DOE/NASA/0008-79/6
NASA CR-159541

(NASA-CR-159541) CERAMIC REGENERATOR SYSTEMS DEVELOPMENT PROGRAM (Ford Motor Co.) 122 p

Unclas
00/07 23458

CERAMIC REGENERATOR SYSTEMS DEVELOPMENT PROGRAM

C. A. Fucinari, J. N. Lingscheit, and J. K. Vallance
Research Staff
Ford Motor Co.

March 1979

Prepared for
NATIONAL AERONAUTICS AND SPACE ADMINISTRATION
Lewis Research Center
Under Contract DEN 3-8

For
U.S. DEPARTMENT OF ENERGY
Division of Transportation Energy Conservation
Heat Engine Highway Vehicle Systems Program

NOTICE

1. Report No.	2. Government Accession No.	3. Recipient's Catalog No.
NASA CR-159541	DE83 013285	

4. Title and Subtitle	5. Report Date
Ceramic Regenerator Systems Development Program Progress Report for Period July 1, 1978 to December 31, 1978	March, 1979
	6. Performing Organization Code
7. Author(s) C. A. Fucinari, J. N. Lingscheit, and J. K. Vallance	8. Performing Organization Report No.
	10. Work Unit No.
9. Performing Organization Name and Address Research Staff Ford Motor Co. Dearborn, Michigan 48121	11. Contract or Grant No. Den 3-8
12. Sponsoring Agency Name and Address Department of Energy Division of Transportation Energy Conservation Washington, D.C. 20545	13. Type of Report and Period Covered Contractor Report
	14. Sponsoring Agency Report No. DOE/NASA/0008-79/6

15. Supplementary Notes Interim Report. Prepared under Interagency Agreement EC-77-A-31-1040

Project Manager, Thomas J. Miller, Transportation Propulsion Division, NASA Lewis Research Center, Cleveland, Ohio 44135

16. Abstract

The primary objectives of the DOE/NASA Ceramic Regenerator Design and Reliability Program is to develop ceramic regenerator cores that can be used in passenger car and industrial/truck gas turbine engines.

The major cause of failure of early gas turbine regenerators was found to be chemical attack of the ceramic material. Improved materials and design concepts aimed at reducing or eliminating chemical attack were placed on durability test in Ford 707 industrial gas turbine engines late in 1974.

This report describes the results of 10,745 hours of turbine engine durability testing accumulated during the period from July 1, 1978 to Dec. 31, 1978. Two materials, aluminum silicate and magnesium aluminum silicate, continue to show promise. Three aluminum silicate cores have attained the durability objective of 10,000 hours at 800°C (1472°F). Another aluminum silicate core shows minimal evidence of chemical attack after 7632 hours at 982°C (1800°F).

The results obtained during this period in ceramic material screening tests, aerothermodynamic performance tests, stress analysis, cost studies, and material specifications are also included in this report.

17. Key Words (Suggested by Author(s))	18. Distribution Statement
Heat Exchangers Ceramic Regenerator Systems Ceramic Materials Heat Exchanger Manufacturing	Unclassified — unlimited STAR Category 85 DOE Category UC-96

19. Security Classif. (of this report)	20. Security Classif. (of this page)	21. No. of Pages	22. Price*
Unclassified	Unclassified	120	—

*For sale by the National Technical Information Service, Springfield, Virginia 22161

DOE/NASA/0008-79/6
NASA CR-159541

CERAMIC REGENERATOR SYSTEMS DEVELOPMENT PROGRAM

C. A. Fucinari, J. N. Lingscheit, and J. K. Vallance
Research Staff
Ford Motor Co.

March 1979

Prepared for
National Aeronautics and Space Administration
Lewis Research Center
Cleveland, Ohio 44135
Under Contract DEN 3-8

For
U.S. DEPARTMENT OF ENERGY
Division of Transportation Energy Conservation
Heat Engine Highway Vehicle Systems Program

TABLE OF CONTENTS

TABLE OF CONTENTS

TABLE OF CONTENTS

LIST OF ILLUSTRATIONS

LIST OF ILLUSTRATIONS

LIST OF ILLUSTRATIONS

LIST OF ILLUSTRATIONS

Page No.

LIST OF ILLUSTRATIONS

LIST OF ILLUSTRATIONS

LIST OF TABLES

SUMMARY

Since the NASA/Ford Ceramic Regenerator Program is organized by tasks, the results obtained during the July 1, 1978 to December 31, 1978 period will also be summarized by Task.

Task I — Core Durability Testing at 800°C.

Approximately 6403 hours of engine durability test (12,806 core hours) at 800°C (1472°F) were completed from July 1, 1978 to Dec. 31, 1978 on cores made from chemically-resistant materials and mounted with a rim support and drive system.

Turbine engine durability tests on aluminum silicate regenerator cores show that this material is relatively impervious to chemical attack. Nine cores of this material have each accumulated over 5000 hours of engine test at 800°C (1472°F), and three cores have attained the durability objective of 10,000 hours with a minimal amount of chemical attack damage.

A high thermal expansion MAS core has accumulated 5381 hours at 800°C (1472°F). A MAS core made from a more advanced material having lower thermal expansion characteristics and greater strength was recently placed on durability test and has now accumulated 2717 hours.

One thin-wall AS core has now accumulated 9616 hours of engine test.

Separations in the elastomer-matrix bond region have occurred on all thin-wall cores bonded using the conventional technique. Utilization of a high-compliance elastomer system shows promise of solving this problem. Two different high compliance elastomer configurations are now on test, with one having accumulated 7840 hours.

The cement holding the hub inserts in place failed in five out of the first fifteen AS cores that have undergone engine test. A hub configuration which utilizes a solid ceramic ring around the hub insert is now on test, and one unit has accumulated 7840 hours.

In order to attain a more maintenance free system, the spring and fixed roller ball bearings in the mounting system in all the engines have been replaced by solid graphite bearings. Over 2677 hours have been accumulated on spring roller bearings and 2384 hours on the fixed roller bearings with little or no wear.

Task II — Core Durability Testing at 1000°C (1832°F).

A total of 8684 core-hours at 1000°C (1832°F) were accumulated during this period.

About 7623 hours of engine test at an average regenerator inlet temperature of 982°C (1800°F) have been accumulated on a thick-wall aluminum silicate core, and 5314 hours at this temperature have been accumulated on a thin-wall AS core. Neither core shows any signs of thermal or chemical attack damage after this exposure.

A second core made from an advanced MAS material was placed on test at 1000°C (1832°F) towards the end of the report period and accumulated 110 hours.

Task III — Material Screening Tests.

Four new materials (3-MAS, 1-LAS/MAS) have been introduced into the laboratory testing program.

A second set of matrix inserts, representing five different materials (3-MAS, 1-LAS, 1-AS) have been analyzed subsequent to the completion of the accelerated corrosion testing program. The MAS materials were unaffected by the test, while the LAS and AS materials experienced some increase in thermal expansion.

Two full sized regenerator cores (1-MAS, 1-AS thin-wall) successfully completed the accelerated corrosion testing program.

Task IV — Aerothermodynamic Performance.

A total of thirty-three matrix fin configurations have been tested at the present time. Twenty-one rectangular, eight sinasoidal, two isosceles triangular, and two hexagonal configurations comprise the present matrix sample size.

The first attempt to evaluate the effect of flow interruption in the axial direction was completed during this report period. The wavy flow passage increased the heat transfer and pressure drop characteristics 20% and 17.5%, respectively, for a 2% improvement in overall fin efficiency.

Task V — Design Studies of Advanced Regenerator Systems

The Supplier D MAS-2 material physical properties have been more fully characterized by evaluating specimens from three different matrices using Weibull statistics.

The tangential shear strength of a limited number of specimens of Supplier A thin-wall aluminum silicate material was determined.

Task VI — Thermal Stability Tests of Ceramics

During this reporting period, thermal stability testing was completed on the sample sets being evaluated at: 1000°C (1832°F), with sodium present; 1100°C (2012°F), without sodium present; 1100°C (2012°F), with sodium present; and 1200°C (2192°F), with sodium present.

Five MAS materials (those of Suppliers C, D, E, I, and J) are judged to have potential for regenerator service at 1000°C (1832°F). The AS material of Supplier A and the LAS material of Supplier B may also be useful at this temperature.

At 1100°C (2012°F) the four MAS materials tested (those of Suppliers C, D, E, and I) appear to have a physical and chemical stability necessary for regenerator service at this elevated temperature. The LAS, LAS/MAS, and AS materials tested are not recommended for service above 1000°C (1832°F).

The data at 1200°C (2192°F) should be completed during the next report period.

Task VII — Manufacturing Cost Studies

A comparison of conventional and zero-wind fabrication costs was completed. Data for two regenerator core configurations indicate a production cost increase ranging from 15% to 26%, depending on core configuration.

Task VIII — Core Material and Design Specification.

A core material and design specification for a regenerative heat exchanger intended for operation at 800°C (1472°F) has been completed. Input, in the forms of laboratory data and engine testing of full size regenerator cores at 1000°C (1832°F), continue to be gathered toward the goal of a high temperature material and design specification.

Task IX — Project Management

The program completion date has been extended from June 30, 1979 to December 31, 1979 at no additional cost to NASA. This extension will allow an additional 2000 and 13000 core test hours to be accumulated at 1000°C (1472°F) and 800°C, respectively. In addition, this extension will permit other suppliers to develop full-size cores for test evaluation.

Task X — Reporting Requirements

Publication of the "Semi-Annual Progress Reports" and "Topical Reports" are on schedule.

INTRODUCTION

Since 1965, Ford Motor Company has been engaged in developing a ceramic regenerator system for use in gas turbine engines. Over 100,000 hours of engine operating experience have been accumulated on a sample of approximately 1,000 regenerator cores fabricated of lithium aluminum silicate (LAS) and produced by two suppliers.

Because of unexpected failures of the LAS regenerator, in 1973 Ford started a series of controlled durability tests using the 707 turbine engine. When these tests were terminated in August 1973, 11 core failures had occurred out of a sample of 30 cores on test. It was determined that the failures were primarily caused by a severe chemical attack on the LAS material used. These test data showed that these regenerators had a B_{10} life of 600 hours and an average life of 1600 hours.

Late in 1973, an engineering research program was initiated to solve the regenerator core failure problem. The primary objective of this program is to develop ceramic regenerator cores that can be used in passenger car and industrial/truck gas turbine engines and other industrial waste heat recovery systems. Specific durability objectives are defined as achieving a B_{10} life of 10,000 hours on a truck/industrial gas turbine engine duty cycle at a regenerator inlet temperature of 800°C (1472°F).

In late 1973 Ford funded several companies to develop new ceramic regenerator materials. By 1973, new materials, including aluminum silicate (AS) and a magnesium aluminum silicate (MAS) were screened in laboratory and engine tests and found to have acceptable resistance to chemical attack. Regenerator cores made from new materials were placed on durability test late in 1974 and early in 1975.

The Ford 707 industrial turbine is being used as the test bed to evaluate these new regenerator materials and concepts. Since 1974, over 98,445 engine test hours (196,890 core hours) have been accumulated on regenerator systems. Core durability testing will continue in 1979 in an effort to demonstrate the B_{10} life of 10,000 hours required for an industrial gas turbine engine regenerator.

Late in 1974, the Alternate Automotive Power Systems Division of the Environmental Protection Agency joined with Ford Motor Company in an "Automotive Gas Turbine Ceramic Regenerator Design and Reliability Program." In early 1975, this program was transferred to the newly-formed Energy Research and Development Administration (ERDA), and since 1976 this program has been under the direction of the National Aeronautics and Space Administration (NASA). A description of the work conducted in these programs is contained in References 1 through 6.

The present DOE/NASA cost-sharing program with Ford Motor Company continues the ceramic regenerator design and development work that was started under the original EPA/FORD contract. This latest program is subdivided into ten major tasks. These tasks are:

Task I — Core Durability Testing at 800°C (1472°F)
Task II — Core Durability Testing at 1000°C (1832°F)
Task III — Material Screening Tests
Task IV — Aero-Thermodynamic Performance
Task V — Design Studies of Advanced Regenerator Systems
Task VI — Ceramic Thermal Stability Tests
Task VII — Manufacturing Cost Studies
Task VIII — Core Material and Design Specifications
Task IX — Program Management
Task X — Reporting Requirements

The technical progress in each of these tasks for the period from July 1, 1978 to December 31, 1978 is recorded in the following sections of this report.

DISCUSSION OF RESULTS
TASK I. CORE DURABILITY TESTING AT 800°C (1472°F)
I.A. INTRODUCTION

Reference 1 describes the engine test results obtained by Ford Motor Company on lithium aluminum silicate ceramic regenerators used in the 707 turbine engine up to the end of 1973. These regenerator cores were mounted at the hub and driven through ceramic pins cemented into the rim. These data showed that chemical attack was the major cause of failure, and that this type of regenerator core configuration would have a B_{10} life of 600 hours and a B_{50} life of 1600 hours. A B_{10} life of 600 hours was obtained from a Weibull Analysis of the failures in this sample, and means that 10% of the regenerators of this configuration will fail in less than 600 hours of engine test. A B_{50} life of 1600 hours means that 50% of the regenerators will fail in less than 1600 hours of engine exposure.

By 1975 AS and MAS regenerators had been successfully fabricated, and these materials showed promise in both laboratory and accelerated engine tests. They were placed on long term durability tests and the results are reported in References 2 to 6. The total accumulation of engine test hours since the start of the test program on January 1, 1974 is 98,445 hours (196,890 core hours). With respect to the current program with NASA, a total of 67,266 core hours have been accumulated, which is just below the program objective of 68,000 core hours.

I.B. STATUS

I.B.1. Durability Record of Aluminum Silicate Regenerators

To date 23 different aluminum silicate (AS) regenerators, fabricated by Supplier A, have been engine tested in the Ford 707 turbine. While all these cores are constructed from the same material, they can be broken down into two classifications depending upon their wall thickness. The original aluminum silicate configuration has an average matrix wall thickness of 0.11 mm (.0043 in.). In 1976, a high-performance, thin-wall configuration with a wall thickness of 0.07 mm (.0026 in.) was started on durability test.

Eleven thick-wall AS cores are being tested at 800°C (1472°F) under identical operating conditions and these cores make up the control sample on which durability projections will be based. The durability status of these cores is shown in Figure 1.B.1.1. About 67,000 core hours of engine test have been accumulated on this aluminum silicate sample with three cores having attained the durability objective of 10,000 hours. At least two failures are required before a Weibull Failure Analysis can be undertaken. There have been no failures of cores made from this material so a failure analysis cannot be started. A reliability projection, however can now be made if the shape of the Weibull failure curve is estimated. Using Weibull theory and a sample consisting of the six highest-hour AS cores, together with an estimated failure curve slope, a B_{10} life of 6000 hours can be projected with slightly over 50% confidence. With the same theory, a B_{10} life of 3500 hours can be projected for AS material with almost 100% confidence. A B_{10} life of 3500 hours might be acceptable for an automotive application.

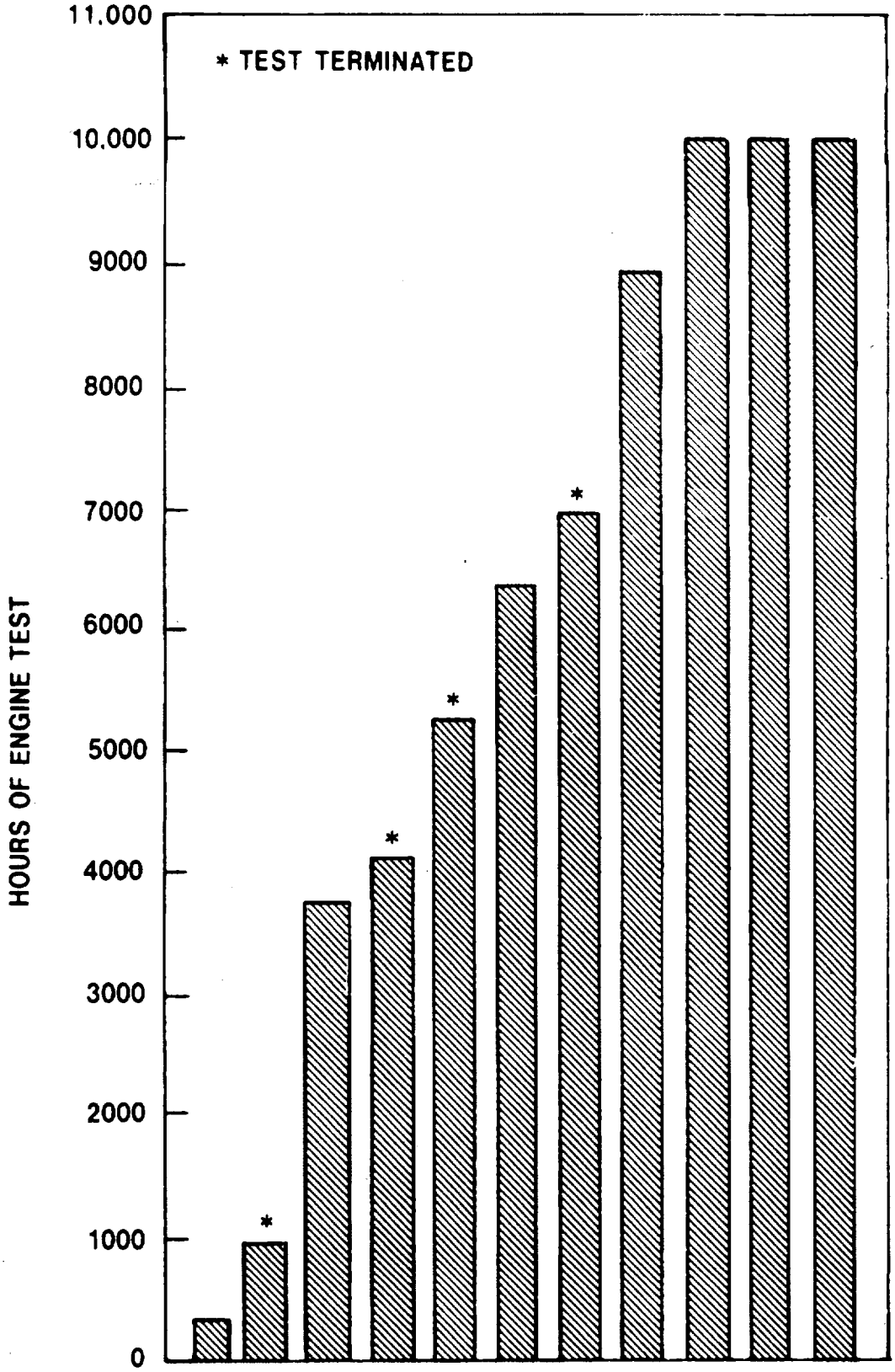

Figure I.B.1.1 — Durability Record of Thick-Wall AS Regenerators Operating at 800°C (1472°F).

Seven thin-wall AS cores have also been engine tested at 800°C (1472°F) as shown in Figure 1.B.1.2 and one core has accumulated over 9600 hours.

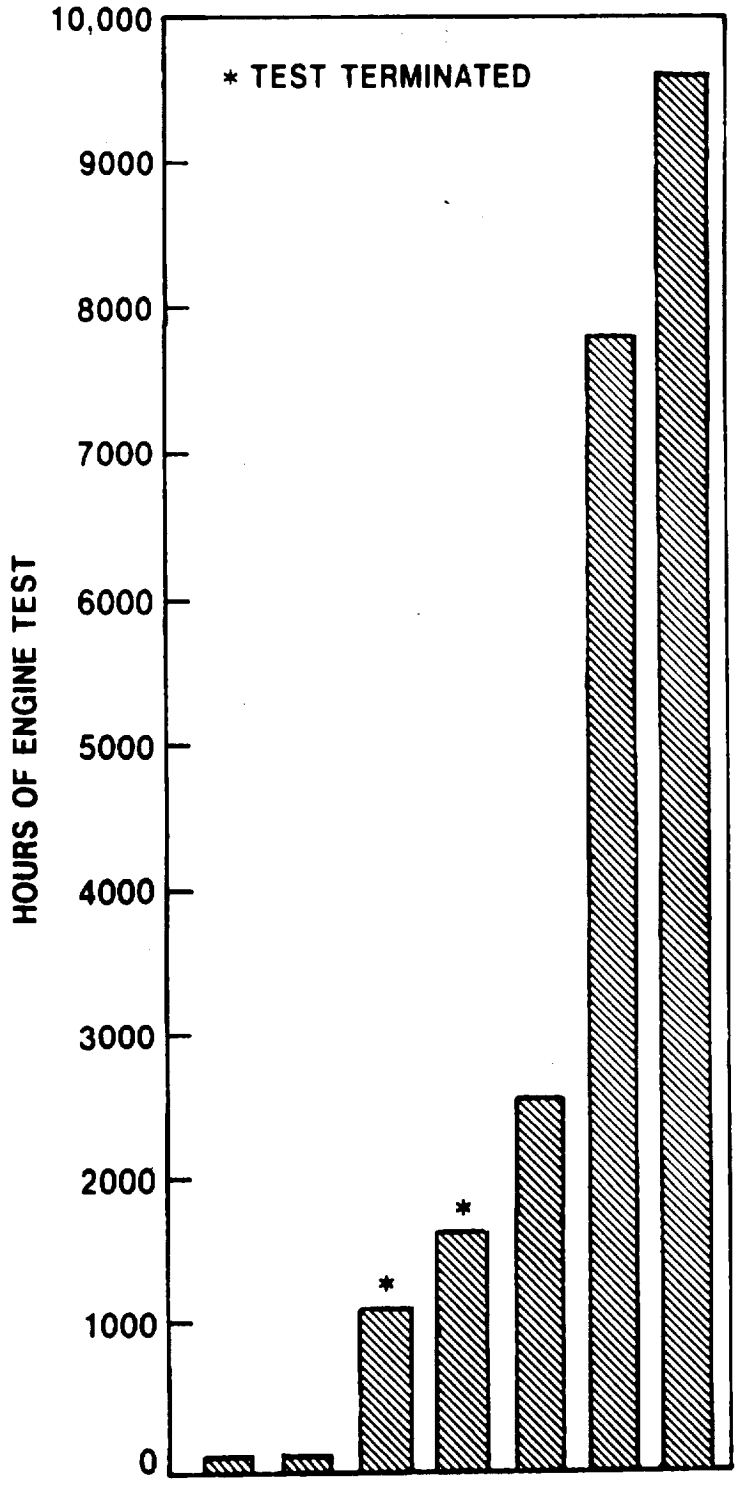

Figure I.B.1.2 — Durability Record of Thin-Wall AS Regenerators Operating at 800°C (1472°F).

The running history of all of Supplier A's AS cores that have been engine tested are shown in Figure 1.B.1.3. This figure also includes the five cores tested at 1000°C (1832°F) and described in Section II.B. Almost 100,000 hours of engine test have been accumulated on this material. None of these cores show any serious signs of thermal distress or chemical attack damage. To date, a total of eleven AS cores have accumulated over 4,000 hours and eight cores have each accumulated over 6,000 hours of engine test without visual distress.

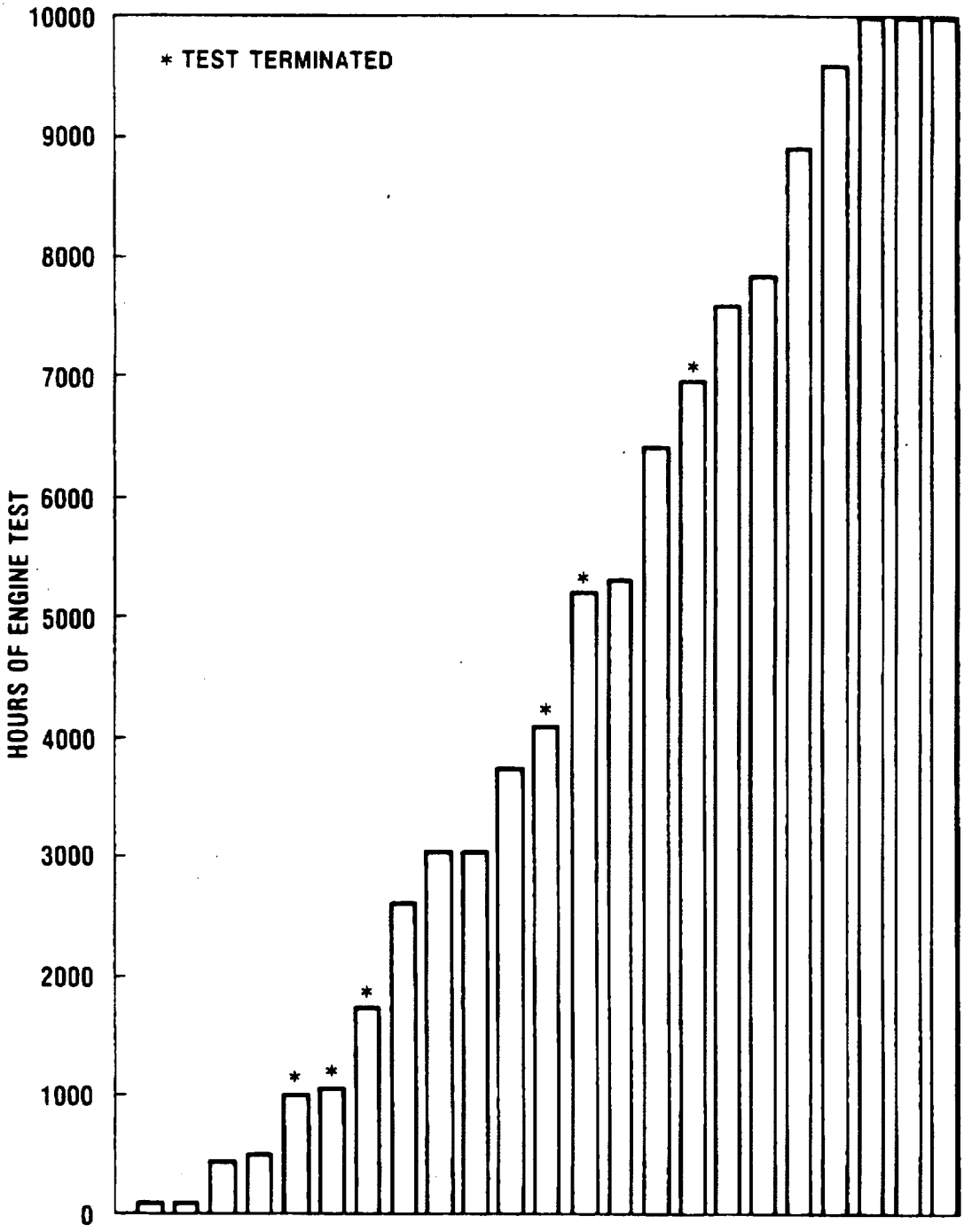

Figure I.B.1.3 — Durability Record of All AS Regenerators Tested in the Ford 707 Turbine Engine

It is planned to continue testing AS regenerators for the remainder of 1979 to acquire additional long-term durability data.

I.B.2. Durability Record of Magnesium Aluminum Silicate Regenerators

Engine tests of MAS regenerators made from first generation or early material and fabricated by Supplier D are described in References 1 to 4. The testing of these cores was terminated when the cement holding the hubs or center sections in place failed and caused damage in this region. One of these cores accumulated 5381 total hours of engine test (Reference 4).

Thermal stress cracks developed in this high-hour, first generation MAS core after 200 hours of engine operation, but remained stable throughout the rest of the test. An analysis conducted on this MAS material showed that at the operating temperature of 800°C (1472°F) the rim thermal stress safety factor could be substantially below unity. The material in the rim area therefore, would be expected to fail and develop thermal cracks (Reference 4).

In late 1977, Supplier D successfully fabricated several cores made from a new MAS material which is stronger and has a lower thermal expansion coefficient than the material used in the original three cores. One of these second-generation MAS cores has now accumulated 2717 hours of engine test. A summary of the operating experience on first and second generation MAS cores is shown in Figure I.B.2.1.

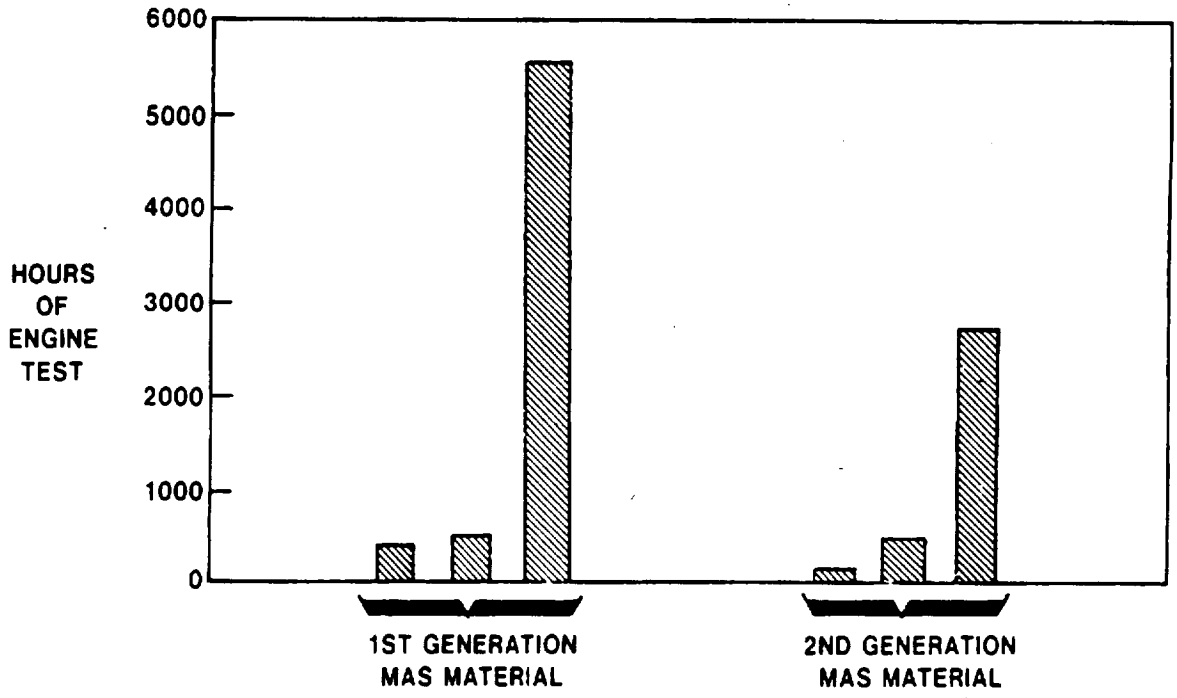

Figure I.B.2.1 — Durability Record of First and Second Generation MAS Regenerators.

It is planned to continue testing at least one of the second generation cores of Supplier D at 800°C (1472°F). A core of this material is also being evaluated at 1000°C (1832°F) and the results are reported in Section II.B of this report.

I.B.3. Hub Cement Failures

As reported in References 2 and 3 the cement holding the hub insert in place failed in five different AS cores out of the first 15 that were engine tested in the 707 turbine. In each case, the failure was attributed to improper composition or improper processing of the cement itself. When properly processed the cement has good durability potential as evidenced by the Weibull distribution for cores processed with Supplier A cold or foam cement (Figure I.B.3.1). It should be noted that two of the three cores that have attained the durability objective of 10,000 hours at 800°C (1472°F) contain the original Supplier A cement at the hub.

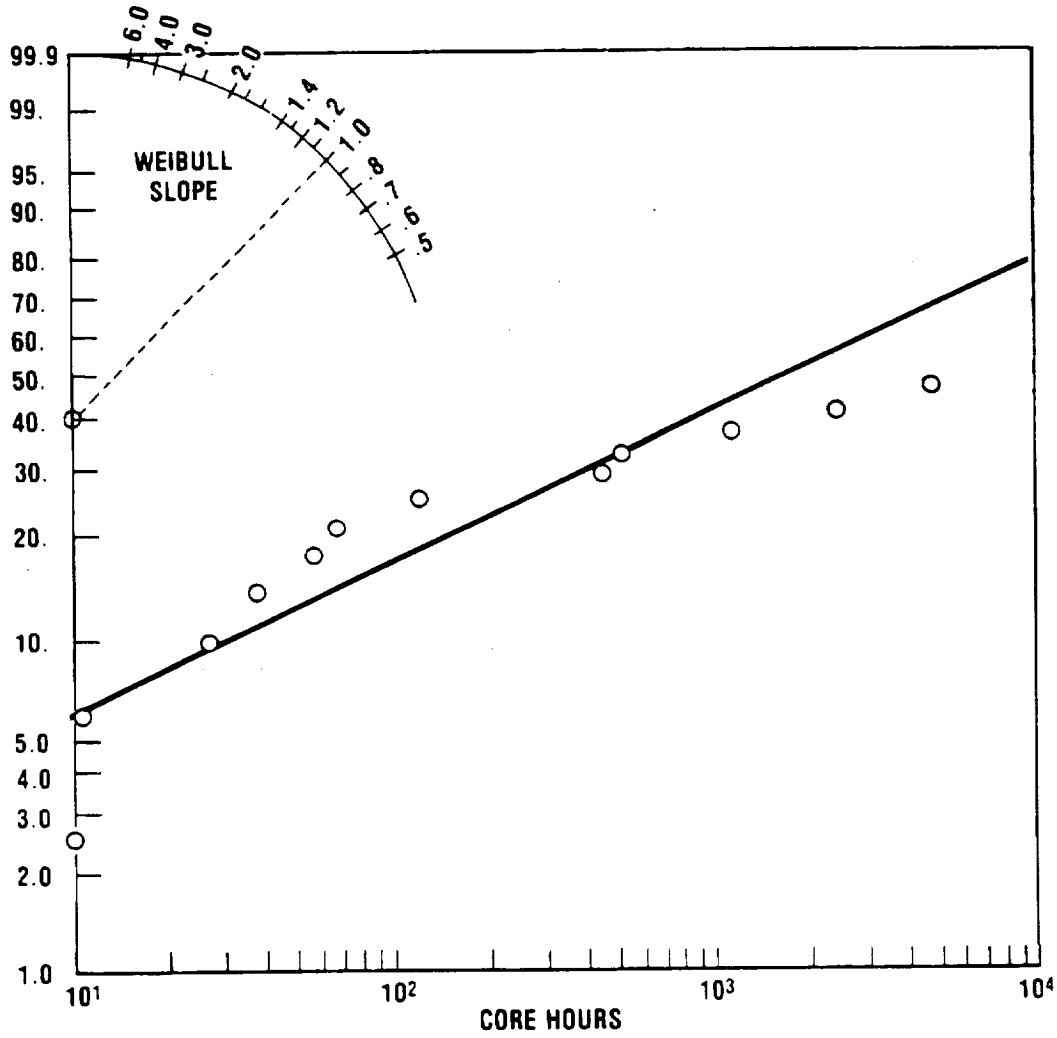

Figure I.B.3.1 — Failure History of AS Cores with Supplier A Foam Cement

Several different concepts aimed at improving the reliability in this area have been engine tested (Reference 3). The most successful configuration consists of a matrix hub cemeted into a thin, 6.4 mm (.25 in.) wide, solid ceramic ring and this subassembly is then cemented into the matrix. The ceramic ring allows better control of temperature during the firing of the cement, and it also provides a better match of the thermal expansion characteristics of the insert-matrix bond area to the rest of the matrix.

All currently active AS cores that have undergone hub failures have been repaired to this configuration, and all new cores received from Supplier A have been built with this design. As a result, eight cores with this new hub configuration have been on durability test since late 1976, and their durability record is shown in Figure I.B.3.2. One of these cores has accumulated over 7000 hours. One low-hour failure occurred during 1977, and after extensive investigation the cause of this failure is still unexplained.

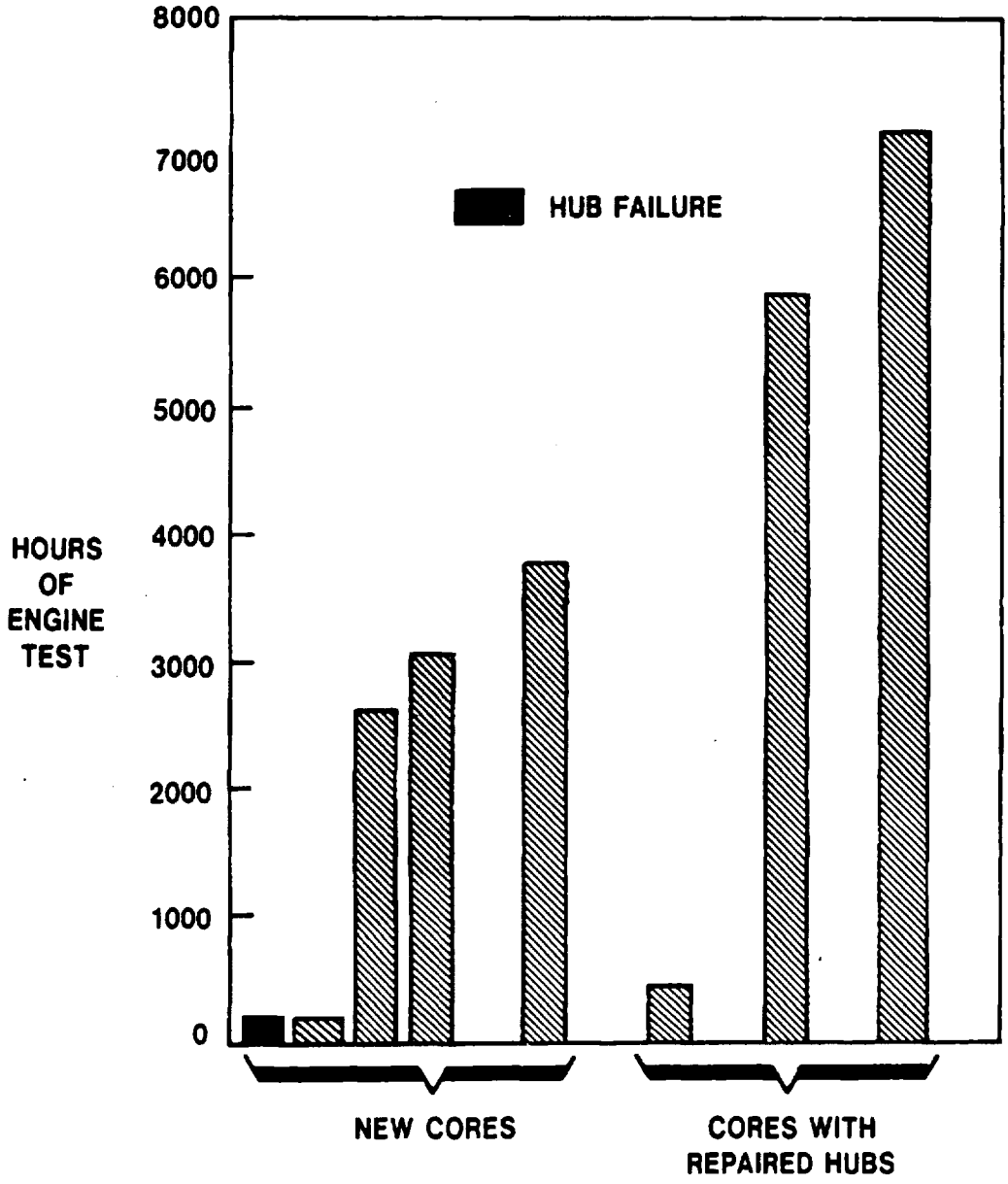

Figure I.B.3.2 — Durability Record of Cores with Solid Ceramic Ring Around Hub Insert.

These hub failures are still not considered to be a serious, fundamental problem. Hubs utilizing a solid ceramic ring around the hub insert appears to have a better durability record than the original hub configuration. More engine test hours are needed to determine the durability life of this concept.

I.B.4 Matrix — Elastomer Bond Separation

Reasonably good durability has been obtained with the elastomer bonded ring gear on the thick-wall AS cores. The results obtained with the same elastomeric drive on the thin-wall AS core have not been as successful. Since the thin-wall matrix has a thinner cross section, it is weaker and has less capability for carrying mechanical loads. Every thin-wall AS core, bonded with the same procedure used with the thick-wall cores, has had a separation in the elastomer-matrix bond area. The operating history is shown in Figure I.B.4.1. Experimental and analytical evidence presented in Reference 4 shows that the eventual solution to this problem is the development of a high-compliance, elastomer system in which the modulus of the elastomer is reduced at least 70%. This conclusion is supported by engine operating experience, also presented in Figure I.B.4.1, which shows that a 50% reduction in modulus is inadequate and failures will occur with this arrangement.

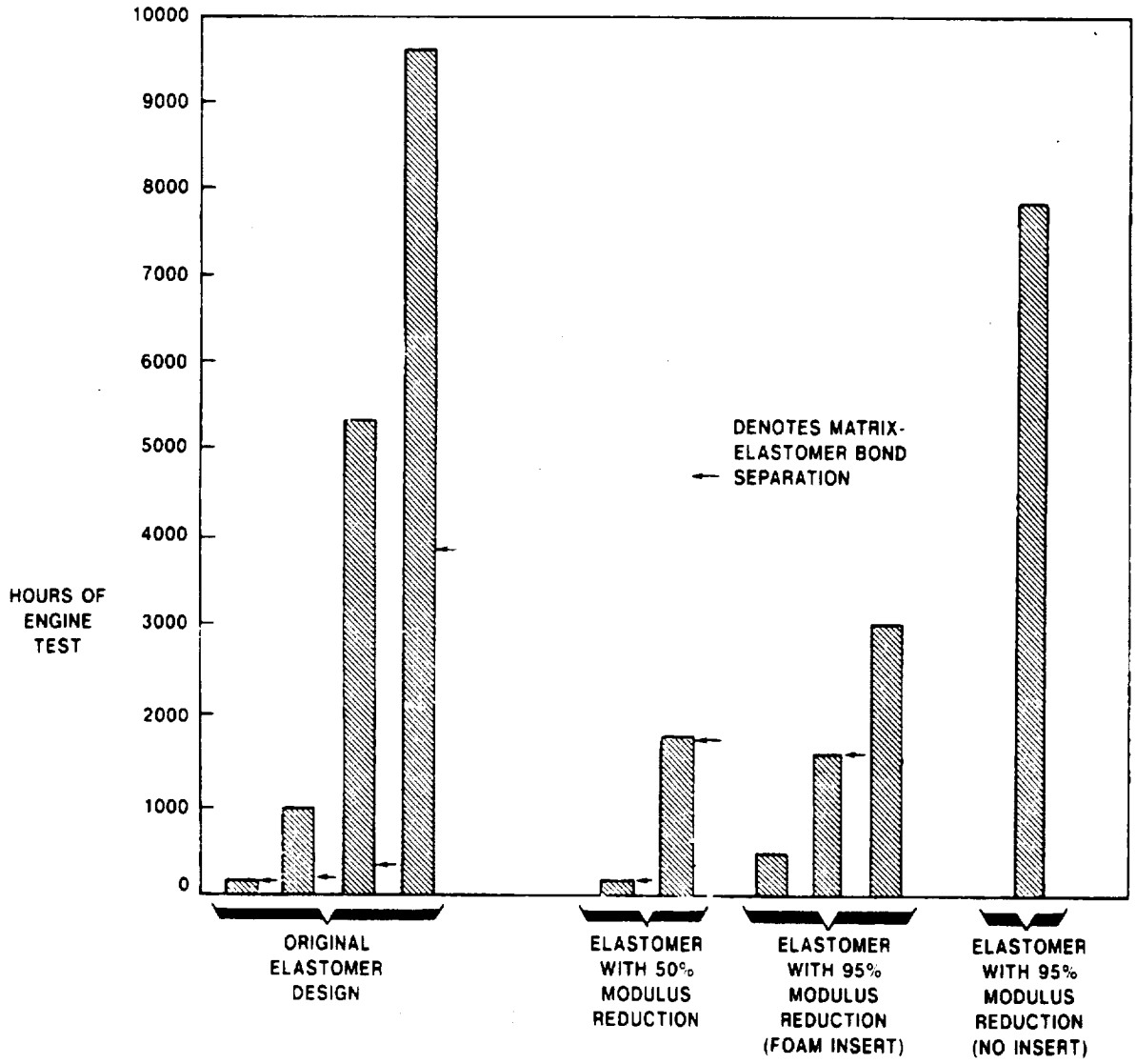

Figure I.B.4.1 — Durability Record of Thin-Wall, AS Regenerators Utilizing Different Elastomer Bonding Approaches.

Two different regenerator configurations are now on test in which the modulus of the elastomer has been reduced by 90-95%. One of these assemblies has now accumulated 7840 hours of engine test (Figure I.B.4.1). This configuration incorporates slots in the elastomer (Figure I.B.4.2) to reduce the modulus. In the other configuration these slots are filled with foam rubber. It is believed that the second configuration with the foam rubber functions identically to the first during engine operation, provided the foam is not continuously bonded to the matrix or ring gear. Use of the foam rubber simplifies the gear-elastomer assembly process.

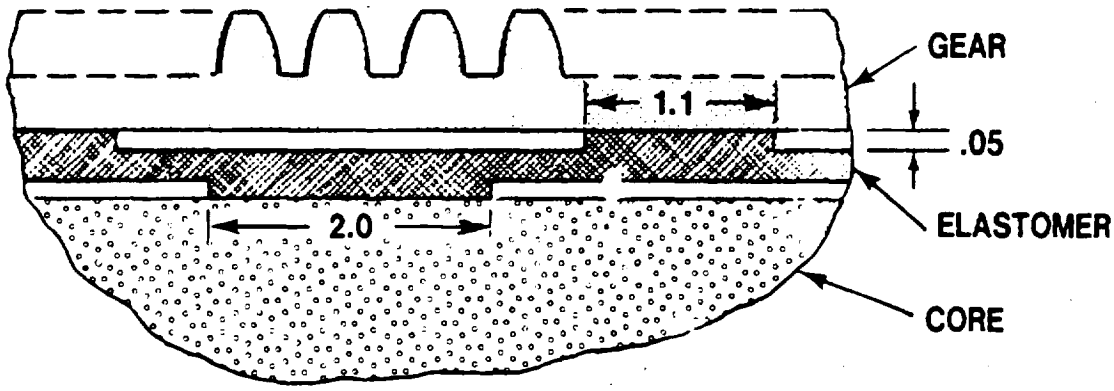

Figure I.B.4.2 — High Compliance Elastomer Design.

It is planned to continue testing this slotted design through the remainder of the program, and all thick and thin-wall cores will be elastomerically bonded in the future with this configuration. The data accumulated to date suggest that this approach may result in the successful elastomeric bonding of the ring gear to thin-wall AS cores.

I.B.5 Drive and Support System

In 1974, the design and development of a rim-mount system was initiated to replace the hub-mounting system then in use in the Ford 707 turbine. The ring gear is supported at three points (Figure I.B.5.1). Except for the pinion location, the rollers were mounted on ball bearings. The ball bearings were inspected every 350 to 400 hours in an effort directed at anticipating any difficulties in the drive system before damaging a high-hour regenerator matrix. As a precautionary measure, the bearings were regreased after each inspection.

In an effort to develop a more maintenance-free system, some of the ball bearings were replaced with a solid graphite bearing. This graphite bearing along with its outer steel roller or tire is shown in Figure I.B.5.2. The graphite bearing is held in the steel tire with snap rings. The durability record of these graphite bearings is shown in Figure I.B.5.3. In the spring roller location the bearing carries a 222N (50 lb) load and in the fixed roller location it carries 1355N (305 lb) load. None of these bearings have failed and the wear appears satisfactory. The high hour spring-roller, graphite bearing now has 2677 hours of engine operation and the highest hour fixed-roller, graphite bearing has 2384 hours.

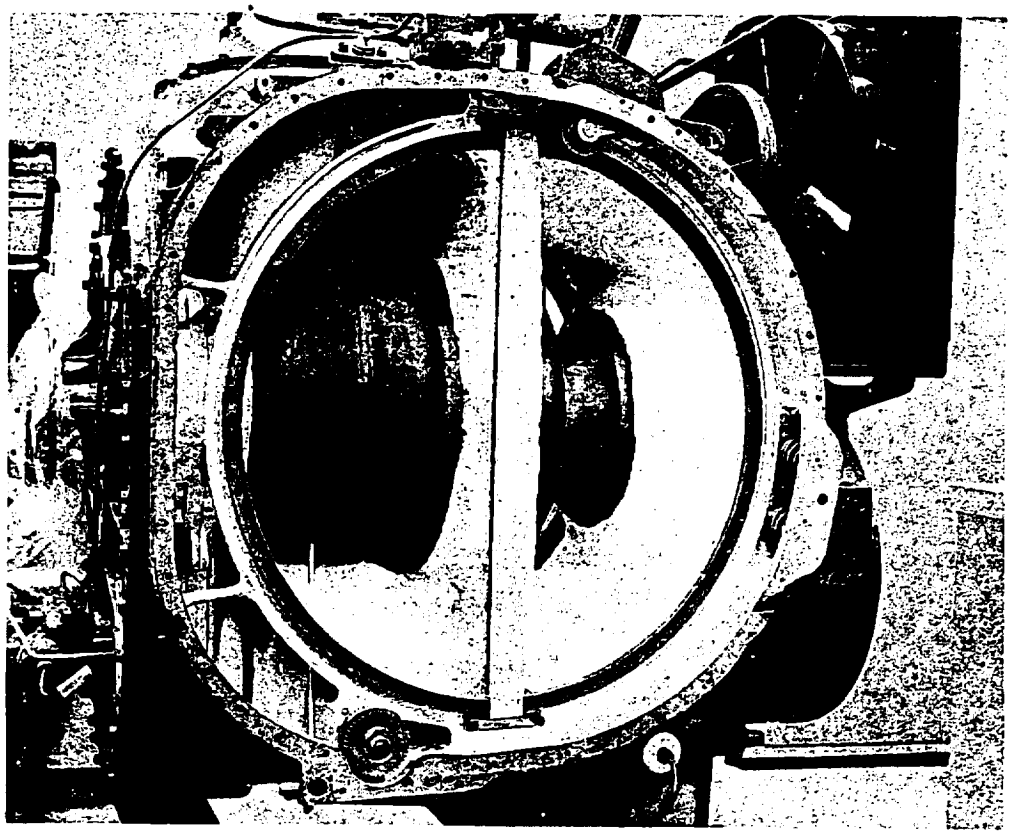

Figure I.B.5.1 — Photograph of Ford 707 Turbine Engine Housing Showing Modifications Required to Incorporate the Present Rim-Support System.

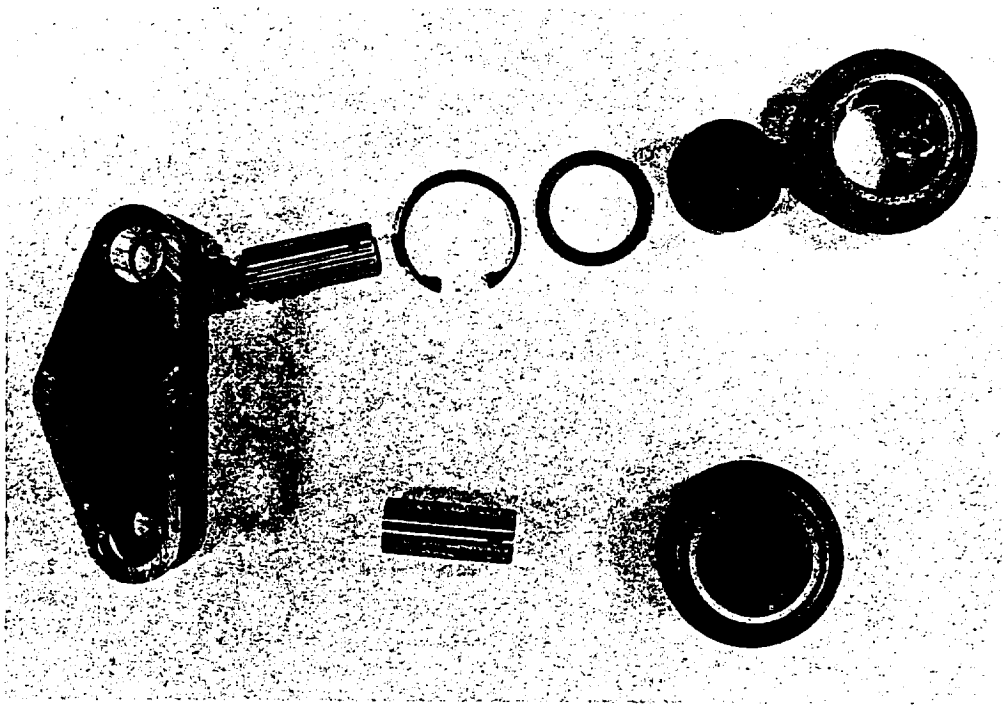

Figure I.B.5.2 — Photograph Showing Graphite Bearing, Outer Race Support Ring, Shaft, Snap Ring, and Yoke.

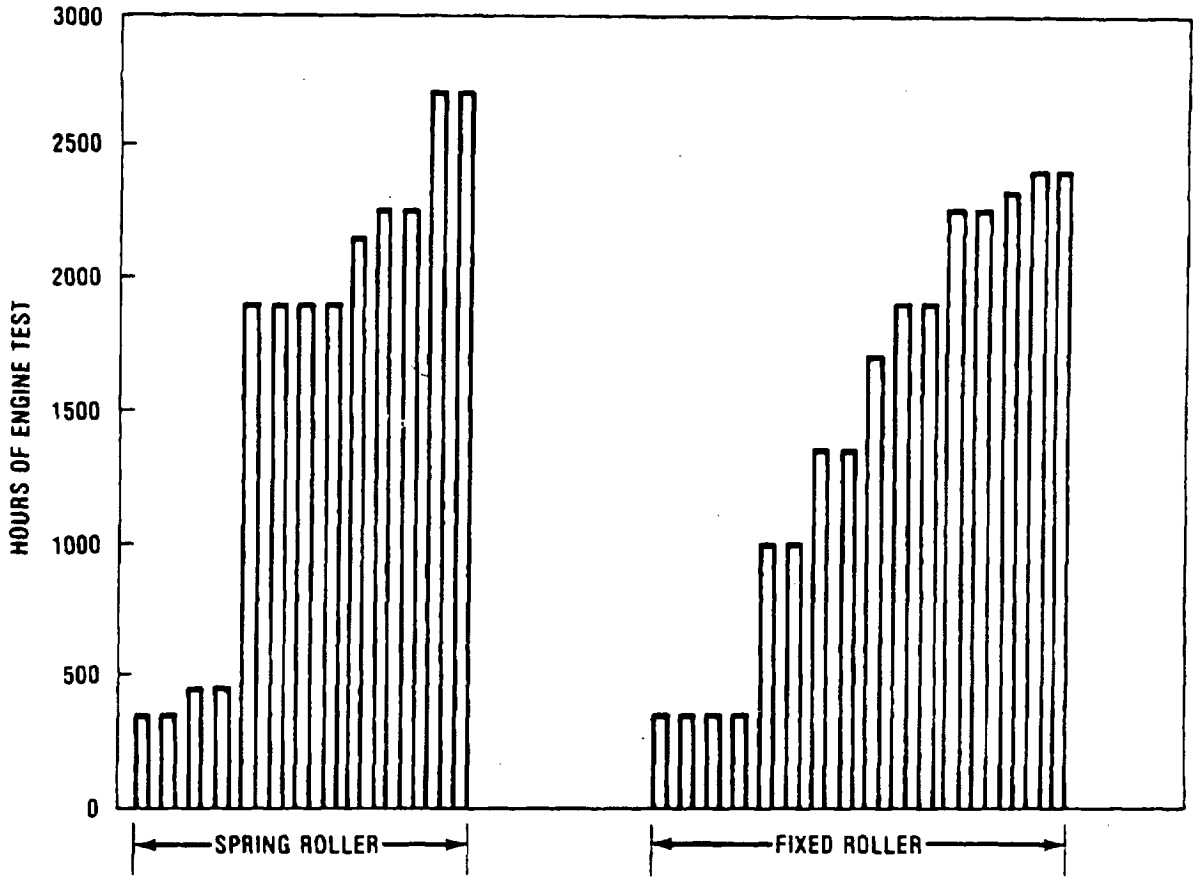

Figure I.B.5.3. — Durability Record of Graphite Bearings in the Fixed Roller and Spring Roller Locations

Because of the encouraging results to date with the graphite bearings, all of the engines currently on test have been converted from ball bearings to graphite in the regenerator drive system. During the next report period the wear data on these graphite bearings will be closely monitored.

At the present time, thirteen engines have been on test with the current three-point support system. No major difficulties have been encountered after 314, 1562, 2054, 2185, 2240, 2628, 3057, 4096, 4722, 5581, 5950, 7784 and 8260 hours for a total of 50,433 operating hours.

I.C. PROBLEM AREAS

Two problem areas exist and they are: failures of the cement bonding the hub insert to the matrix and separation at the elastomer-matrix interface in the thin-wall AS regenerator. The first problem is discussed in Section I.B.3 and the second is discussed in Section I.B.4. Corrective action consists of a ceramic ring for the first problem and high-compliance elastomer design for the second problem. Hardware incorporating these changes is continuing on engine test.

I.D. FUTURE PLANS

During the next report period, engine testing of the thick and thin-wall AS cores and the MAS core will be continued. The durability of the high-compliance, slotted elastomer configuration, the ceramic-ring hub insert, and the graphite bearings will be carefully monitored.

I.E. TASK SUMMARY

Approximately 6403 hours of engine durability test (12806 core hours) at 800°C (1472°F) were completed from July 1 to Dec. 31, 1978 on cores made from chemically-resistant materials and mounted with a rim support and drive system. This brings the total core hours accumulated to 67,266, which is just below the program objective of 68,000 hours.

Turbine engine durability tests on aluminum silicate regenerator cores show that this material is relatively impervious to chemical attack. Nine cores of this material have each accumulated over 5000 hours of engine test at 800°C (1472°F), and three cores have attained the durability objective of 10,000 hours with a minimal amount of chemical attack damage.

A high thermal expansion MAS core has accumulated 5381 hours at 800°C (1472°F). A MAS core made from a more advanced material having lower thermal expansion characteristics and greater strength was recently placed on durability test and has now accumulated 2717 hours.

One thin-wall AS core has now accumulated 9616 hours of engine test.

Separations in the elastomer-matrix bond region have occurred on all thin-wall cores bonded using the conventional technique. Utilization of a high-compliance elastomer system shows promise of solving this problem. Two different high compliance elastomer configurations are now on test, with one having accumulated 7840 hours.

The cement holding the hub inserts in place failed in five out of the first fifteen AS cores that have undergone engine test. A hub configuration which utilizes a solid ceramic ring around the hub insert is now on test, and one unit has accumulated 7840 hours.

The spring and fixed roller ball bearings in the mounting system in all the engines have been replaced by solid graphite bearings. Over 2677 hours have been accumulated on spring roller bearings and 2384 hours on the fixed roller bearings with little or no wear.

TASK II CORE DURABILITY TESTING AT 1000°C (1832°F)

II.A. INTRODUCTION

Since the fourth quarter of 1975, a special 707 turbine engine has been operated at elevated regenerator inlet temperatures. Throughout the test the engine has been operated at an average regenerator inlet temperature of 982°C (1800°F) with excursions of 30°C (52°F) above and below this value being permitted. These regenerator inlet temperatures are obtained by operating the engine at 1065-1080°C (1950-1975°F) turbine inlet temperatures at 60 to 65% gasifier spool speed and low power turbine speeds.

The objective of Task II of the DOE/NASA Ceramic Regenerator Program was to accumulate 6000 core-hours during the second half of 1978 at an inlet temperature of 1000°C (1832°F). With respect to the current program with NASA, which has been extended through December 31, 1979, a total of 17,532 core hours have been accumulated. The program objective is 22,000 core hours at 1000°C (1472°F).

II.B. STATUS

As discussed in Reference 5, a program change was initiated in the first quarter of 1978 so that in the second quarter two of the 800°C (1472°F) engines would be converted to 1000°C (1832°F) engines. This would increase the number of hours of test at 1000°C (1832°F) per quarter from 1000 core-hours to 3000 core-hours. The conversion of the two engines was completed in the second quarter, and a total of 8684 core-hours of 1000°C (1832°F) test were completed on the three engines during the second half of 1978.

The thermal stress safety factor for aluminum silicate at these temperatures was determined in Reference 2. This material has a thermal stress safety factor of about 7.5 at 1000°C (1832°F). Providing the material is thermally stable, the aluminum silicate regenerator should have no problems with thermal stresses at this temperature. The safety factor for the MAS material is believed to be about unity (Reference 5), but more material property data must be generated before this MAS safety factor can be more accurately defined. It is anticipated that localized cracks may be formed in this material, but these cracks are not expected to propogate. Similar cracks were formed in an early MAS core tested at 800°C (1472°F) and these local cracks remained stable for over 5000 hours of engine test.

The present Task II status is summarized in Figure II.B.1 and shows that the highest-hour thin-wall AS core has now accumulated 5314 hours at an average inlet temperature of 982°C (1800°F). A failure at the elastomer bond-matrix interface occurred in this thin-wall core after 271 hours. The failure is typical of thin-wall AS cores bonded with the original process. The core has been rebonded and returned to test. This failure mode and the corrective action are described in Section I.B.4. A second thin-wall core was terminated after 443 hours when excessively damaged by a MAS core failure on the opposite side of the engine. The highest hour thick-wall AS core has 7623 hours at this temperature.

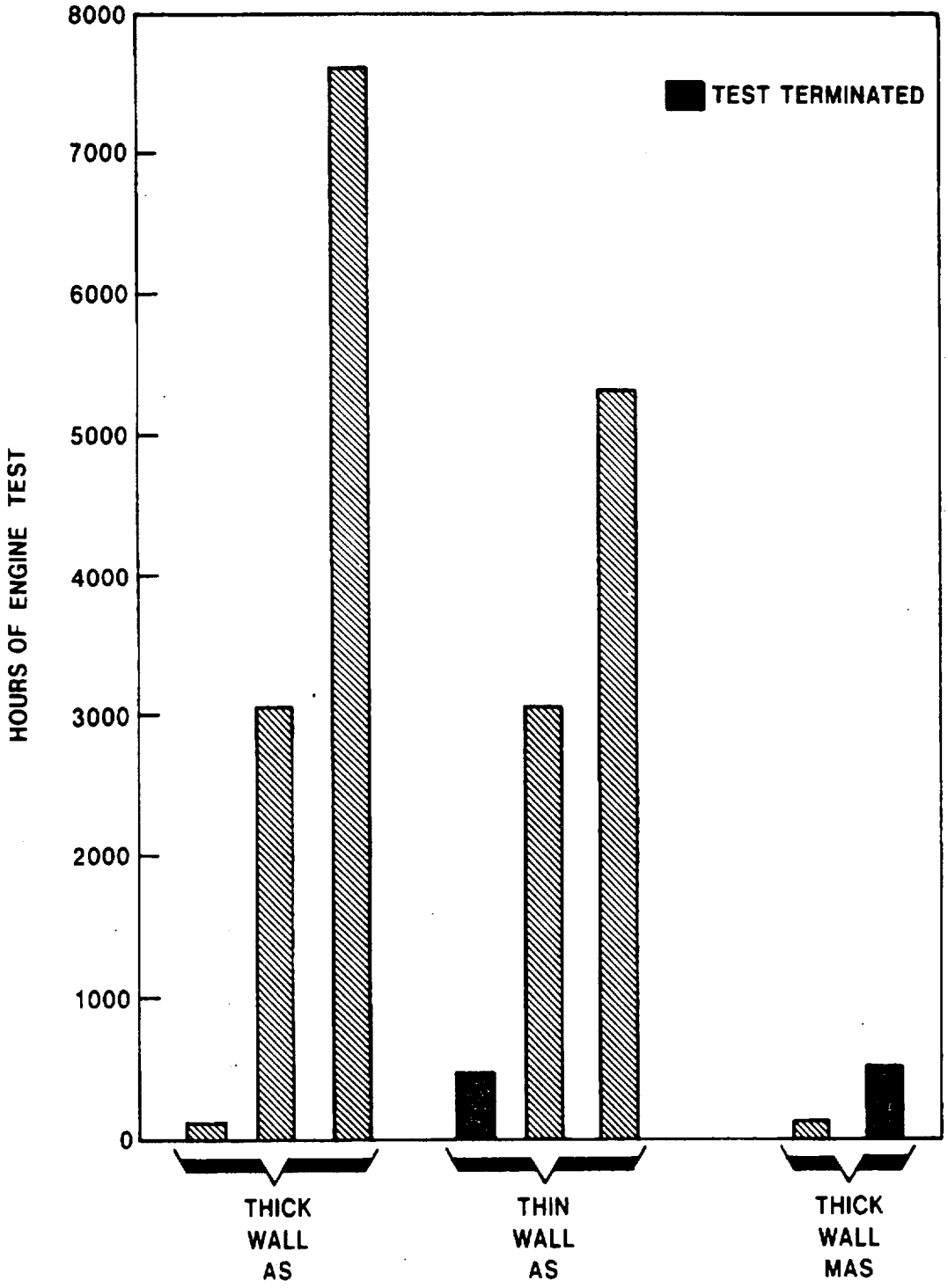

Figure II.B.1 — Durability Record of Regenerators Operating at 1000°C (1832°F)

The first MAS core tested at this temperature was terminated after a hub cement failure. The core, which was fabricated with the supplier D MAS-2 material, appeared to be void of thermal cracks in the rim after 473 hours. A second core of this material was installed in the high temperature engine and has accumulated 110 hours.

II.C. PROBLEM AREAS

The primary limitation to accumulating durability at 1000°C (1832°F) engine condition for the supplier D MAS-2 material is the lack of a reliable cement for attaching the matrix hub insert. This may continue to be a problem for the remainder of the program, since resources are not available to increase development effort in this area.

II.D. FUTURE PLANS

Testing of the thick and thin-wall AS cores and MAS core described above will continue at 1000°C (1832°F) during the remainder of 1979.

II.E. TASK SUMMARY

About 7623 hours of engine test at an average regenerator inlet temperature of 982°C (1800°F) have been accumulated on a thick-wall aluminum silicate core, and 5314 hours at this temperature have been accumulated on a thin-wall AS core. Neither core shows any signs of thermal or chemical attack damage after this exposure.

A second core made from an advanced MAS material was placed on test at 1000°C (1832°F) towards the end of this report period and accumulated 110 hours.

TASK III MATERIAL SCREENING TESTS

III.A. INTRODUCTION

A number of ceramic materials offer the potential for service as gas turbine regenerators at 800°C (1472°F). The number of basic materials are few, but the compositional variations and combinations employing those ceramic materials increase the number of viable candidates to a relatively impressive size. It is the goal of this task to bring some order to the nominees for regenerator ceramics by evaluating the materials (in matrix form) in the laboratory and in the engine environment. The successful completion of this charter will yield a ranking of materials reflecting life and stability in the rather hostile environments found in the gas turbine engine. Commensurate with the execution of this ranking will be the indication of materials found unsuitable for regenerator duty.

Many of the data of this task and of Task VI, "Thermal Stability Tests of Ceramics" are presented in graphical form. The graphing convention is consistent with that used in previous reports, and the symbol legends will be included, when needed, as part of each graph.

III.B. STATUS

III.B.1 Laboratory Tests

During this reporting period, four new materials were procured, prepared, and introduced into the laboratory testing program. Three materials are MAS (two fabricated by a wrapping technique and one by extrusion) and one is an improved LAS/MAS composition (fabricated by wrapping). Both cold face and hot face testing of these materials has begun, and preliminary results will be reported next period.

III.B.2. Accelerated Corrosion Testing — Matrix Inserts

The second test core, containing matrix inserts of five experimental materials (3-MAS, 1-LAS, 1-AS) had completed accelerated corrosion testing in the salt ingestion engine during the previous reporting period. Activity in this sub-task during the current period has concentrated on completing the analyses of the tested specimens. Atomic absorption analysis and thermal expansion comparisons are reported in this section.

Atomic absorption analyses for some chemical constituents found in the matrix insert samples after accelerated corrosion testing are reported in Tables III.B.2.1 through III.B.2.3 for testing periods of 50, 100, and 150 hours, respectively. Samples were selected for each test interval, from the hot face and the cold face of each experimental material and the AS host core.

Analyses for selected ions were carried out on a water solution of the samples to determine the species found on the material surface. One would expect a sodium concentration due to the salt introduced during the course of the test. If sufficient ion-exchange had taken place between the salt compound and the material lattice, exchanged species (peculiar to the particular material being tested) may be detected at the sample surface.

Sample	Position	Solution	% Na_2O	% Li_2O	% MgO
Supplier D	Cold Face	Water	0.050		0.013
MAS	" "	Acid	0.041		7.750
Supplier D	Hot Face	Water	0.080		0.005
MAS	" "	Acid	0.066		7.720
Supplier C	Cold Face	Water	0.030		
MAS	" "	Acid	0.062		8.150
Supplier C	Hot Face	Water	0.030		
MAS	" "	Acid	0.065		8.280
Supplier E	Cold Face	Water	0.010		0.001
MAS #2	" "	Acid	0.012		7.750
Supplier E	Hot Face	Water	0.020		0.001
MAS #2	" "	Acid	0.125		7.710
Supplier B	Cold Face	Water	0.030	0.004	
AS	" "	Acid	0.001	N.D.	
Supplier B	Hot Face	Water	0.070	N.D.	
AS	" "	Acid	0.078	N.D.	
Supplier B	Cold Face	Water	0.030	0.030	
LAS	" "	Acid	0.028	1.340	
Supplier B	Hot Face	Water	N.D.	N.D.	
LAS	" "	Acid	0.140	1.590	
Host Core	Cold Face	Water	0.030	0.005	
AS	" "	Acid	0.005	N.D.	
Host Core	Hot Face	Water	0.010	N.D.	
AS	" "	Acid	0.077	N.D.	

N.D. = Not Detected
Blank = No Analysis

Table III.B.2.1. — Chemical Analyses After 50 Hours of Accelerated Corrosion Testing as Matrix Inserts

Sample	Position	Solution	% Na_2O	% Li_2O	% MgO
Supplier D	Cold Face	Water	0.090		0.019
MAS	" "	Acid	0.040		7.580
Supplier D	Hot Face	Water	0.090		0.005
MAS	" "	Acid	0.090		7.840
Supplier C	Cold Face	Water	0.050		0.001
MAS	" "	Acid	0.060		8.160
Supplier C	Hot Face	Water	0.070		0.001
MAS	" "	Acid	0.070		8.200
Supplier E	Cold Face	Water	0.020		N.D.
MAS #2	" "	Acid	0.130		7.580
Supplier E	Hot Face	Water	0.040		N.D.
MAS #2	" "	Acid	1.140		7.840
Supplier B	Cold Face	Water	0.070	N.D.	
AS	" "	Acid	0.010	N.D.	
Supplier B	Hot Face	Water	0.100	N.D.	
AS	" "	Acid	0.140	N.D.	
Supplier B	Cold Face	Water	0.070	0.030	
LAS	" "	Acid	0.040	1.540	
Supplier B	Hot Face	Water	0.004	N.D.	
LAS	" "	Acid	0.200	1.560	
Host Core	Cold Face	Water	0.050	N.D.	
AS	" "	Acid	0.010	N.D.	
Host Core	Hot Face	Water	0.009	N.D.	
AS	" "	Acid	0.110	0.020	

N.D. = Not Detected
Blank = No Analysis

Table III.B.2.2. — Chemical Analyses After 100 Hours of Accelerated Corrosion Testing as Matrix Inserts

Sample	Position	Solution	% Na_2O	% Li_2O	% MgO
Supplier D	Cold Face	Water	0.090		0.020
MAS	" "	Acid	0.040		7.940
Supplier D	Hot Face	Water	0.110		0.010
MAS	" "	Acid	0.070		7.880
Supplier C	Cold Face	Water	0.060		0.002
MAS	" "	Acid	0.060		8.060
Supplier C	Hot Face	Water	0.070		0.002
MAS	" "	Acid	0.060		8.140
Supplier E	Cold Face	Water	0.030		0.001
MAS #2	" "	Acid	0.110		7.500
Supplier E	Hot Face	Water	0.050		0.001
MAS #2	" "	Acid	0.120		7.730
Supplier B	Cold Face	Water	0.090	0.005	
AS	" "	Acid	0.010	N.D.	
Supplier B	Hot Face	Water	0.120	N.D.	
AS	" "	Acid	0.130	0.020	
Supplier B	Cold Face	Water	0.090	0.040	
LAS	" "	Acid	0.030	1.520	
Supplier B	Hot Face	Water	0.030	N.D.	
LAS	" "	Acid	0.250	1.580	
Host Core	Cold Face	Water	0.050	0.003	
AS	" "	Acid	0.010	N.D.	
Host Core	Hot Face	Water	0.030	N.D.	
AS	" "	Acid	0.100	0.020	

N.D. = Not Detected
Blank = No Analysis

Table III.B.2.3. — Chemical Analyses After 150 Hours of Accelerated Corrosion Testing as Matrix Inserts

A second solution, the tested material dissolved in acid, was analyzed for selected constituents to determine the exchange, if of a detectable level, of material ions with sodium ions as a result of the accelerated corrosion test environment. This solution represents the bulk chemical composition of the experimental material, and the results of the analysis of this solution ideally will not be affected by the surface sodium chloride concentration.

Atomic absorption analysis detects ionic species, and the concentrations are reported in terms of a corresponding, stable oxide. The analyses carried out in this subtask were for sodium and magnesium in MAS materials and for sodium and lithium in AS compositions.

A comparison of Tables III.B.2.1, III.B.2.2, and III.B.2.3; representing 50, 100, and 150 hours, respectively, of accelerated corrosion testing of matrix inserts yields several pertinent observations. As is to be expected, the surface accumulation of salt (water solutions) increases with test time. This indicates a sodium chloride buildup on the core surfaces with test time.

The MAS and the AS materials, including the host core, seem to incorporate a small concentration of sodium into the lattice. This concentration appears to level off after 100 test hours. The Supplier B LAS, while superior in sodium resistance to previous LAS compositions, does not exhibit a leveling off of sodium pickup, but continues to evidence increasing bulk concentrations of sodium. Of interest is the diminished lithium concentration of the cold face of the Supplier B LAS material relative to the hot face, indicating that acid leaching at the cold face may be a more severe problem at 800°C (1472°F) than is ion exchange at the hot face. The MAS compositions generally appear to be quite resistant to sodium corrosion under these test conditions.

To aid in the evaluation of each material's reaction to the accelerated corrosion testing procedure, the thermal expansion behavior between room temperature and 800°C (1472°F) of the tested material is determined by differential dilatometry and compared to the original thermal expansion response. Those data, for the five matrix insert materials are graphically presented in Figures III.B.2.1 through III.B.2.5. Please note the scale differences among the figures.

An inspection of these figures indicates the relatively benign reaction of the MAS materials to airborne sodium chloride at 800°C (1472°F). The thermal expansion behavior of these materials (Figures III.B.2.1, III.B.2.2, and III.B.2.3) are essentially unchanged by exposure to the accelerated corrosion test conditions for a period of 150 hours.

The thermal expansions of the Supplier B-AS (Figure III.B.2.4) and the LAS material (Figure III.B.2.5) have both undergone significant changes as a result of 150 hours of exposure to accelerated corrosion testing as matrix inserts. Both materials have been made less contractive to the point where the LAS is slightly expansive. Evidently the sodium uptake by these materials results in a "stuffing" of the crystalline lattice due to the size disparity between the sodium and the lithium ions. This ionic replacement creates a lattice deformed by residual strain, thereby changing the reaction of the unit

cell to changes in temperature. The degree of this reaction is expected to vary directly with the amount of ion exchange incurred, explaining the more pronounced change in thermal expansion behavior experienced by the LAS material. Again, it is worthy of note that these differences, assuming no change in reaction mechanism, will become more pronounced with time.

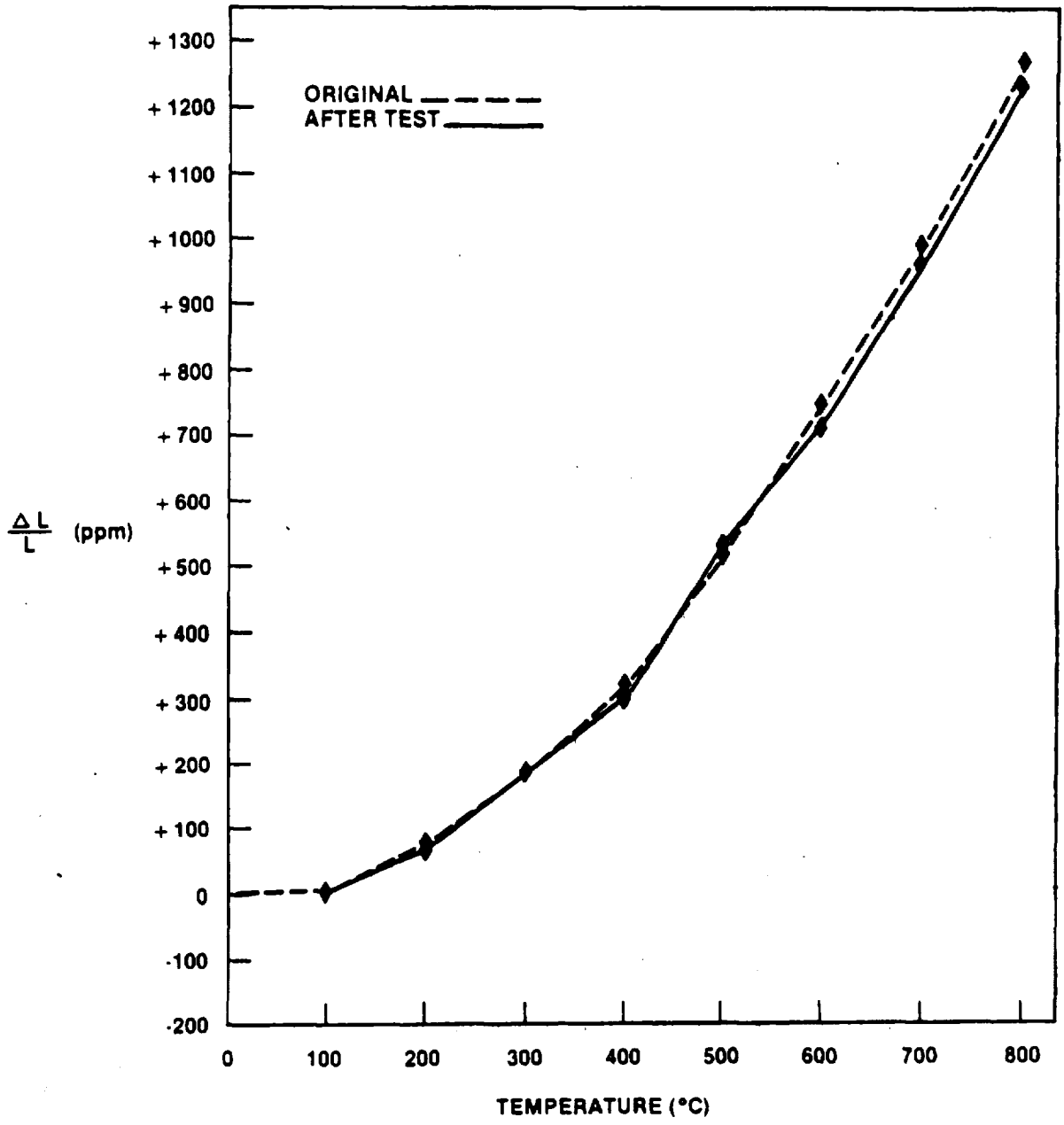

Fig. III.B.2.1. — Supplier D, MAS; Thermal Expansion Behavior Before and After 150 Hours of Accelerated Corrosion Testing as a Matrix Insert

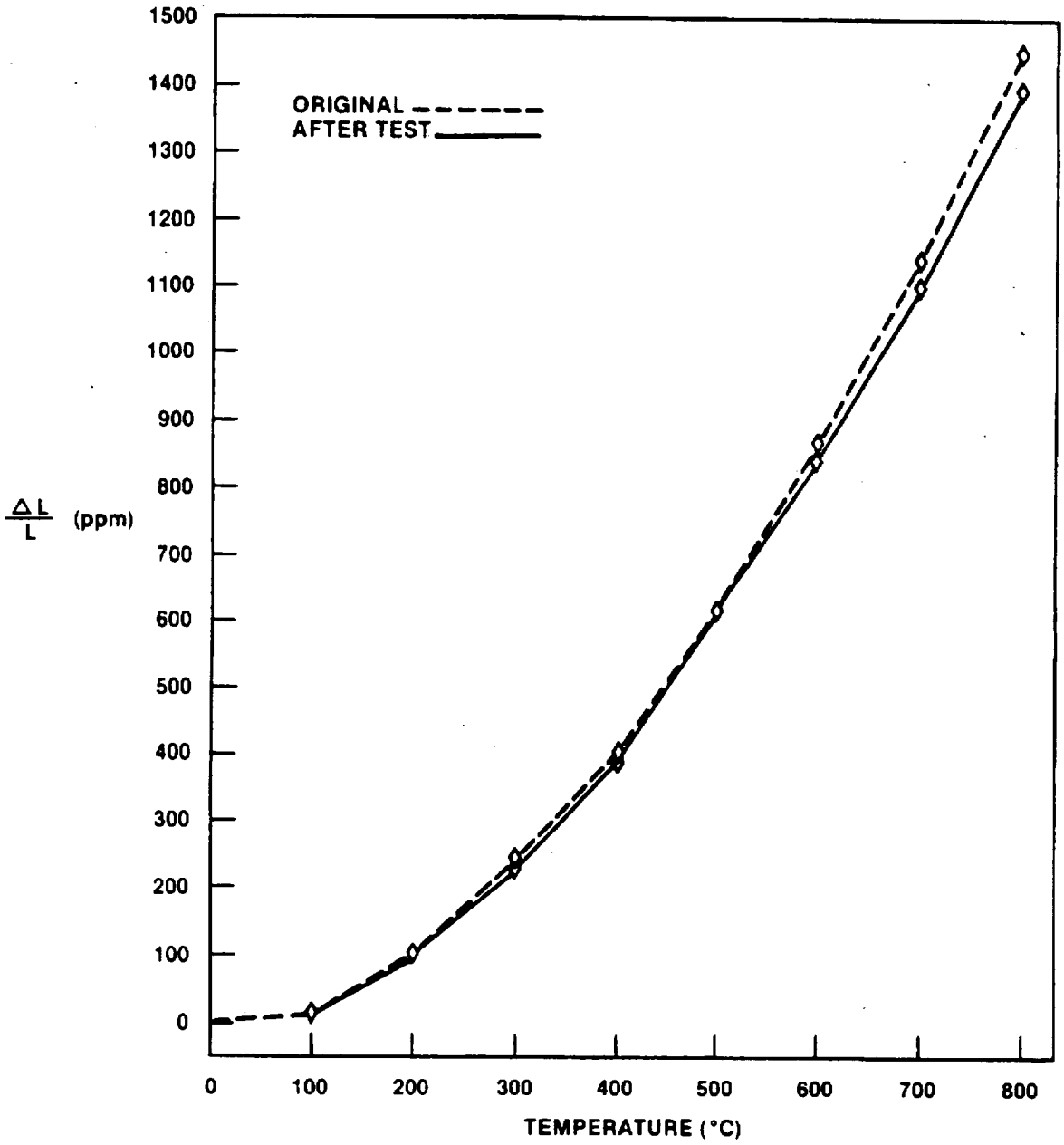

Fig. III.B.2.2. — Supplier C, MAS; Thermal Expansion Behavior Before and After 150 Hours of Accelerated Corrosion Testing as a Matrix Insert

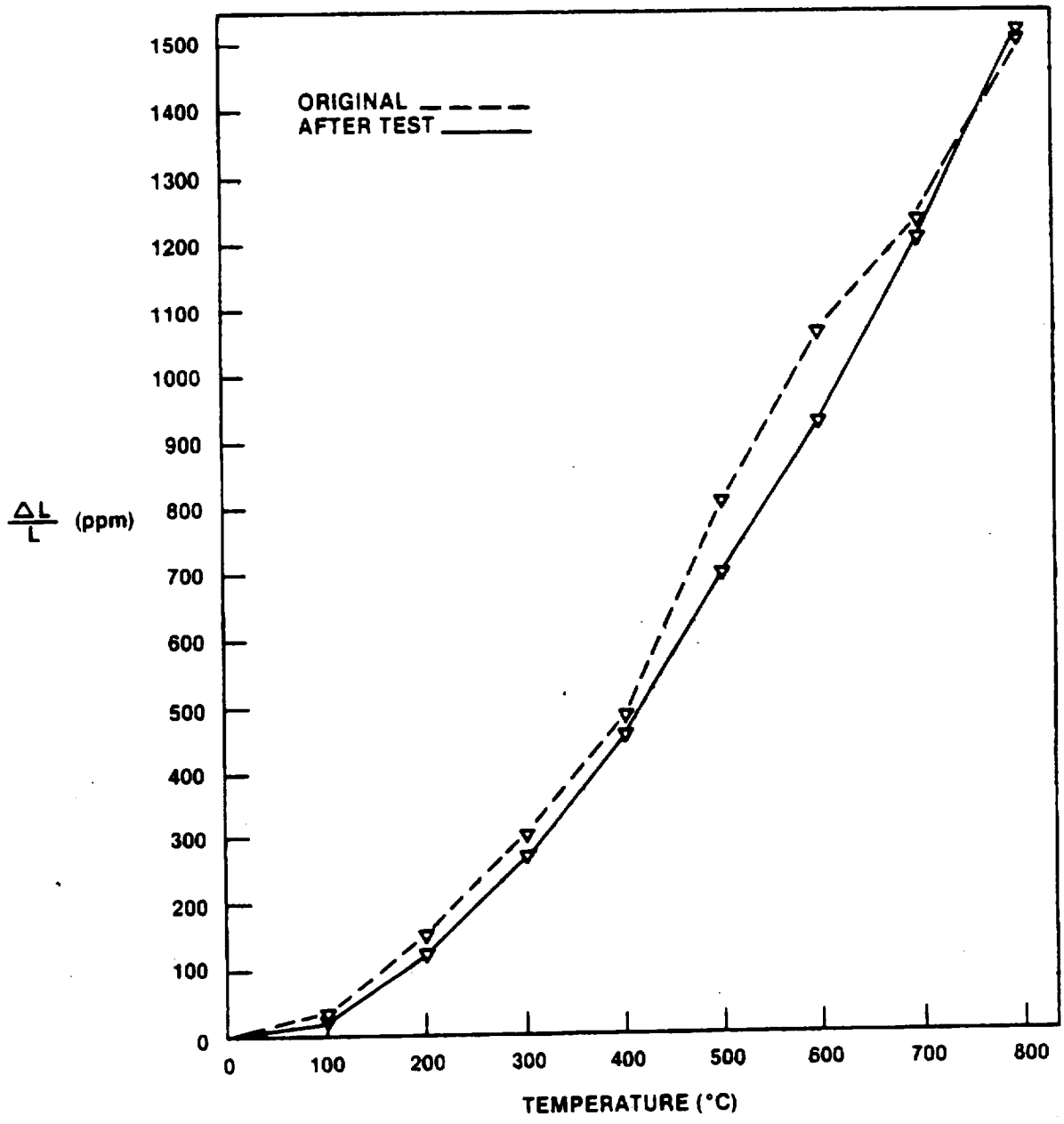

Fig. III.B.2.3. — Supplier E, MAS #2; Thermal Expansion Behavior Before and After 150 Hours of Accelerated Corrosion Testing as a Matrix Insert

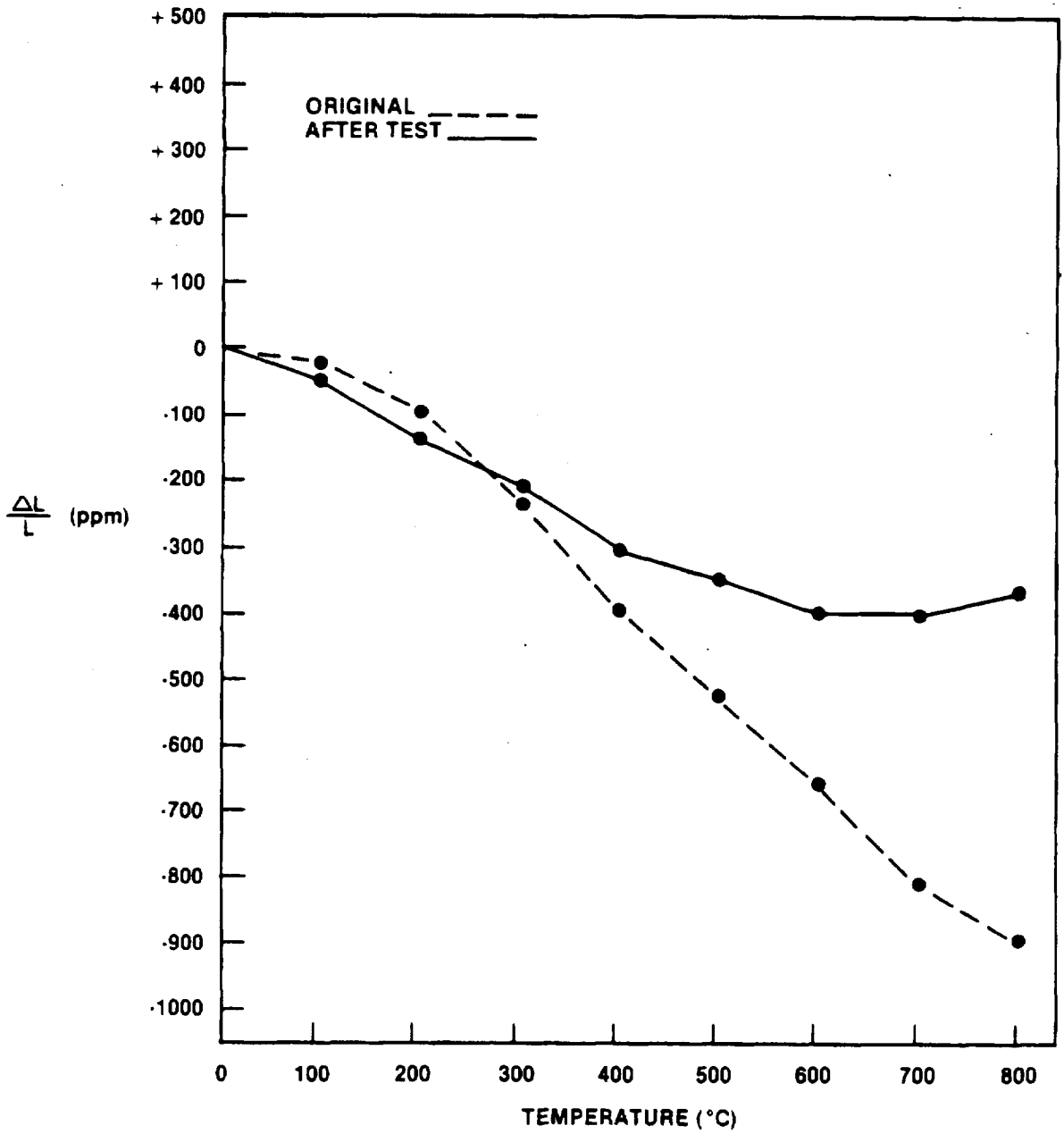

Fig. III.B.2.4. — Supplier B, AS; Thermal Expansion Behavior Before and After 150 Hours of Accelerated Corrosion Testing as a Matrix Insert

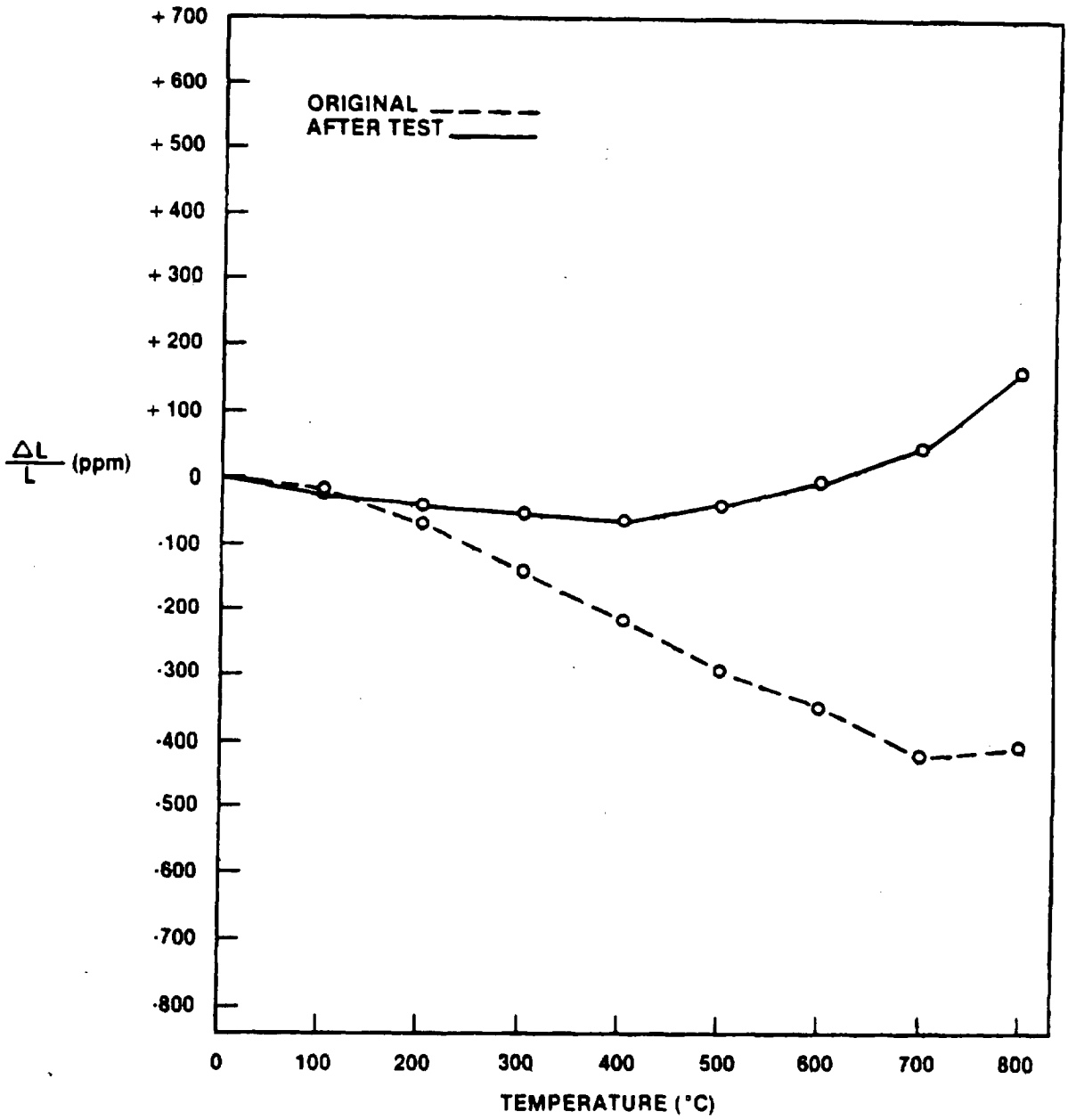

Fig. III.B.2.5. — Supplier B, LAS; Thermal Expansion Behavior Before and After 150 Hours of Accelerated Corrosion Testing as a Matrix Insert

III.B.3 Accelerated Corrosion Testing — Full Size Cores

As was reported at the end of the last period (Reference 6), two full size regenerator cores had been introduced into the accelerated corrosion testing program, utilizing the Ford 707 gas turbine engine modified to accommodate the aspiration of road salt. The first core tested, an MAS composition of Supplier D, has accumulated 250 hours of test time. During this reporting period, this core has completed the testing schedule and then has run for an additional 150 hours under the accelerated corrosion test conditions, as it was used as an engine core during the testing of other candidate materials.

The second full size test core, an MAS composition from Supplier C, failed during the initial stages of the testing program. This core did not appear to be properly densified during firing, and the failure encountered is not interpreted as a material shortcoming.

A third full size test core, an AS material from Supplier A fabricated in a thin-wall configuration, was introduced into the accelerated corrosion testing program during this reporting period, and the goal of 500 test hours was achieved. The chemical analyses (atomic absorption spectrophotometry) were completed during this reporting period and are tabularly reported for the MAS core of Supplier D (Table III.B.3.1) and the AS core (thin wall) of Supplier A (Table III.B.3.2). The analyses were carried out at 50 hour intervals; however, during periods of extraordinary salt ingestion, the test hours are doubly weighted. This condition occurred once in the course of the test cycle and was traced to a malfunction in the salt feed mechanism which resulted in continuous, rather than periodic, salt ingestion.

The chemical analyses for sodium and magnesium during the accelerated corrosion testing of a full size core of MAS from Supplier D are presented in Table III.B.3.1. The data indicate a salt build-up on the core surface with time, and the extreme deposition resulting from the equipment malfunction was indicated. These data were corrobated by visual inspections during the sampling procedure, as the salt build-up is quite discernible to the naked eye. It would appear that little or no sodium is being taken up by the material on the cold face side of the core. Except for the 500 hour sample, the sodium level appears to be constant with time. The 500 hour samples were taken after a heavy salt deposition period.

It appears that there is a more significant sodium incorporation into the material on the hot face side of the core. The relative sodium concentrations between the cold side and the hot side data support the contention that one should see more ion exchange at the elevated temperature. Perhaps the most dramatic statement of the test is the pragmatic observation that this MAS core survived 650 hours of accelerated corrosion testing without chemical or physical impairment. This testing was done after 1200 previous hours of engine testing to evaluate cold face acid attack. This core continues to function in a durability test engine having accumulated an additional 750 hours of engine time for a total of 2717 hours.

Sodium analyses during the accelerated corrosion testing of a full size core of the AS composition of Supplier A are presented in Table III.B.3.2. Experience during the matrix insert test program (Section III.B.2) indicated that analyzing for additional constituents was not necessary. The surface deposition of large quantities of sodium is indicated by the initial analyses of the water solutions. The initial test interval (60 hours) is doubly weighted due to excessive salt ingestion. The surface concentrations decrease during subsequent test periods and tend to become constant. Consistent with prior salt ingestion tests, the surface build-up of sodium chloride is more pronounced on the cold face of the regenerator core.

A comparison of the sodium levels in the bulk material indicate sodium uptake at both the cold face and the hot face of the material. The cold face concentrations are quite low compared to that found at the hot face. The concentrations at both faces increase with time. Again, it should be pointed out that this core survived the accelerated corrosion testing scheduling without any undue deterioration.

Test Time	Position	Solution	% Na_2O	% MgO
50 Hours	Cold Face	Water	0.070	0.023
50 Hours	Cold Face	Acid	0.048	7.660
50 Hours	Hot Face	Water	0.030	0.007
50 Hours	Hot Face	Acid	0.182	7.870
100 Hours	Cold Face	Water	0.100	0.032
100 Hours	Cold Face	Acid	0.050	7.720
100 Hours	Hot Face	Water	0.050	0.009
100 Hours	Hot Face	Acid	0.200	7.720
150 Hours	Cold Face	Water	0.130	0.040
150 Hours	Cold Face	Acid	0.040	7.660
150 Hours	Hot Face	Water	0.070	0.009
150 Hours	Hot Face	Acid	0.180	7.870
200 Hours	Cold Face	Water	0.240	0.040
200 Hours	Cold Face	Acid	0.030	7.810
200 Hours	Hot Face	Water	0.060	0.010
200 Hours	Hot Face	Acid	0.170	7.880
258 Hours	Cold Face	Water	0.250	0.040
258 Hours	Cold Face	Acid	0.030	7.830
258 Hours	Hot Face	Water	0.070	0.010
258 Hours	Hot Face	Acid	0.200	7.910
300 Hours	Cold Face	Water	0.380	0.040
300 Hours	Cold Face	Acid	0.030	7.800
300 Hours	Hot Face	Water	0.060	0.010
300 Hours	Hot Face	Acid	0.190	7.870
350 Hours	Cold Face	Water	0.190	0.030
350 Hours	Cold Face	Acid	0.030	7.850
350 Hours	Hot Face	Water	0.050	0.010
350 Hours	Hot Face	Acid	0.230	7.930
400 Hours	Cold Face	Water	0.190	0.030
400 Hours	Cold Face	Acid	0.030	7.930
400 Hours	Hot Face	Water	0.020	0.010
400 Hours	Hot Face	Acid	0.210	7.910
500 Hours	Cold Face	Water	0.370	0.010
500 Hours	Cold Face	Acid	0.270	7.720
500 Hours	Hot Face	Water	0.760	0.040
500 Hours	Hot Face	Acid	0.030	7.790
550 Hours	Cold Face	Water	0.680	0.040
550 Hours	Cold Face	Acid	0.030	7.750
550 Hours	Hot Face	Water	0.040	0.010
550 Hours	Hot Face	Acid	0.710	7.770
600 Hours	Cold Face	Water	0.790	0.040
600 Hours	Cold Face	Acid	0.030	7.740
600 Hours	Hot Face	Water	0.010	0.001
600 Hours	Hot Face	Acid	0.740	7.760
650 Hours	Cold Face	Water	0.670	0.040
650 Hours	Cold Face	Acid	0.030	7.810
650 Hours	Hot Face	Water	0.020	0.004
650 Hours	Hot Face	Acid	0.570	7.830

Table III.B.3.1. — Chemical Analyses of Supplier D-MAS Full Size Core During Accelerated Corrosion Testing

Test Time	Position	Solution	% Na_2O
120 Hours	Cold Face	Water	1.110
120 Hours	Cold Face	Acid	0.030
120 Hours	Hot Face	Water	1.480
120 Hours	Hot Face	Acid	0.070
170 Hours	Cold Face	Water	0.590
170 Hours	Cold Face	Acid	0.090
170 Hours	Hot Face	Water	0.030
170 Hours	Hot Face	Acid	3.030
220 Hours	Cold Face	Water	0.540
220 Hours	Cold Face	Acid	0.070
220 Hours	Hot Face	Water	0.020
220 Hours	Hot Face	Acid	2.620
270 Hours	Cold Face	Water	0.600
270 Hours	Cold Face	Acid	0.080
270 Hours	Hot Face	Water	0.010
270 Hours	Hot Face	Acid	3.310
320 Hours	Cold Face	Water	0.650
320 Hours	Cold Face	Acid	0.120
320 Hours	Hot Face	Water	0.020
320 Hours	Hot Face	Acid	2.830
370 Hours	Cold Face	Water	0.560
370 Hours	Cold Face	Acid	0.110
370 Hours	Hot Face	Water	0.020
370 Hours	Hot Face	Acid	2.790
420 Hours	Cold Face	Water	0.660
420 Hours	Cold Face	Acid	0.120
420 Hours	Hot Face	Water	0.015
420 Hours	Hot Face	Acid	2.760
500 Hours	Cold Face	Water	0.620
500 Hours	Cold Face	Acid	0.110
500 Hours	Hot Face	Water	0.015
500 Hours	Hot Face	Acid	3.040

Table III.B.3.2. — Chemical Analyses of Supplier A - AS Full Size Core During Accelerated Corrosion Testing

III.C. PROBLEM AREAS

There are no current problems with the materials screening tests.

III.D. FUTURE PLANS

Laboratory testing of the four new materials will be pursued. Additional matrix inserts and full-size regenerator cores will be tested under accelerated corrosion conditions, as they become available.

III.E. TASK SUMMARY

Four new materials (3-MAS, 1-LAS/MAS) have been introduced into the laboratory testing program. A second set of matrix inserts, representing 5 different materials (3-MAS, 1-LAS, 1-AS) have been analyzed subsequent to the completion of the accelerated corrosion testion program. The MAS materials were unaffected by the test, while the Supplier B LAS and AS materials both experienced some increase in thermal expansion. Two full sized regenerator cores (1-MAS, 1-AS thin-wall) successfully completed the accelerated corrosion testing program.

TASK IV AEROTHERMODYNAMIC PERFORMANCE

IV.A. INTRODUCTION

The matrix fin configuration selected for a given heat exchanger, under specific engine conditions, has a significant influence on the level of thermal stress and aerothermodynamic performance. In order to evaluate aerothermodynamic performance of prospective fin configurations, a shuttle rig was designed and fabricated (Section Q in Reference 1).

The essential parameters required for accurate heat exchanger performance prediction are the basic heat transfer (J= Stanton-Prandtl No. = Colburn No. = C_2RE^{X2}) and pressure drop (F = Fanning Friction Factor = C_1/RE) characteristics of the matrix fin geometry being evaluated as a function of a nondimensional flow parameter (RE = Reynold's No.). In order to obtain the basic heat transfer and pressure drop data, a transient technique similar to the "sliding drawer" technique described in Reference 7 was used. By determining the maximum slope of the fluid temperature difference curve during the cooling transient, the Colburn No. of the test matrix can be determined for each flow condition (Reynold's No.). The theoretical basis for this measurement technique is described in Reference 7.

In addition to the dependence on the maximum slope of the fluid temperature difference curve during the cooling transient, the level of the heat transfer characteristics (Colburn No.) is dependent on the fin parameter values utilized for data reduction. This was previously discussed in Section Q in Reference 1. Utilizing the present technique, the pertinent fin parameters required for data reduction are highly dependent on the accuracy of the wall density (ρW) value of the matrix material.

Since erroneous estimates of the fin parameters can introduce significant discrepancies in the F and J curves, an alternate set of heat transfer and pressure drop characteristics that eliminates the necessity of estimating fin parameters was derived (Section Q.6 of Reference 1). In addition, the alternate characteristics allow a direct comparison of test data from different sources, since a universal method of determining pertinent fin parameters is non-existent at this time.

IV.B. STATUS

The heat transfer and pressure drop characteristics for the thirty-three matrix fin configurations evaluated in the shuttle rig are listed on Tables IV.B.1. and IV.B.2. The present matrix sample size contains twenty-one rectangular (core no. 2. 3, 6, 8, 9, 12 thru 17, 21 thru 24, 28 thru 33), two hexagonal (core no. 26 and 27), eight sinusoidal (core no. 1, 5, 7, 10, 11, 19, 20 and 25) and two isosceles triangular (core no. 4 and 18) fin configurations. In addition, the present sample size represents a good cross-section of the different manufacturing processes which are currently being evaluated as follows:

1. Supplier A — Corrugating or extrusion
2. Supplier B — Stacked extruded tubes
3. Supplier C — Corrugating
4. Suppliers D and E — Calendering
5. Supplier I — Extrusion
6. Supplier J — Embossing or stamped sheets

CODE:

R — RECTANGULAR
I.T. — ISOSCELES TRIANGULAR
S.T. — SINUSOIDAL TRIANGULAR
H — HEXAGONAL

$$F = C_1 RE^{X_1}$$

$$J = C_2 RE^{X_2}$$

$$\frac{\Delta P.P}{L} = C \quad \frac{WT^{1.673}}{AF}$$

$$\frac{NTU}{L} = A \left[\frac{AFT^{0.673}}{W}\right] - X_2$$

CORE NO.	SUP-PLIER	TYPE OF FIN	X FINS/CM. (FINS/IN.)	Y ROWS/CM. (ROWS/IN.)	N HOLES/CM.2 (HOLES/IN.2)	S MM. (IN.)	D MM. (IN.)	H MM. (IN.)	PN MM. (IN.)	A.R. PN/H	ρ_w LB/CC.	L/DH	σ	DH MM. (IN.)	β M.2/M.3 (FT.2/FT.3)	C X 10^5	A X 10^2	C_1	X_1	C_2	X_2	J/F @ RE = 100	A_c CM.2 (IN.2)
1	A	S.T.	11.8 (29)	13.0 (33)	143 (924)	.100 (.0043)	.100 (.0043)	.889 (.0350)	1.813 (.0714)	2.75	2.20 (137.0)	121	873	.500 (.0232)	424 (1392)	1.30	4.85	13.4	- 1	3.34	- 1	.249	183 (18)
2	B	R	11.4 (29)	12.2 (31)	140 (888)	.193 (.0076)	.193 (.0076)	.627 (.0247)	.879 (.0346)	1.40	1.55 (97.0)	107	500	.655 (.0258)	3684 (1114)	1.23	4.11	14.0	- 1	4.19	- 1	.298	183 (18)
3	D	R	8.3 (21)	8.7 (22)	71.6 (462)	.216 (.0085)	.216 (.0085)	.940 (.0370)	1.211 (.0477)	1.29	1.40 (92.8)	72	600	.966 (.0381)	2765 (843)	84	2.18	14.9	- 1	4.18	- 1	.281	96 (15.2)
4	I	I.T.	15.8 (40)	9.1 (23)	142.8 (920)	.135 (.0053)	.135 (.0053)	.978 (.0382)	1.270 (.0500)	1.31	1.56 (97.1)	121	542	.888 (.0232)	4356 (1328)	1.11	5.11	10.8	- 1	3.83	- 1	.361	72 (11.2)
5	C	S.T.	9.8 (25)	15.4 (39)	151 (975)	.135 (.0053)	.135 (.0053)	.816 (.0263)	2.032 (.0800)	3.05	1.43 (89.8)	176	569	.401 (.0158)	5688 (1734)	2.25	10.2	9.1	- 1	.82	- 8	.171	183 (18)
6	D	R	6.9 (17.5)	7.5 (19)	51.5 (332)	.300 (.0118)	.300 (.0118)	1.936 (.0488)	1.450 (.0571)	1.48	1.47 (91.4)	67	618	1.092 (.0430)	2253 (687)	.815	1.86	10.7	- 1	4.28	- 1	.256	46 (7.1)
7	C	S.T.	5.1 (13)	6.3 (16)	32.2 (208)	.178 (.0070)	.178 (.0070)	1.419 (.0586)	3.086 (.1536)	2.77	1.51 (94.3)	53	737	1.315 (.0518)	2240 (683)	.33	17.4	10.6	- 1	.324	- 5	.174	183 (18)
8	E	R	4.1 (10.5)	14.4 (36.5)	59.4 (383)	.284 (.0112)	.213 (.0084)	.482 (.019)	2.418 (.0952)	8.0	2.40 (149.8)	89	611	.787 (.0310)	3183 (940)	1.10	3.85	10.4	- 1	8.65	- 1	.302	96 (9.3)
9	E	R	5.3 (13.5)	15.8 (39.5)	82.8 (533)	.306 (.015)	.229 (.009)	.411 (.0162)	1.86 (.074)	4.87	2.34 (146.3)	100	585	.645 (.0254)	3128 (954)	1.66	4.20	17.6	- 1	8.8	- 1	.287	101 (15.6)
10	A	S.T.	14.6 (37)	14.4 (36.5)	209.8 (1351)	.066 (.0026)	.066 (.0026)	.536 (.0240)	1.374 (.0841)	2.18	2.00 (130.4)	128	787	.548 (.0216)	5609 (1707)	1.66	5.9	10.3	- 1	3.29	- 1	.202	183 (18)
11	A	S.T.	6.3 (16)	10.2 (26)	64.6 (416)	.127 (.0050)	.127 (.0050)	.851 (.0335)	3.175 (.1250)	3.73	2.20 (137.3)	91	720	.775 (.0305)	3716 (1133)	.76	2.35	14.6	- 1	2.78	- 1	.192	183 (18)
12	A	R	7.5 (17.0)	7.1 (18)	49.6 (320)	.290 (.0114)	.290 (.0114)	1.123 (.0442)	1.427 (.0562)	1.27	1.67 (104.2)	82	634	1.130 (.0446)	2244 (684)	.46	1.75	10.5	- 1	5.0	- 1	.383	96 (15.2)
13	A	S	5.6 (14.2)	5.6 (14.2)	31.3 (202)	.274 (.0108)	.274 (.0108)	1.514 (.0596)	1.788 (.0704)	1.16	1.63 (101.6)	47	718	1.467 (.0566)	1896 (578)	.25	4.43	18.2	- 1	1.44	- .75	.256	96 (15.2)
14	E	R	8.1 (15.5)	8.3 (21)	58.5 (326)	.305 (.012)	.381 (.015)	.837 (.033)	1.84 (.0845)	1.99	2.39 (149.3)	78	567	1.82 (.0402)	2181 (665)	.82	2.3	13.9	- 1	8.12	- 1	.365	62 (9.6)
15	E	R	8.1 (15.5)	11.0 (28)	87.3 (434)	.100 (.0075)	.330 (.013)	.584 (.023)	1.638 (.0645)	2.85	2.34 (145.8)	85	558	.822 (.0324)	2711 (827)	1.00	6.04	18.7	- 1	1.88	- .87	.212	84 (9.8)
16	D	R	8.6 (18.8)	8.7 (17.0)	44.2 (286)	.315 (.0124)	.315 (.0124)	1.179 (.0464)	1.511 (.0567)	1.20	1.51 (94.2)	68	625	1.188 (.0467)	2186 (642)	44	1.30	17.1	- 1	4.18	- 1	.243	46 (7.1)
17	E	R	3.2 (8.0)	15.4 (39.0)	49.1 (312)	.388 (.0142)	.241 (.0085)	.609 (.0161)	3.175 (.125)	7.75	2.31 (144.4)	98	588	.713 (.0281)	3136 (887)	1.45	8.0	18.3	- 1	3.09	- .88	.293	84 (9.8)
18	A	I.T.	7.8 (20)	4.7 (12)	37.4 (240)	.257 (.0101)	.257 (.0101)	1.859 (.0732)	2.540 (.1000)	1.37	1.53 (95.5)	60	653	1.183 (.0458)	2244 (684)	.48	8.29	15.6	- 1	1.00	- .72	.233	101 (15.6)
19	A	S.T.	15.0 (38)	13.6 (34.5)	203.9 (1311)	.061 (.0024)	.061 (.0024)	.676 (.0266)	1.336 (.0526)	1.98	2.10 (131.0)	122	787	.570 (.0278)	5422 (1653)	1.38	8.68	18.1	- 1	3.94	- 1	.245	183 (18)
20	A	S.T.	18.8 (27.5)	14.6 (37)	157.4 (1018)	.066 (.0026)	.066 (.0026)	.620 (.0244)	1.846 (.0777)	2.88	2.18 (136.3)	107	788	.562 (.0233)	5264 (1605)	1.36	5.83	18.4	- 1	3.18	- 1	.195	96 (15.2)

Table IV.B.1 — Shuttle Rig Matrices (1-20).

CODE:

R — RECTANGULAR
I.T. — ISOSCELES TRIANGULAR
S.T. — SINUSOIDAL TRIANGULAR
H — HEXAGONAL

$F = C_1 RE^{X_1}$

$J = C_2 RE^{X_2}$

$$\frac{\Delta P.P}{L} = C \left(\frac{WT}{AF}\right)^{1.673}$$

$$\frac{NTU}{L} = A \left[\frac{AFT}{W}^{0.673}\right]^{-X_2}$$

CORE NO.	SUP-PLIER	TYPE OF FIN	X FINS CM	Y ROWS CM	N HOLES CM²	S MM (IN.)	B MM (IN.)	H MM (IN.)	PH MM (IN.)	AR PH H	Pw gM CC	L DH	σ	DH MM (IN.)	β M² M³	C X10⁵	A X10²	C_1	X_1	C_2	X_2	J/F @ RE-100	A_F CM² (IN.²)
			FINS IN.	ROWS IN.	HOLES IN.²						LB. FT.³				FT.² FT.³								
21	E	R	5.6 (14.3)	10 (25.3)	56.1 (362)	.223 (.0088)	.279 (.011)	.724 (.0285)	1.78 (.070)	2.45	2.02 (126.2)	71	.637	.991 (.0390)	2572 (784)	.62	4.70	17.1	−1	1.80	−.83	.222	103 (16)
22	E	R	3.9 (10)	15.4 (39)	60.5 (390)	.277 (.0109)	.208 (.0082)	.442 (.0174)	2.54 (.100)	5.75	2.29 (143.2)	94	.608	.739 (.0291)	3290 (1003)	1.28	4.20	18.8	−1	5.37	−1	.286	103 (16)
23	E	R	2.4 (6.2)	16.7 (42.3)	40.6 (262)	.381 (.015)	.191 (.0075)	.406 (.016)	4.09 (.161)	10.0	2.39 (149.1)	95	.618	.737 (.0290)	3355 (1023)	1.43	8.64	21.2	−1	1.62	−.81	.184	103 (16)
24	E	R	4.7 (12)	12.6 (32)	59.5 (384)	.417 (.0164)	.279 (.0110)	.516 (.0203)	2.12 (.0833)	4.10	1.94 (121.0)	89	.521	.790 (.0311)	2637 (804)	1.18	2.45	16.9	−1	4.17	−1	.247	103 (16)
25	C	S.T.	9.8 (25)	12.8 (32.5)	126 (813)	.183 (.0072)	.183 (.0072)	.599 (.0236)	2.03 (.0800)	3.39	2.33 (145.7)	153	.512	.417 (.0164)	4907 (1496)	2.4	4.3	9.4	−1	2.07	−1	.220	103 (16)
26	I	H	6.8 (17.3)	5.9 (15)	40.3 (260)	.323 (.0127)	.323 (.0127)	1.37 (.054)	1.47 (.058)	1.07	1.62 (101.3)	51	.656	1.37 (.054)	1912 (583)	.32	1.1	17.4	−1	4.48	−1	.257	46 (7.1)
27	B	H	15 (38.1)	13 (33)	195 (1260)	.071 (.0028)	.071 (.0028)	.699 (.0275)	.665 (.0262)	.95	2.05 (128)	101	.827	.699 (.0275)	4723 (1440)	.81	4.75	14.4	−1	4.0	−1	.278	46 (7.1)
28	A	R	7.9 (20)	7.9 (20)	62 (400)	.165 (.0065)	.165 (.0065)	1.105 (.0435)	1.27 (.050)	1.15	1.68 (104.6)	64	.756	1.105 (.0435)	2736 (834)	.37	1.85	15.1	−1	4.25	−1	.281	103 (16)
29	A	R	6.9 (17.5)	6.9 (17.5)	47.5 (306)	.279 (.011)	.279 (.011)	1.17 (.046)	1.45 (.057)	1.24	1.69 (105.6)	61	.653	1.17 (.0462)	2227 (679)	.38	1.75	15.1	−1	5.25	−1	.348	103 (16)
30	J	R	4.3 (11.0)	7.9 (20)	34.1 (220)	.752 (.0295)	.452 (.0178)	.818 (.0322)	2.31 (.0909)	2.82	1.85 (115.3)	59	.435	1.07 (.0422)	1624 (495)	.72	.93	15.9	−1	3.49	−1	.219	103 (16)
31	J	R	4.3 (11)	6.7 (17)	29 (187)	.706 (.0278)	.635 (.0250)	.859 (.0338)	2.31 (.0909)	2.69	1.86 (115.8)	62	.398	1.12 (.0440)	1424 (434)	.85	.94	18.7	−1	4.19	−1	.224	103 (16)
32	J	R	8.5 (21.5)	8.3 (21)	70.1 (452)	.257 (.0101)	206 (.0081)	1.00 (.0395)	1.18 (.0465)	1.21	2.08 (129.5)	59	.649	.963 (.0379)	2696 (822)	.67	2.0	17.8	−1	4.06	−1	.228	46 (7.1)
33	D	R	10.6 (27)	13.8 (35)	146.5 (945)	.284 (.0112)	.142 (.0056)	.584 (.023)	.94 (.0370)	1.61	1.42 (88.8)	113	.560	.617 .0243	3628 (1106)	1.50	4.1	14.1	−1	3.97	−1	.282	103 (16)

Table IV.B.2 — Shuttle Rig Matrices (21-33).

During this report period the wall densities (ρW) for matrices 28, 29, 30, 31 and 33 were measured. Consequently, the pertinent fin parameters required for complete data reduction were determined for these matrices.

Matrix samples 28 (Figure IV.B.1) and 29 (Figure IV.B.2) were extruded by Supplier A. The standard performance characteristics, which are based on the actual geometric opening with the wall thickness factored out, are illustrated on Figures IV.B.3 and IV.B.4, respectively. The alternate heat transfer and pressure drop characteristics, which are based on measured test data, are shown on Figures IV.B.5 and IV.B.6 for matrices 28 and 29, respectively.

Matrices 30 (Figure IV.B.7) and 31 (Figure IV.B.8) were fabricated by Supplier J. These samples, which consist of layered stamped sheets, represent the initial attempt to evaluate the effect of interrupting the flow in the axial direction (wavy flow passage). The stamping dies were machined to attain an equivalent rib height (H) and spacing (PH) for each structure. Unlike the straight thru flow passage of matrix 30, a wavy flow passage (Figure IV.B.9) was incorporated for matrix 31.

Figures IV.B.10 and IV.B.11 illustrate the standard performance characteristics for matrices 30 and 31, respectively. The alternate performance characteristics are shown on Figures IV.B.12 and IV.B.13.

The wavy flow passage incorporated in matrix 31 (Figure IV.B.9) resulted in an increase in L/DH of approximately 3%. The effect of interrupting the flow can be estimated by comparing the laminar flow pressure drop (C_1) and heat transfer (C_2) constants for matrices 30 and 31 from Table IV.B.2. Matrix 31 indicates an increase of 20% for the heat transfer constant (C_2) when compared to the straight-thru passage of matrix 30. Concurrently, the wavy flow passage increased the pressure drop constant (C_1) 17.5%. the net result is that the wavy flow passage increased the overall fin efficiency (C_2/C_1) by 2%.

For gas turbine applications,engine horsepower (HP) and specific fuel consumption (SFC) are affected by regenerator pressure drop and heat transfer efficiency, respectively. If SFC is a more important factor for a given engine application, then the wavy flow passage is beneficial. Conversely, the wavy flow passage would be detrimental if HP were the most important consideration.

Matrix 33 (Figure IV.B.14) from Supplier D was fabricated by the calendering method from tooling similar to that used for matrix 2. The standard and alternate heat transfer and pressure drop characteristics are shown on Figure IV.B.15 and IV.B.16, respectively. As expected the standard performance characteristics (Figure IV.B.15) are equivalent to matrix 2 within experimental accuracy.

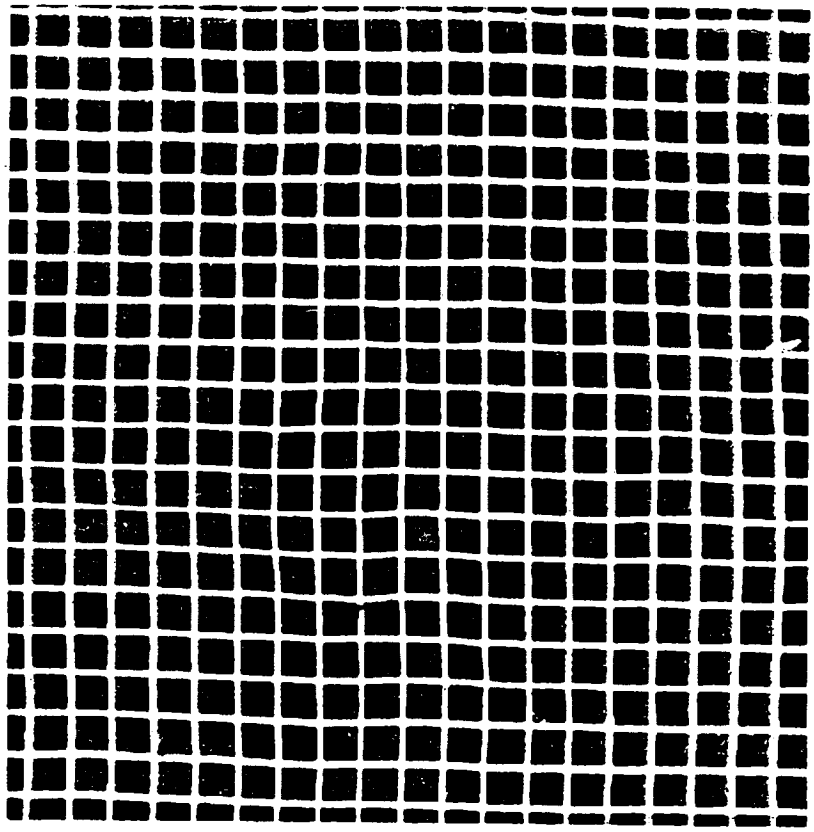

Figure IV.B.1 — Photograph of Matrix 28.

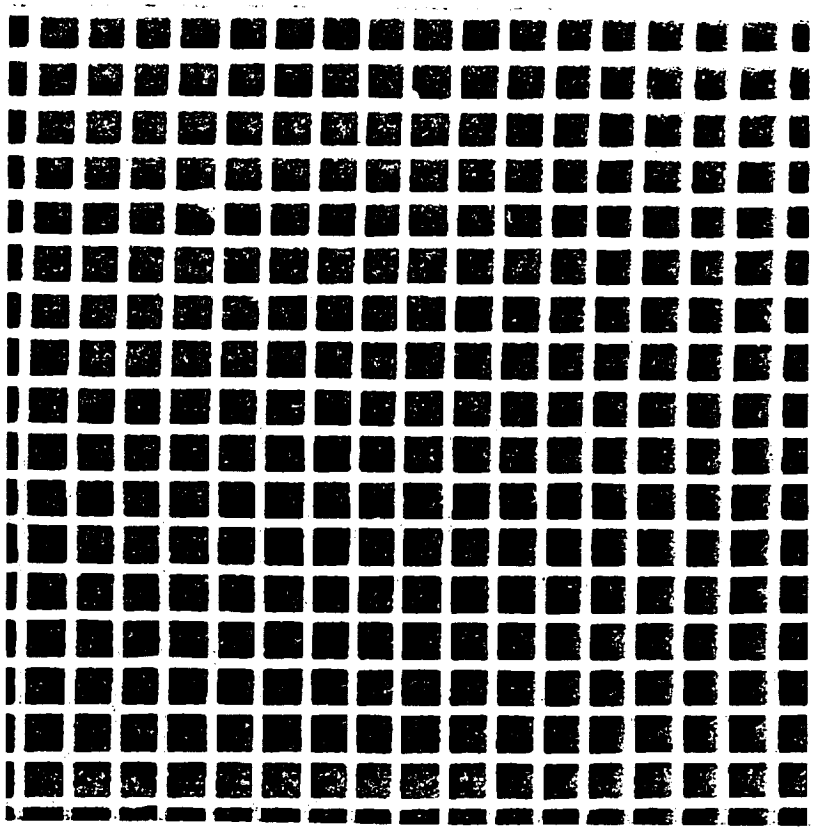

Figure IV.B.2 — Photograph of Matrix 29.

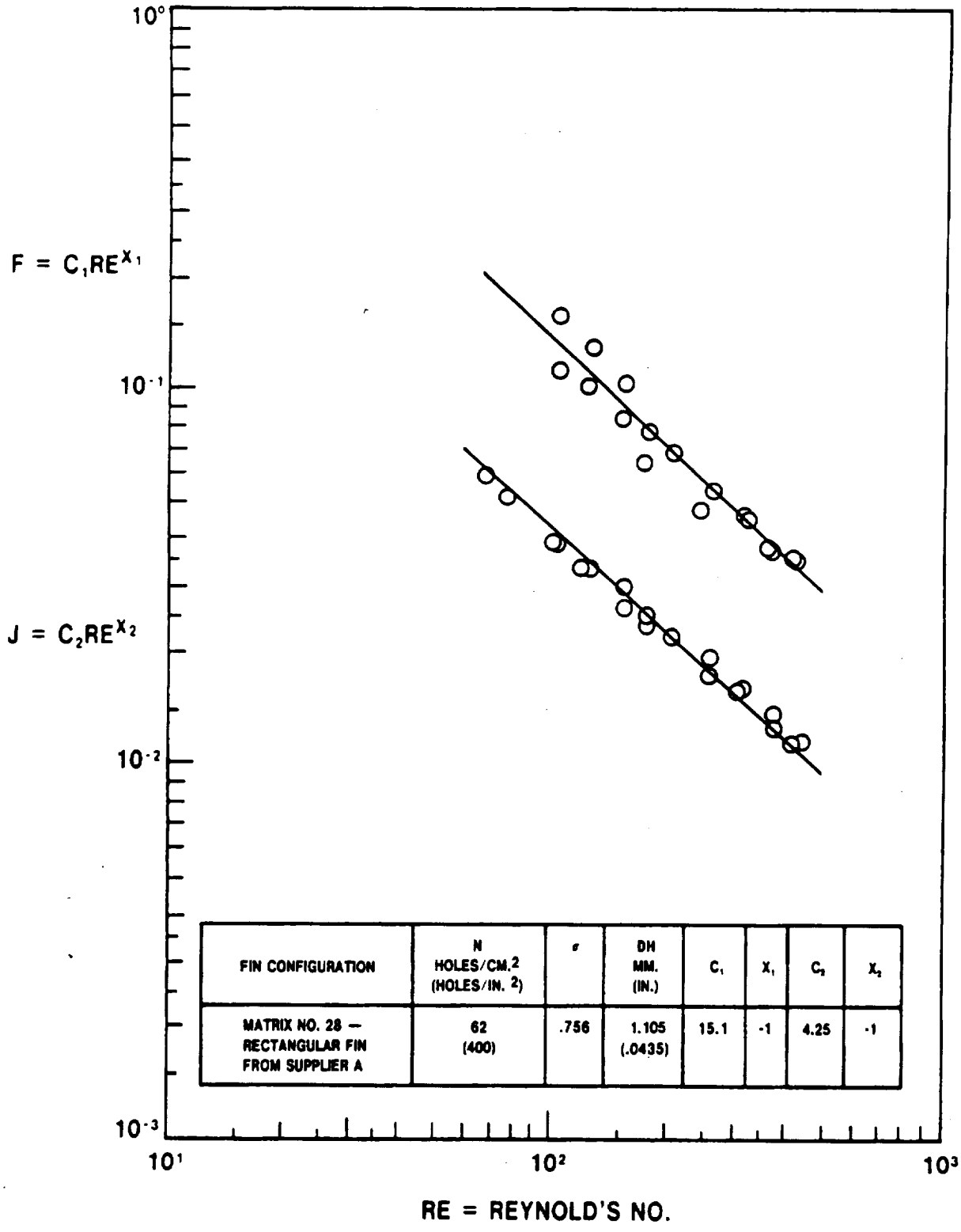

FIN CONFIGURATION	N HOLES/CM.^{2} (HOLES/IN. ^{2})	σ	DH MM. (IN.)	C_1	X_1	C_2	X_2
MATRIX NO. 28 — RECTANGULAR FIN FROM SUPPLIER A	62 (400)	.756	1.105 (.0435)	15.1	-1	4.25	-1

Figure IV.B.3 — Standard Heat Transfer and Pressure Drop Characteristics for Matrix 28.

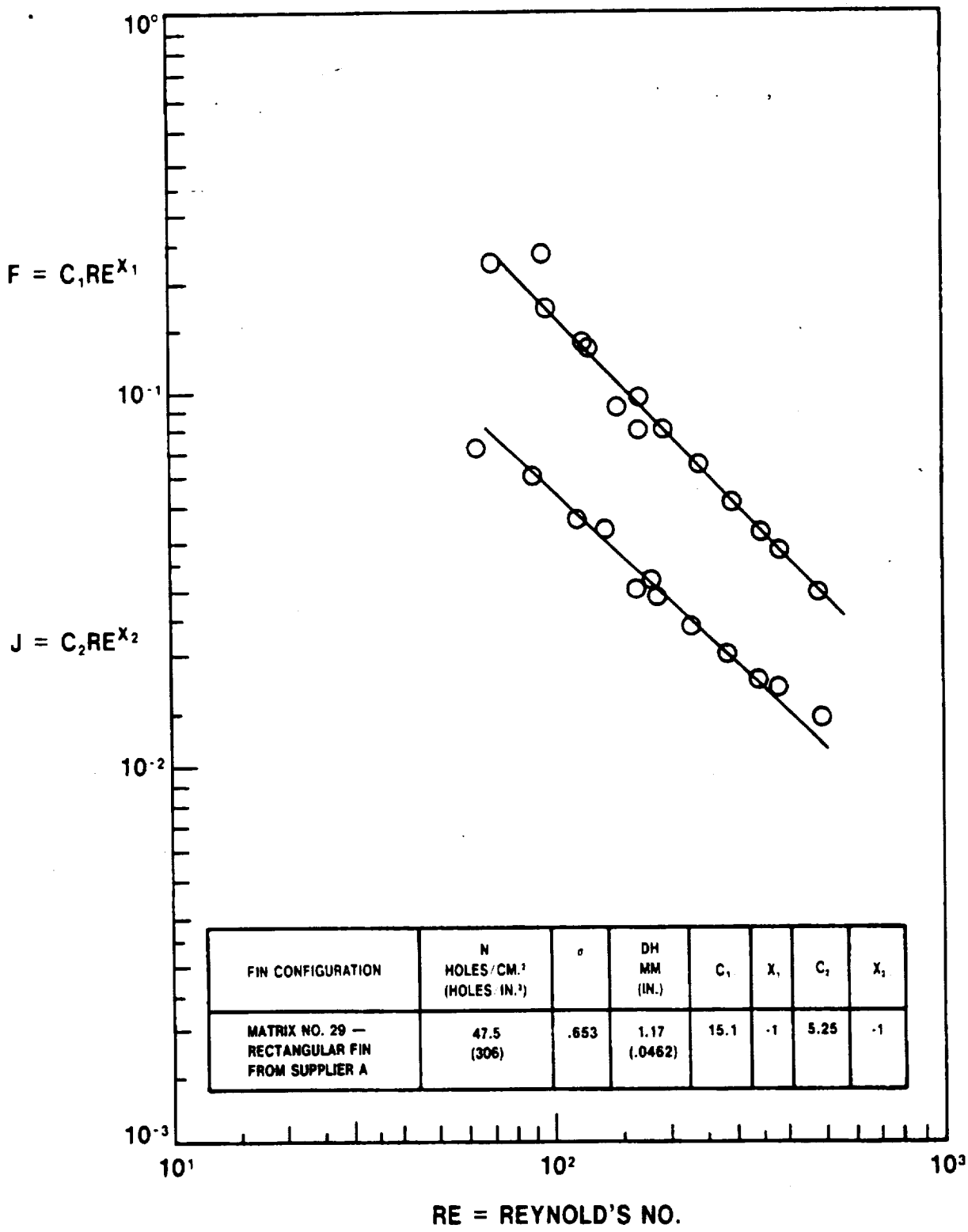

FIN CONFIGURATION	N HOLES/CM.² (HOLES IN.²)	σ	DH MM (IN.)	C_1	X_1	C_2	X_2
MATRIX NO. 29 — RECTANGULAR FIN FROM SUPPLIER A	47.5 (306)	.653	1.17 (.0462)	15.1	-1	5.25	-1

Figure IV.B.4 — Standard Heat Transfer and Pressure Drop Characteristics for Matrix 29.

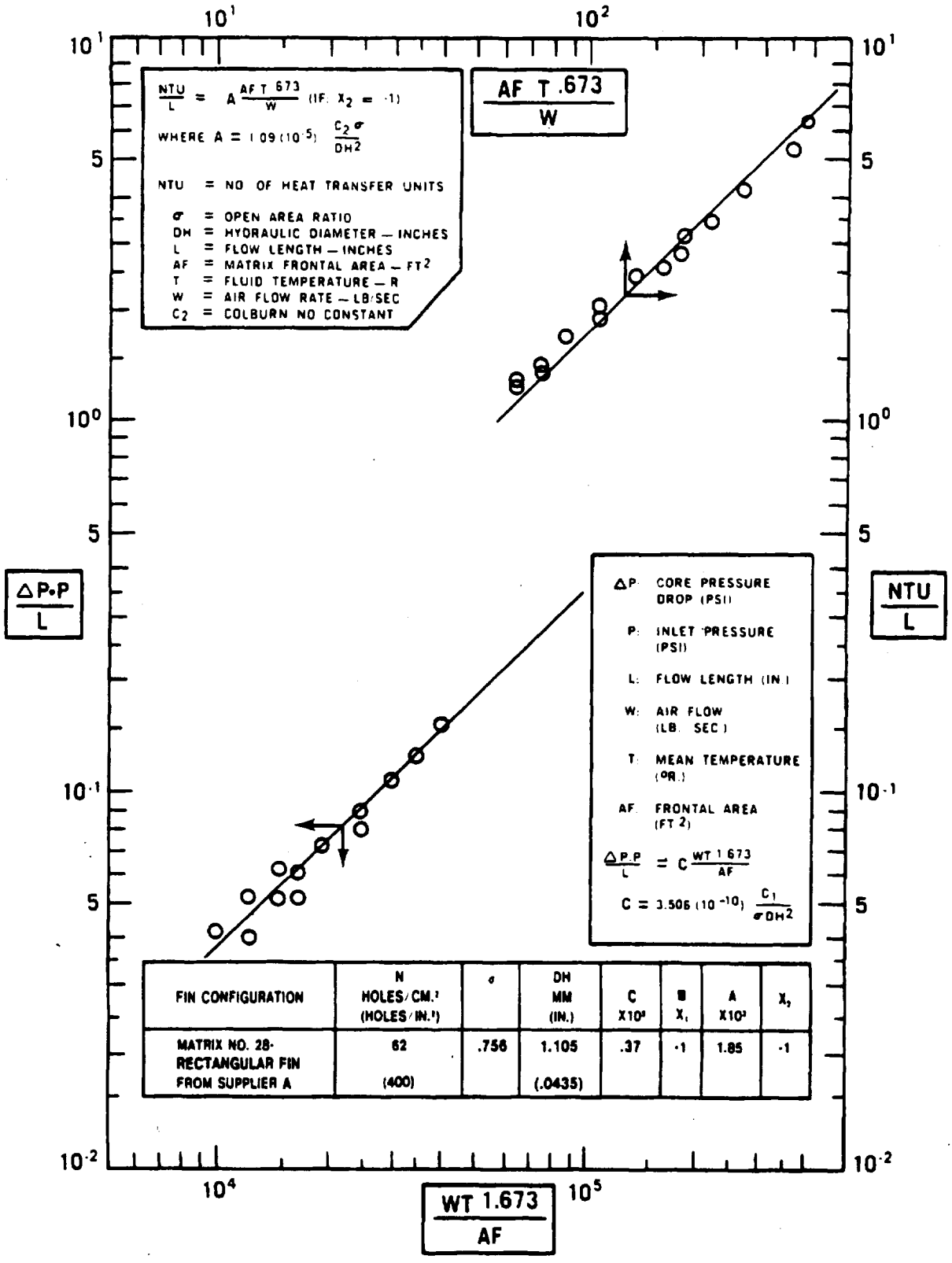

Figure IV.B.5 — Alternate Heat Transfer and Pressure Drop Characteristics for Matrix 28.

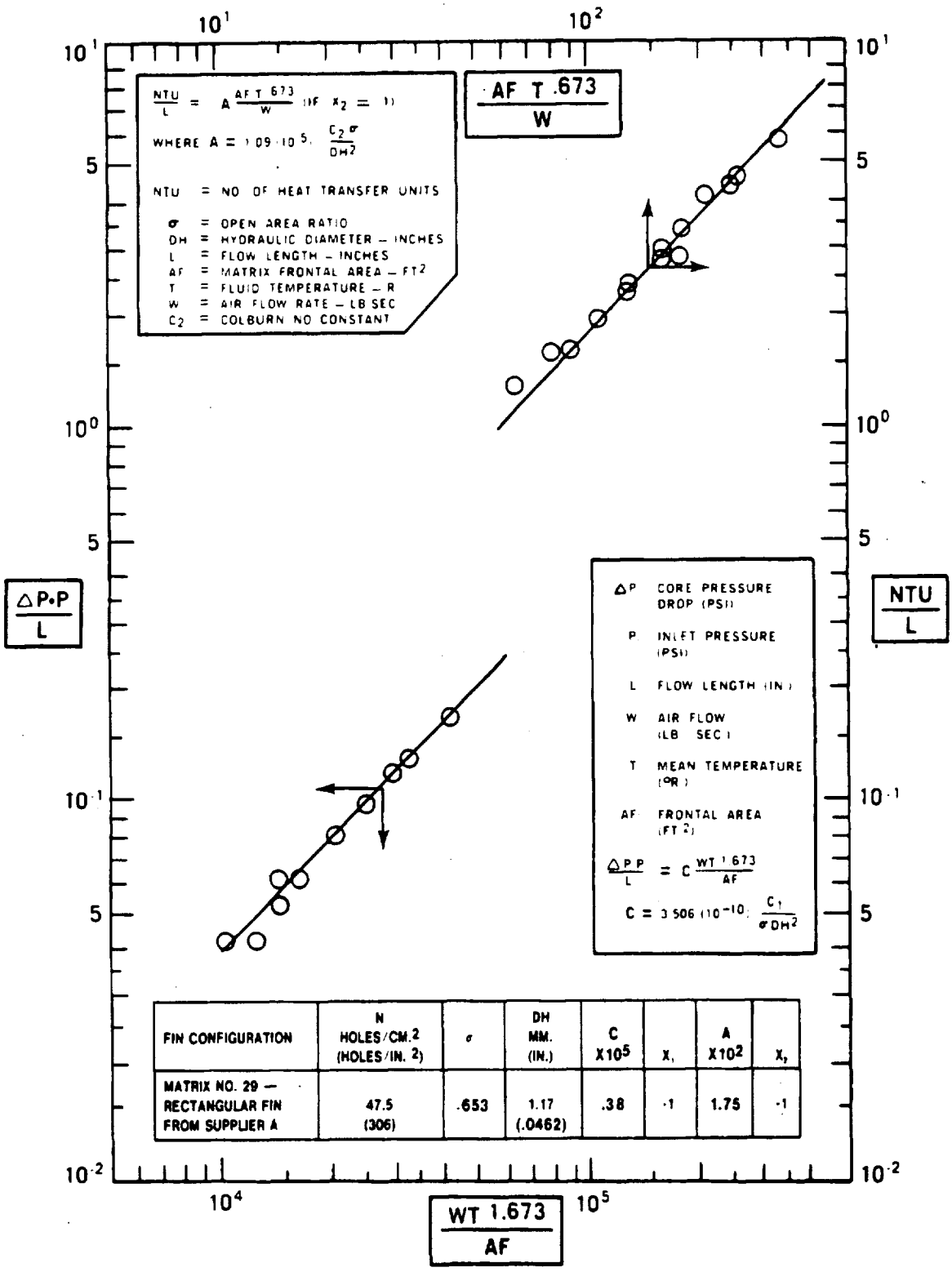

FIN CONFIGURATION	N HOLES/CM.² (HOLES/IN.²)	σ	DH MM. (IN.)	C X10⁵	X_1	A X10²	X_2
MATRIX NO. 29 — RECTANGULAR FIN FROM SUPPLIER A	47.5 (306)	.653	1.17 (.0462)	.38	·1	1.75	·1

Figure IV.B.6 — Alternate Heat Transfer and Pressure Drop Characteristics for Matrix 29.

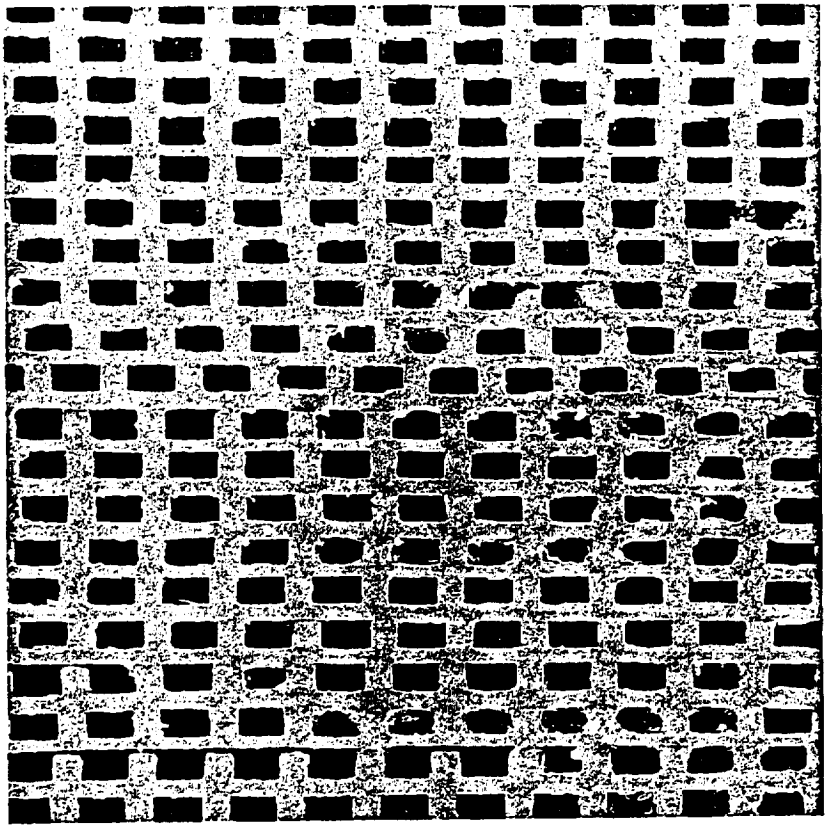

Figure IV.B.7 — Photograph of Matrix 30.

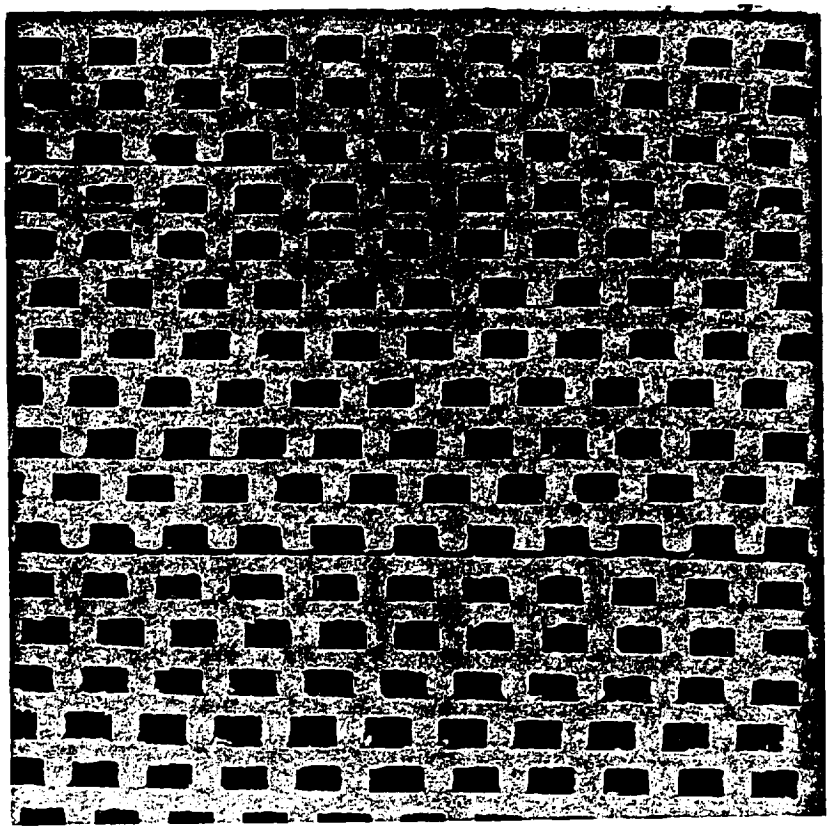

Figure IV.B.8 — Photograph of Matrix 31.

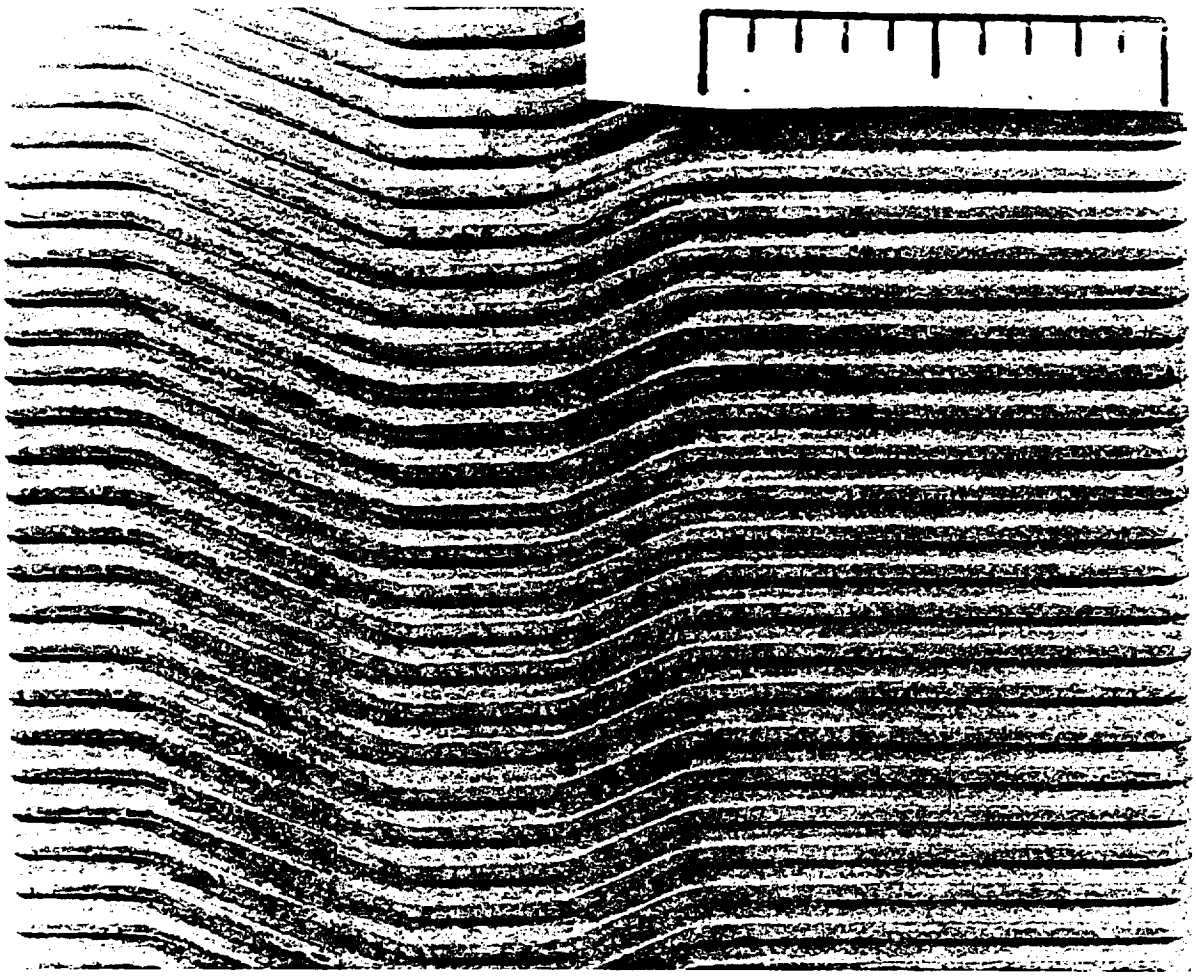

Figure IV.B.9 — Matrix 31 Wavy Flow Passage.

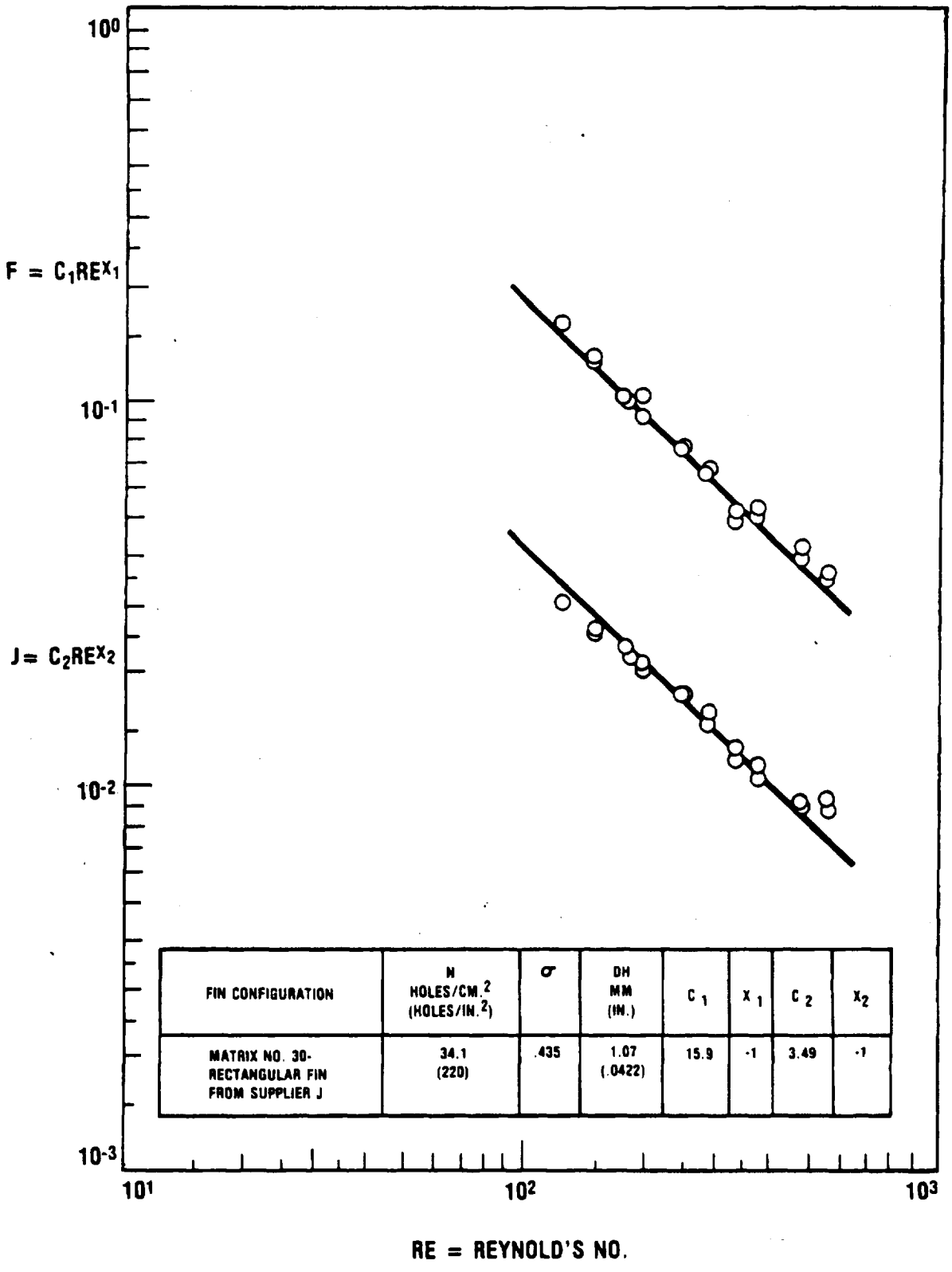

FIN CONFIGURATION	N HOLES/CM.^{2} (HOLES/IN.^{2})	σ	DH MM (IN.)	C_1	X_1	C_2	X_2
MATRIX NO. 30-RECTANGULAR FIN FROM SUPPLIER J	34.1 (220)	.435	1.07 (.0422)	15.9	-1	3.49	-1

Figure IV.B.10 — Standard Heat Transfer and Pressure Drop Characteristics for Matrix 30.

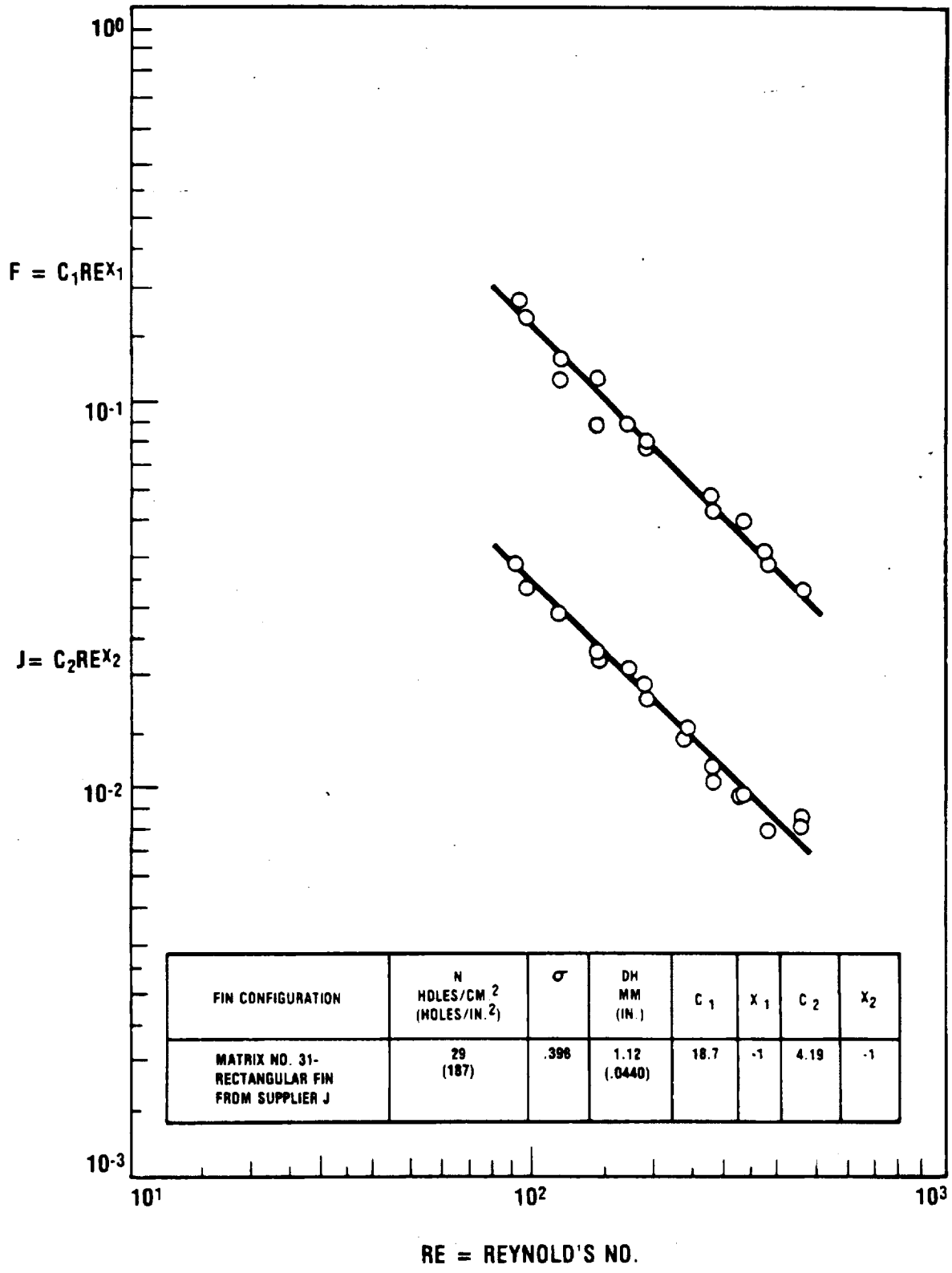

FIN CONFIGURATION	N HOLES/CM ^{2} (HOLES/IN.^{2})	σ	DH MM (IN.)	C_1	X_1	C_2	X_2
MATRIX NO. 31- RECTANGULAR FIN FROM SUPPLIER J	29 (187)	.396	1.12 (.0440)	18.7	-1	4.19	-1

Figure IV.B.11 — Standard Heat Transfer and Pressure Drop Characteristics for Matrix 31.

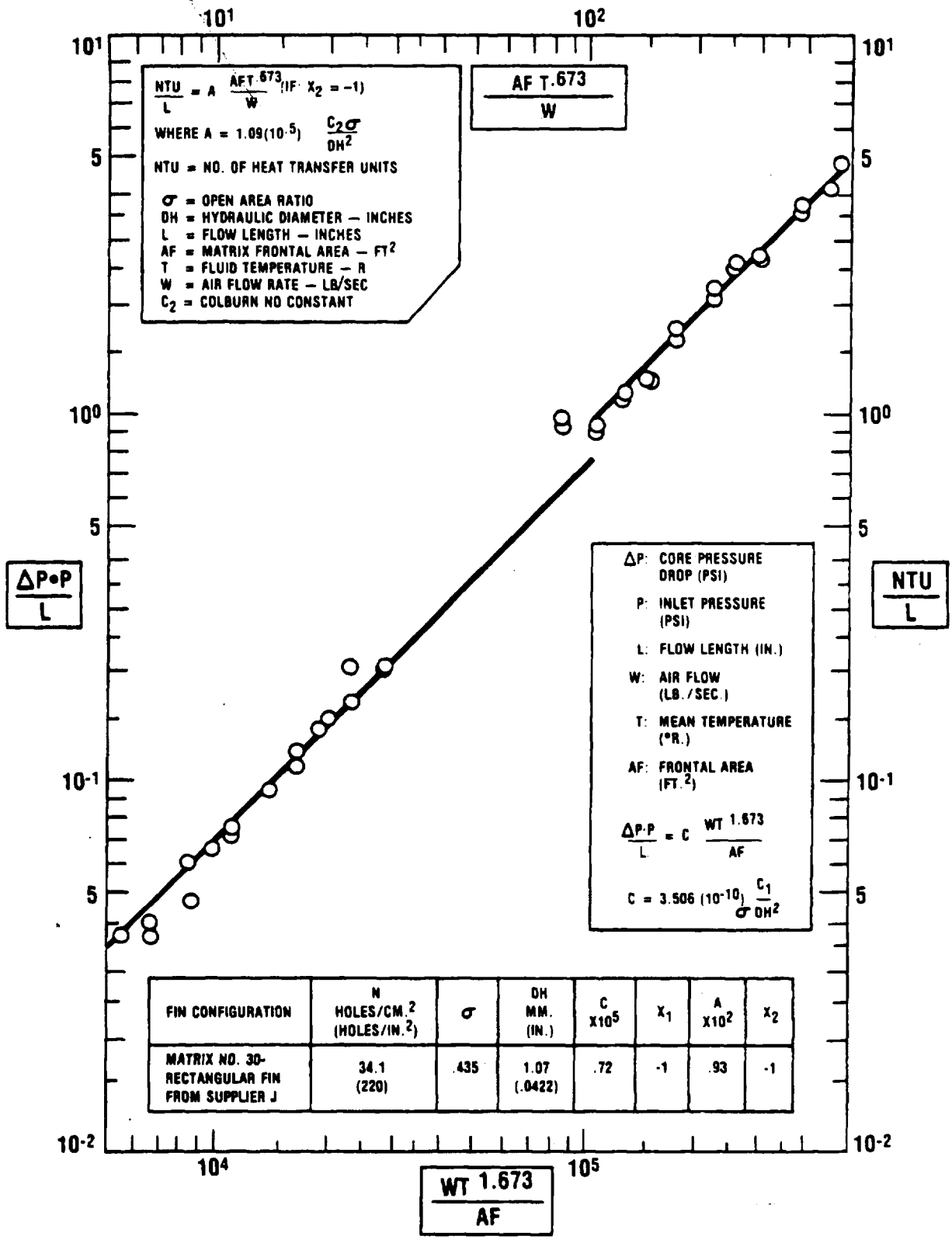

FIN CONFIGURATION	N HOLES/CM.^{2} (HOLES/IN.^{2})	σ	DH MM. (IN.)	C $X10^5$	X_1	A $X10^2$	X_2
MATRIX NO. 30-RECTANGULAR FIN FROM SUPPLIER J	34.1 (220)	.435	1.07 (.0422)	.72	-1	.93	-1

Figure IV.B.12 — Standard Heat Transfer and Pressure Drop Characteristics for Matrix 30.

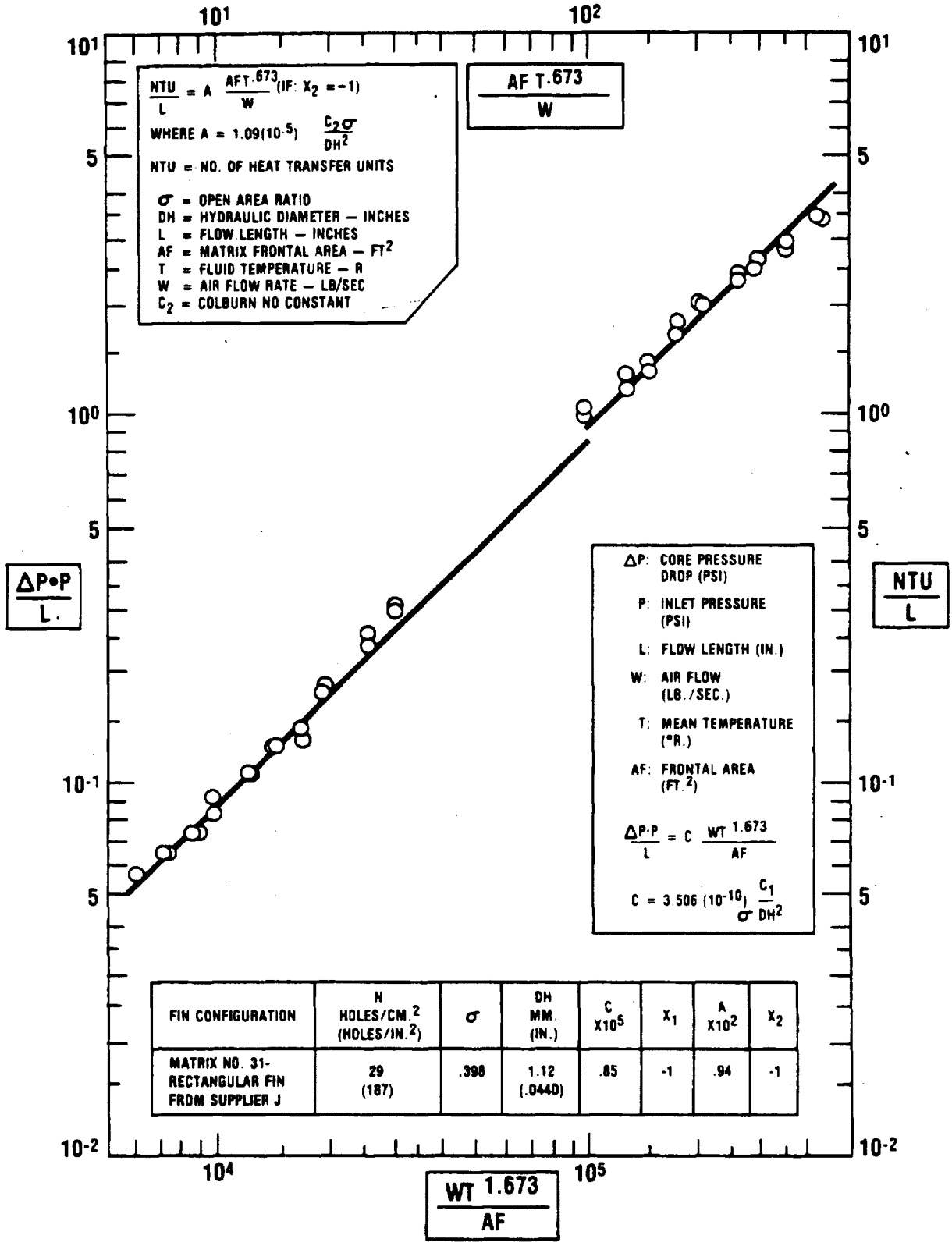

FIN CONFIGURATION	N HOLES/CM.^{2} (HOLES/IN.^{2})	σ	DH MM. (IN.)	C $X10^5$	X_1	A $X10^2$	X_2
MATRIX NO. 31- RECTANGULAR FIN FROM SUPPLIER J	29 (187)	.398	1.12 (.0440)	.85	-1	.94	-1

Figure IV.B.13 — Standard Heat Transfer and Pressure Drop Characteristics for Matrix 31.

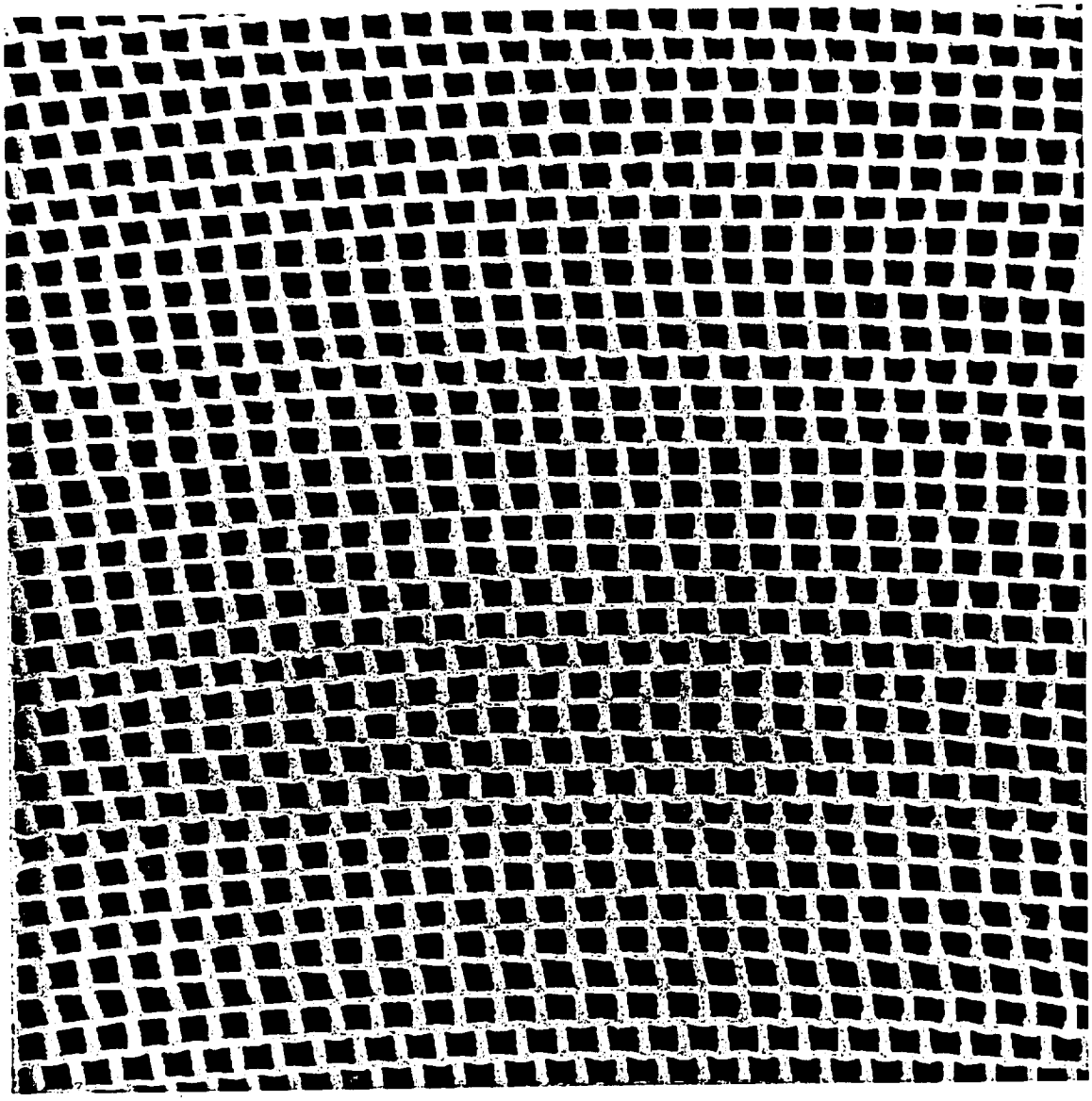

Figure IV.B.14 — Photograph of Matrix 33.

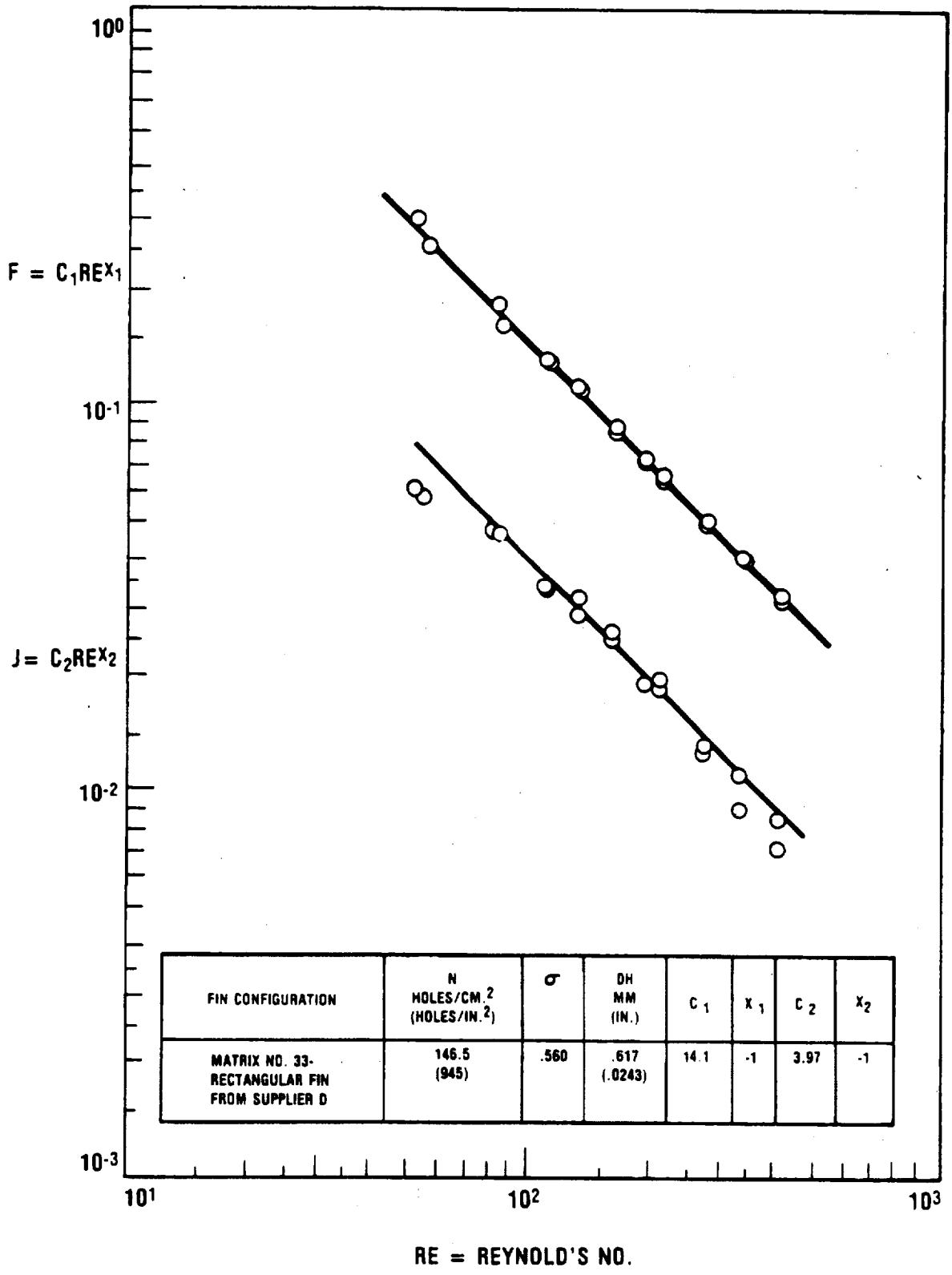

FIN CONFIGURATION	N HOLES/CM.^{2} (HOLES/IN.^{2})	σ	DH MM (IN.)	C_1	X_1	C_2	X_2
MATRIX NO. 33- RECTANGULAR FIN FROM SUPPLIER D	146.5 (945)	.560	.617 (.0243)	14.1	-1	3.97	-1

Figure IV.B.15 — Standard Heat Transfer and Pressure Drop Characteristics for Matrices 32, 3 and 21.

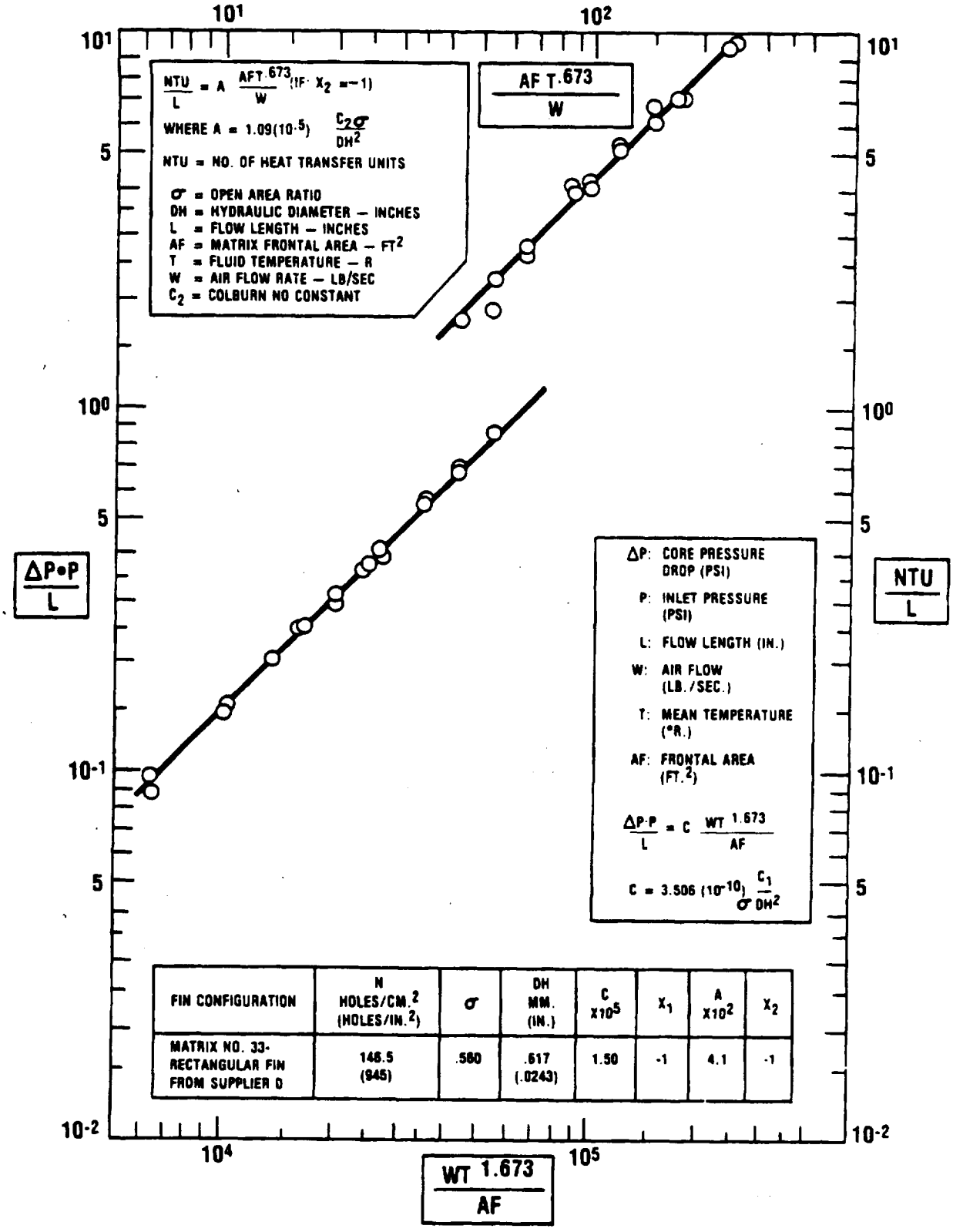

FIN CONFIGURATION	N HOLES/CM.² (HOLES/IN.²)	σ	DH MM. (IN.)	C X10⁵	X_1	A X10²	X_2
MATRIX NO. 33- RECTANGULAR FIN FROM SUPPLIER D	146.5 (945)	.580	.617 (.0243)	1.50	-1	4.1	-1

Figure IV.B.16 — Standard Heat Transfer and Pressure Drop Characteristics for Matrices 32, 3 and 21.

IV.C. PROBLEM AREAS

No major problems exist at this time.

IV.D. FUTURE PLANS

An additional matrix from Supplier J has been received for evaluation during the next report period. Additional matrices are expected from Supplier A and I.

IV.E. TASK SUMMARY

A total of thirty-three matrix fin configurations have been tested at the present time. Twenty-one rectangular, eight sinusoidal, two isosceles triangular and two hexagonal configurations comprise the present matrix sample size.

The first attempt to evaluate the effect of a wavy flow passage was completed during this report period. The wavy flow passage increased the heat transfer and pressure drop characteristics 20% and 17.5%, respectively for a 2% improvement in overall fin efficiency.

TASK V. DESIGN STUDIES OF ADVANCED REGENERATOR SYSTEMS

V.A. INTRODUCTION

Since 1973, design studies of ceramic heat exchanger systems have been carried out in order to analytically evaluate the thermal and structural performance of the various supplier's matrices and to compare different drive, mounting, seal and stress relief schemes. Two types of rotary heat exchangers have been studied: a regenerator sized for the Ford 707 gas turbine engine and a preheater sized for the Ford Stirling engine. The regenerator has a 710 mm (28.2 in) outside diameter and is 77 mm (2.86 in) thick. The preheater has a 460 mm (18.04 in) outside diameter, a 190 mm (7.50 in) inside diameter, and is 41 mm (1.6 in) thick. These ceramic heat exchanger systems have been analyzed for temperature inlet conditions of 800°C (1472°F) and 1000°C (1832°F) (Ref. 1,2). Task V of the NASA/Ford Ceramic Regenerator Program deals with design studies emphasizing regenerator system materials and configurations intended to improve aero-thermo-dynamic performance, reduce thermal stress, and provide for higher temperature operation.

V.B. STATUS

Flexure strength and elastic modulus data for Supplier D MAS-2 regenerator material was initially reported in Reference 5. In order to more accurately characterize the structural integrity of the Supplier D MAS-2 material, test specimens from two additional matrices were evaluated utilizing the four-point bend test. A statistical analysis of the modulli of elasticity (MOE) and rupture (MOR) provides an estimate of the core-to-core variation in matrix strain tolerance (MOR/MOE) which may be expected.

A Weibull failure distribution at a 90% confidence band was determined for each type of specimen from each of the three regenerator cores using a Ford time-sharing library computer program. This program uses a least squares approximation if a statistically significant difference existed between the Weibull distributions for the three different cores. This program uses a two-sided test for significance at the 0.1% level.

Table V.B.1 lists the median B_{10} and B_{50} values of radial and tangential MOR and MOE for the three cores evaluated. Significant differences in the Weibull distributions between cores would seem to be the result of processing variations rather than fundamental material property differences. In light of this, the Weibull distribution was determined for the aggregate data from the three cores to provide an estimate of the greatest range of properties that may be expected. This information is plotted in Figures V.B.1 through V.B.4 and the B_{10} and B_{50} values are listed in Table V.B.2.

In Reference 5, the results of statistical analyses of the radial and tangential MOE and MOR in addition to radial compressive strength of specimens cut from several Supplier A thin-wall aluminum silicate regenerator cores incorporating a sinusoidal triangular fin with a wall thickness of .061 mm (.0024 in.) were reported. As reported in Section I.B.4 this structure has experienced separations in the elastomer-matrix bond area due to the significant reduction in strength associated with the thinner cross-section of the matrix walls. In order to characterize this structure more completely, the tangential shear strength of the matrix was investigated.

CORE NO.	MOR — KPa (PSI) B_{10}	MOR — KPa (PSI) B_{50}	MOE x 10^{-6} — KPa (PSI) B_{10}	MOE x 10^{-6} — KPa (PSI) B_{50}	STRAIN TOLERANCE — PPM B_{10}	STRAIN TOLERANCE — PPM B_{50}
TANGENTIAL ORIENTATION						
1	2067 (300)	2756 (400)	3.38 (.49)	5.34 (.775)	612	516
2	1378 (200)	1929 (280)	5.60 (.813)	6.03 (.875)	245	320
3	1964 (285)	2584 (375)	7.33 (1.064)	7.92 (1.15)	268	326
RADIAL ORIENTATION						
1	1378 (200)	2343 (340)	2.05 (.298)	2.49 (.362)	671	939
2	923 (134)	1516 (220)	2.20 (.319)	3.03 (.44)	420	500
3	785 (114)	1654 (240)	2.76 (.400)	3.24 (.470)	285	511

Table V.B.1 — Statistical Evaluation of Supplier D MAS-2 Physical Properties

Four shear specimens cut from a Supplier A thin-wall regenerator were tested. The test results for the limited number of specimens (Figure V.B.5) indicate an average tangential shear strength of 393 KPa (57 PSI).

For the purpose of calculating the shear stress imposed on a regenerator core by the drive system, we can assume the regenerator to be rigidly clamped at the seal mid-width, and subject to a torque equal to the seal drag torque, which is assumed to be 700 ft.-lb. during a cold start. The maximum shear stress is then estimated to be 131 KPa (19 PSI).

This would indicate that the specimens tested provide a safety factor of 3 against shear failure. A general statement concerning the resistance of the thin-wall matrix to shear stress failure cannot be made, since the number of specimens tested was too small to provide a meaningful statistical evaluation of shear strength.

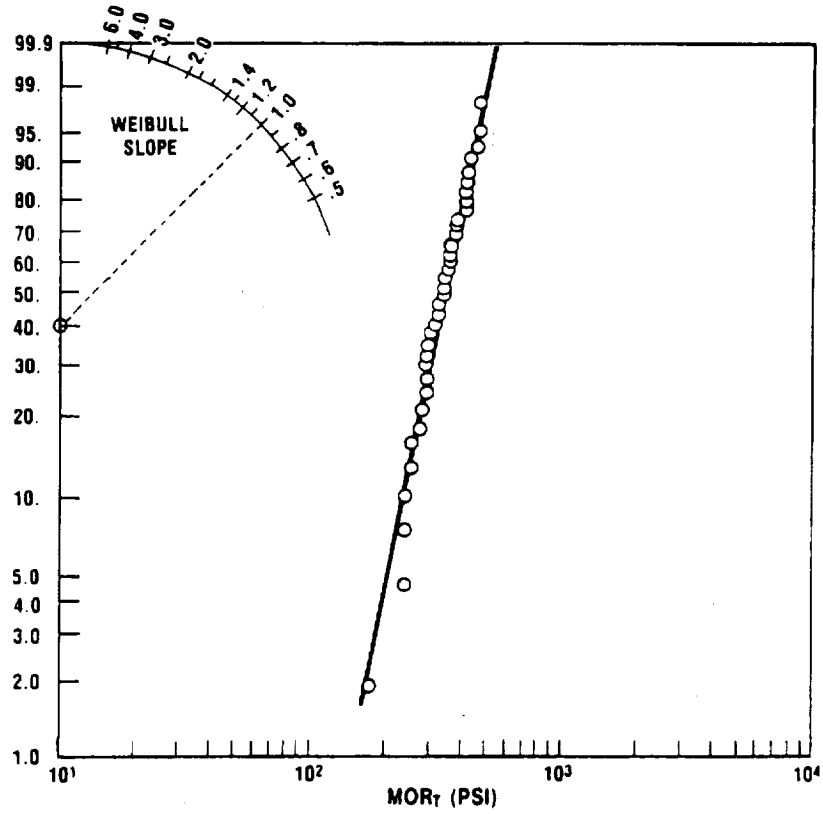

Figure V.B.1 — Supplier D MAS-2 Tangential MOR

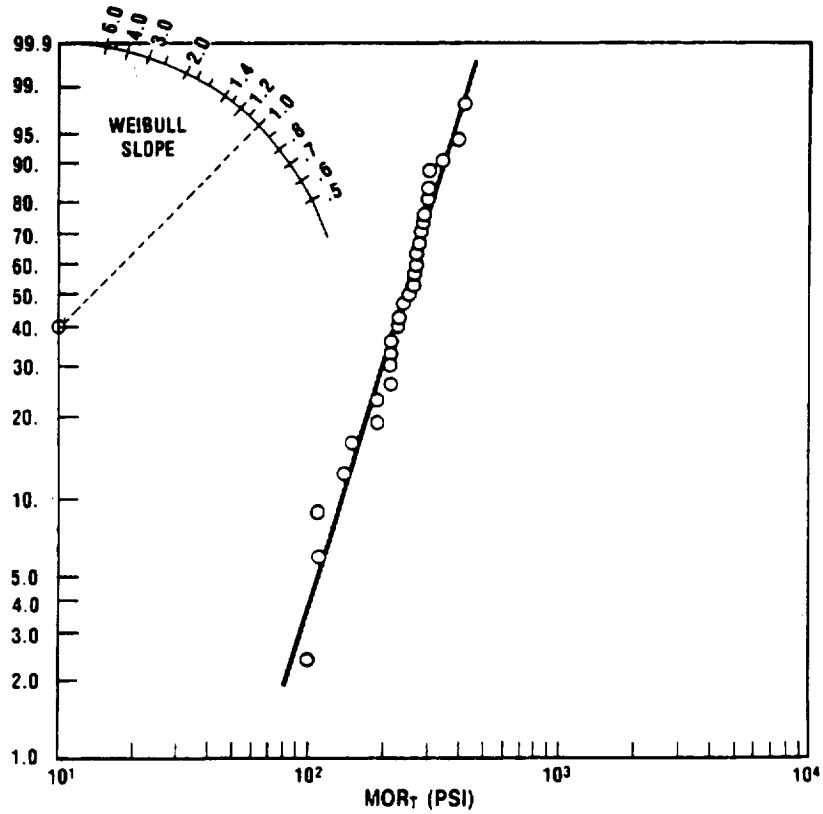

Figure V.B.2 — Supplier D MAS-2 Radial MOR

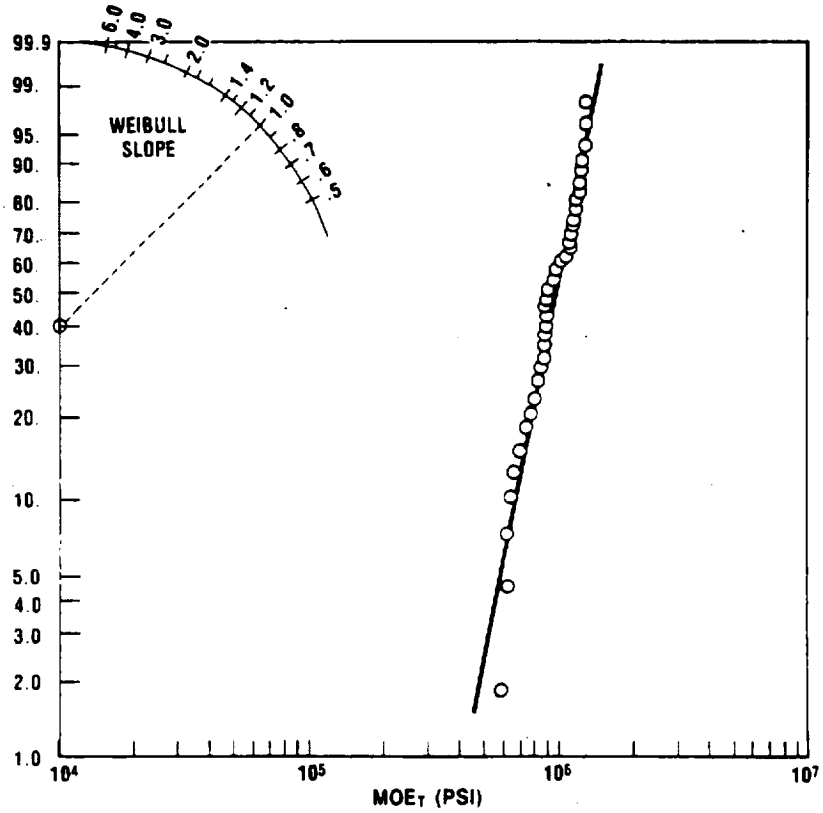

Figure V.B.3 — Supplier D MAS-2 Tangential MOE

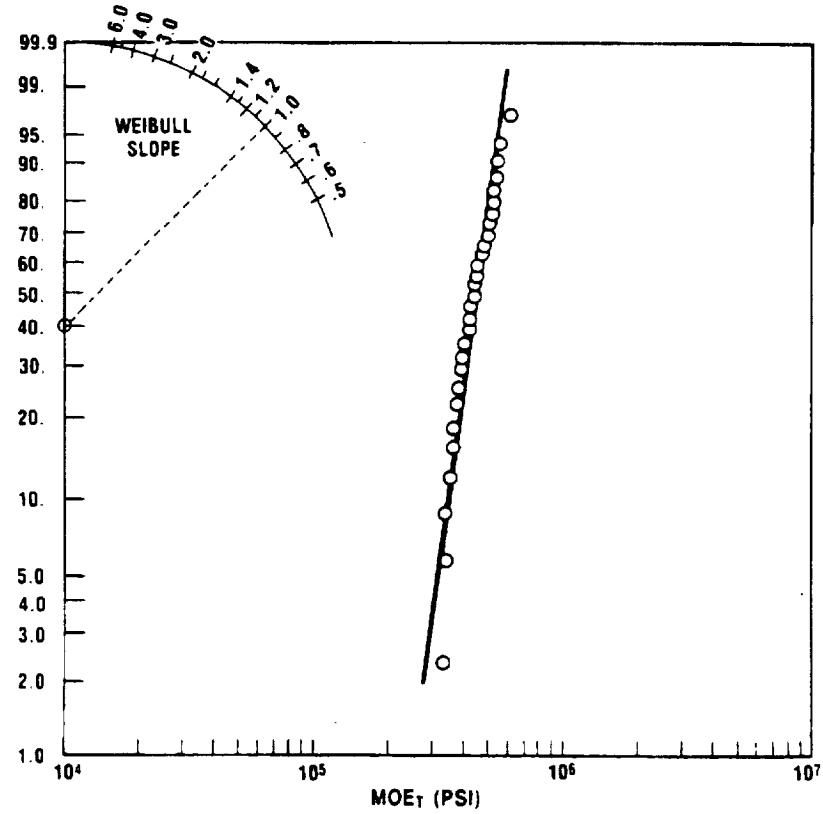

Figure V.B.4 — Supplier D MAS-2 Radial MOE

CODE:

R — RECTANGULAR
I.T. — ISOSCELES TRIANGULAR
S.T. — SINUSOIDAL TRIANGULAR
H — HEXAGONAL
W — WRAPPED
C — CORRUGATED
EX — EXTRUDED
EM — EMBOSSED

SUP-PLIER	TYPE OF FIN	X FINS / CM.	Y ROWS / CM.	N HOLES / CM.²	S MM. (IN.)	B MM. (IN.)	H MM. (IN.)	B_{50} MOR_T Kpa (PSI)	B_{10} MOR_T Kpa (PSI)	B_{50} MOE_T Kpa (PSI)	B_{10} MOE_T Kpa (PSI)	B_{50} MOR_R Kpa (PSI)	B_{10} MOR_R Kpa (PSI)	B_{50} MOE_R Kpa (PSI)	B_{10} MOE_R Kpa (PSI)	B_{50} $COMP_R$ Kpa (PSI)	B_{10} $COMP_R$ Kpa (PSI)	MIN. STRAIN TOL. (PPM)	MAT'L	MFG. PROCESS
		(FINS / IN.)	(ROWS / IN.)	(HOLES / IN.²)						(X10⁻⁶)	(X10⁻⁶)			(X10⁻⁶)	(X10⁻⁶)					
A	S.T.	15.0 (38)	13.6 (34.5)	203.9 (1311)	.061 (.0024)	.061 (.0024)	.676 (.0266)	1998 (290)	1399 (203)	3.1 (.45)	2.14 (.31)	620 (90)	386 (56)	.379 (.055)	.193 (.028)	345 (50)	200 (29)	645	AS	W, C
I	I.T.	15.8 (40)	9.1 (23)	142.6 (920)	.135 (.0053)	.135 (.0053)	.970 (.0382)	2274 (330)	1240 (180)	4.13 (.60)	3.38 (.49)	2274 (330)	1516 (220)	4.31 (.625)	4.07 (.59)	1688 (245)	1226 (178)	528	MAS	EX
D	R	11.4 (29)	12.2 (31)	140 (900)	.193 (.0076)	.193 (.0076)	.627 (.0247)	2412 (350)	1654 (240)	6.75 (.98)	4.62 (.67)	1688 (245)	930 (135)	3.10 (.45)	2.34 (.34)	1309 (190)	944 (137)	357	MAS	W, EM

Table V.B.2 — Matrix Mechanical Properties

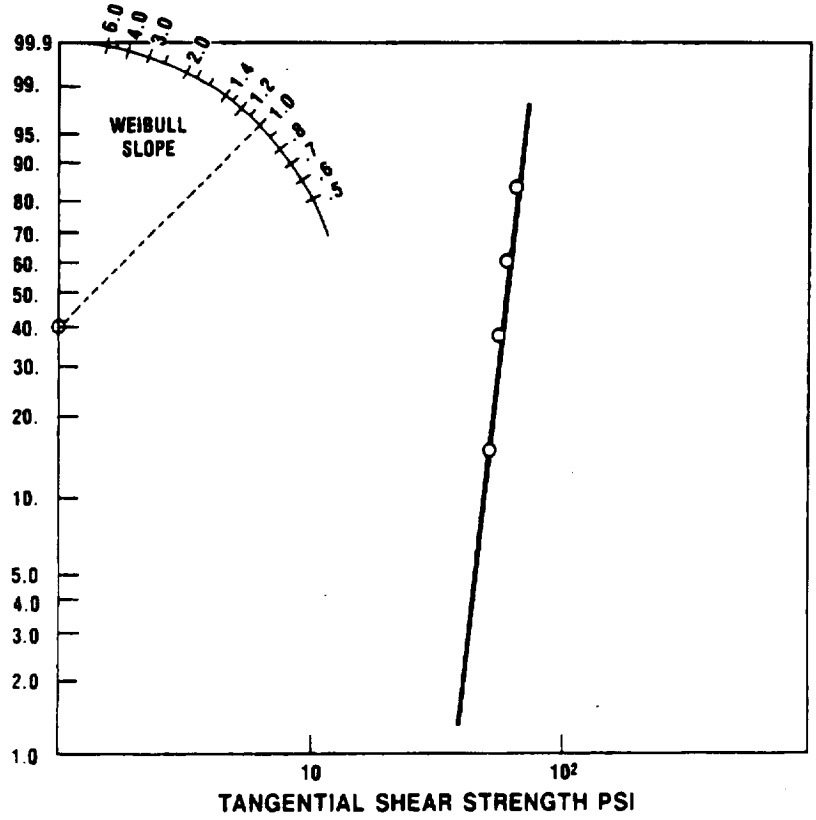

Figure V.B.5 — Supplier A Thin-Wall As Tangential Shear Strength.

V.C. PROBLEM AREAS

There are no current problems.

V.D. FUTURE PLANS

As promising materials are identified through characterization of their thermal expansion and chemical stability, mechanical properties will be evaluated and regenerator systems incorporating these materials will be analyzed for structural integrity.

The three-dimensional finite element stress analysis for Supplier D MAS-2 material will be re-evaluated incorporating the current physical properties.

V.E. TASK SUMMARY

The Supplier D MAS-2 material physical properties have been more fully characterized by evaluating specimens from 3 different matrices using Weibull statistics.

The tangential shear strength of a limited number of specimens of Supplier A thin-wall aluminum silicate material was determined.

TASK VI. THERMAL STABILITY TESTS OF CERAMICS

VI.A. INTRODUCTION

The designers of alternate heat engines continually place higher temperature requirements on the structural materials used in these engines, because higher operating temperatures yield greater engine efficiencies. This demand, in turn, requires that the materials used in the heat exchanger applications must survive at higher operating temperatures. The evaluative task reported here seeks to define the temperature limits of the proposed ceramic regenerator materials by exposing them to high temperatures with and without a corrosive agent (sodium chloride) present. The reaction of each material is measured by evaluating the physical and chemical stability during the course of the testing program.

VI.B STATUS

VI.B.1 1000°C (1832°F) Test Temperature

Ten materials (5-MAS, 2-AS, 1-LAS/MAS, 1-LAS, 1-SiC) plus the 9455 LAS standard had previously been evaluated (Reference 6) at 1000°C (1832°F) without sodium present and the results are repeated on Figure VI.B.1.1. The testing of the original ten experimental materials at 1000°C (1832°F) with sodium present was completed during this reporting period, and a graphical representation of the materials' dimensional stability as a function of test time is presented in Figure VI.B.1.2.

The MAS materials and the LAS material all exhibit good corrosion resistance at 1000°C (1832°F). The LAS/MAS mixture exhibits a progressive growth in this environment similar to its previous exposure without sodium present. This suggests that the material may be thermally unstable, rather than susceptible to sodium attack.

The Supplier A and B AS materials react contractively to the rigors of the sodium stability test. The contraction of the material of Supplier B was so dramatic as to fall off scale, and the numbers to the immediate right of each symbol are the normalized length changes, in parts per million, measured at each time interval.

A comparison of these data with the corresponding test set without sodium present (Figure VI.B.1.1) points out a most interesting observation. The LAS material of Supplier B appears to be more stable (in a dimensional sense) in the sodium-enriched environment. This observation, without further investigation of the change in material behavior as a result of stability testing, may be misleading. This point is raised to encourage the reader to carefully examine the thermal expansion comparisons offered for each tested material in Figures VI.B.1.3 through VI.B.1.13. Please note the scale differences among the figures. A comparison between the figures in this report and those corresponding figures for similar testing without sodium present included in the previous report (Reference 6), together with the dimensional stability data, enable one to draw more meaningful conclusions.

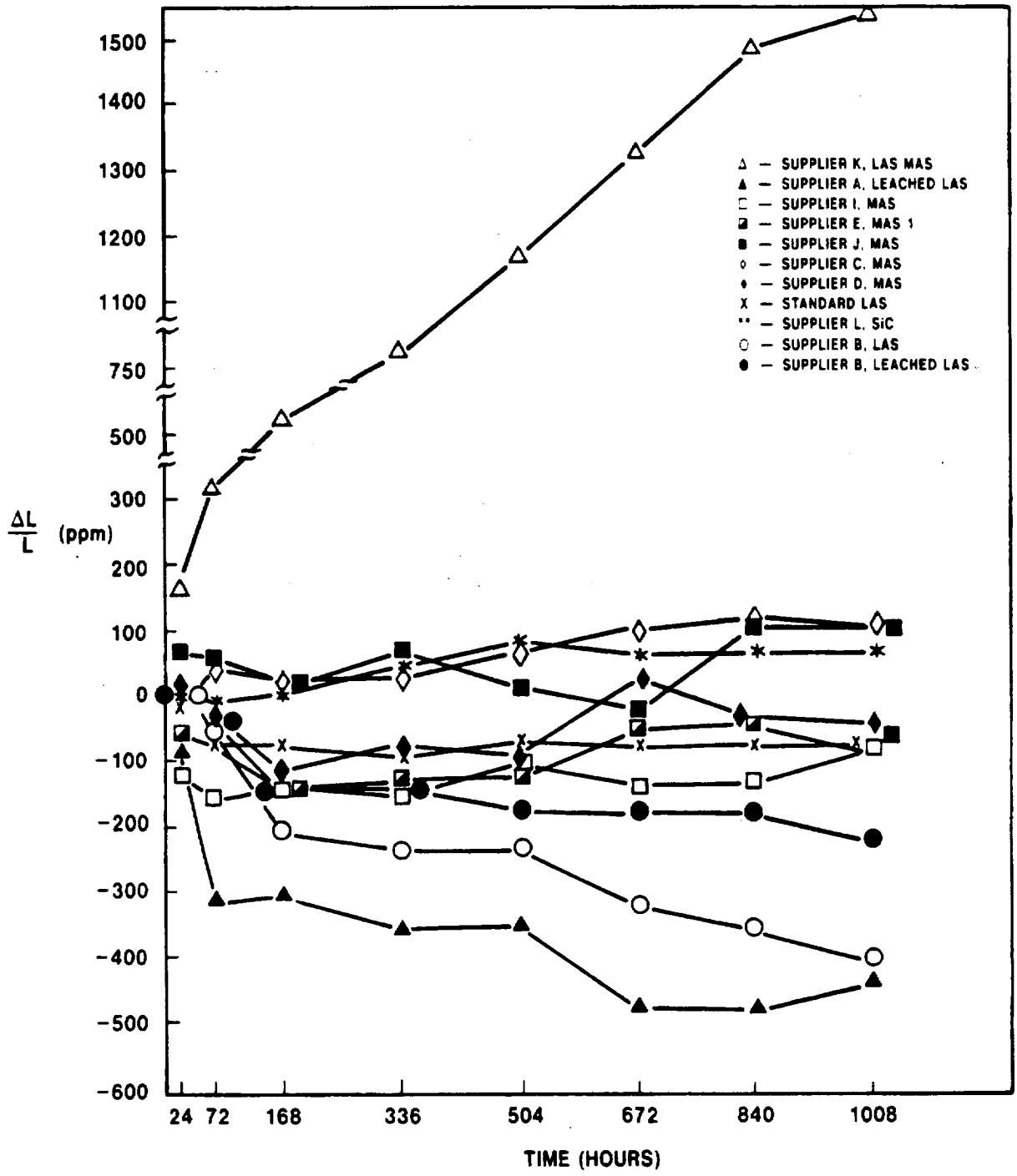

Figure VI.B.1.1 Physical Stability of Various Materials at 1000°C (1832°F).

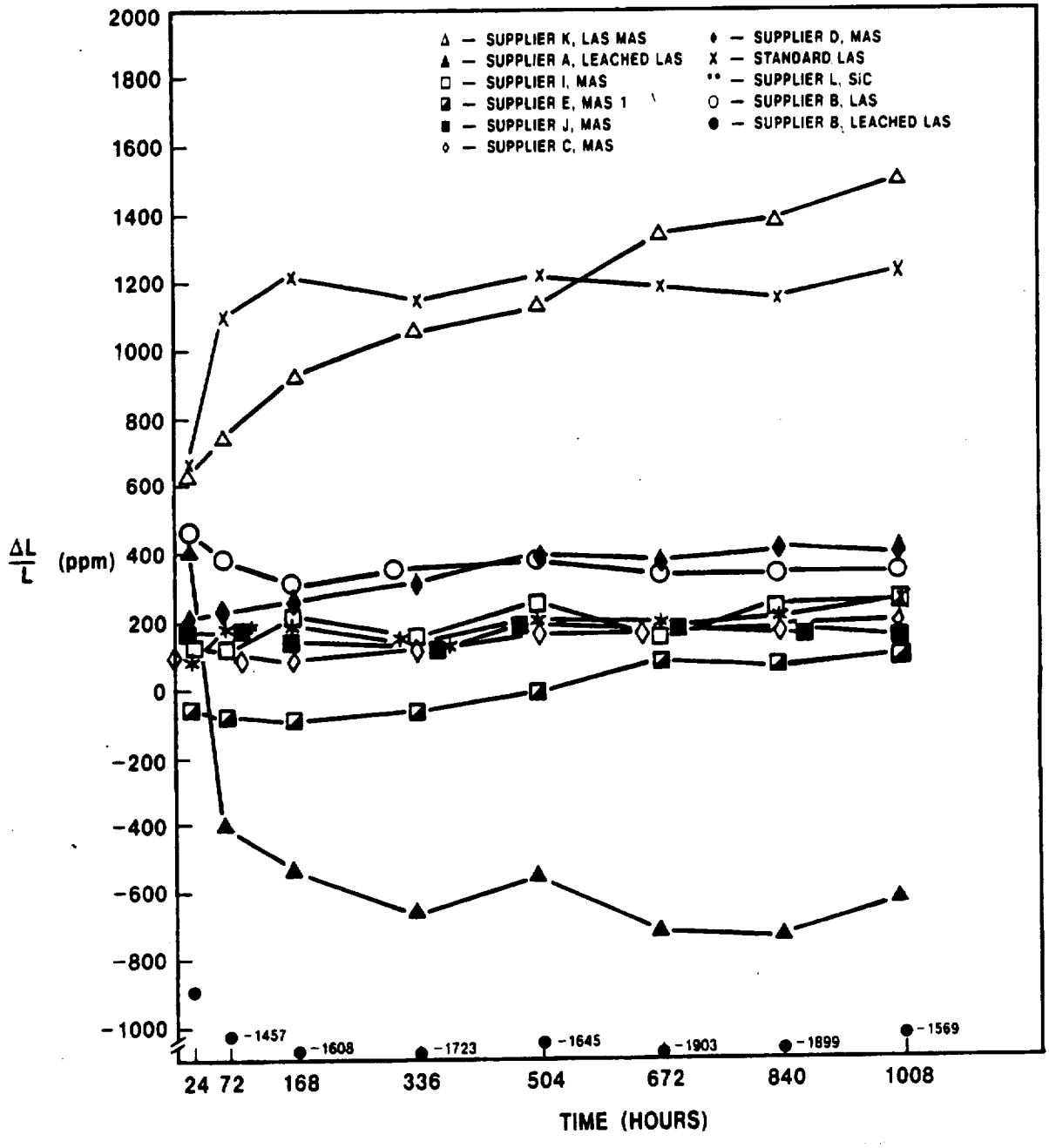

Figure VI.B.1.2 Physical Stability of Various Materials at 1000°C (1832°F) with Sodium Present.

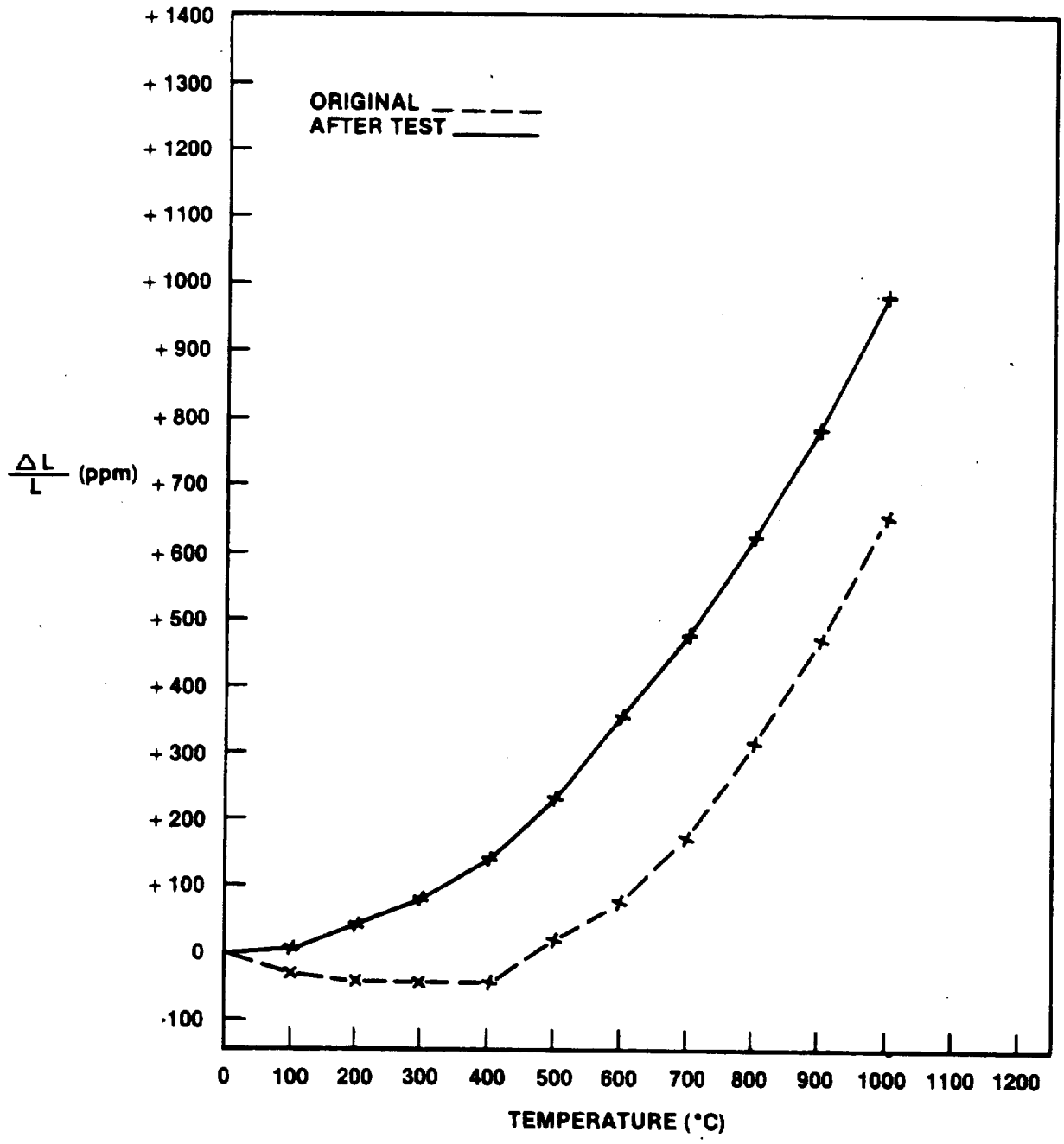

Figure VI.B.1.3 9455 LAS Standard; Thermal Expansion Behavior Before and After 1000°C (1832°F) Thermal Stability Testing with Sodium Present.

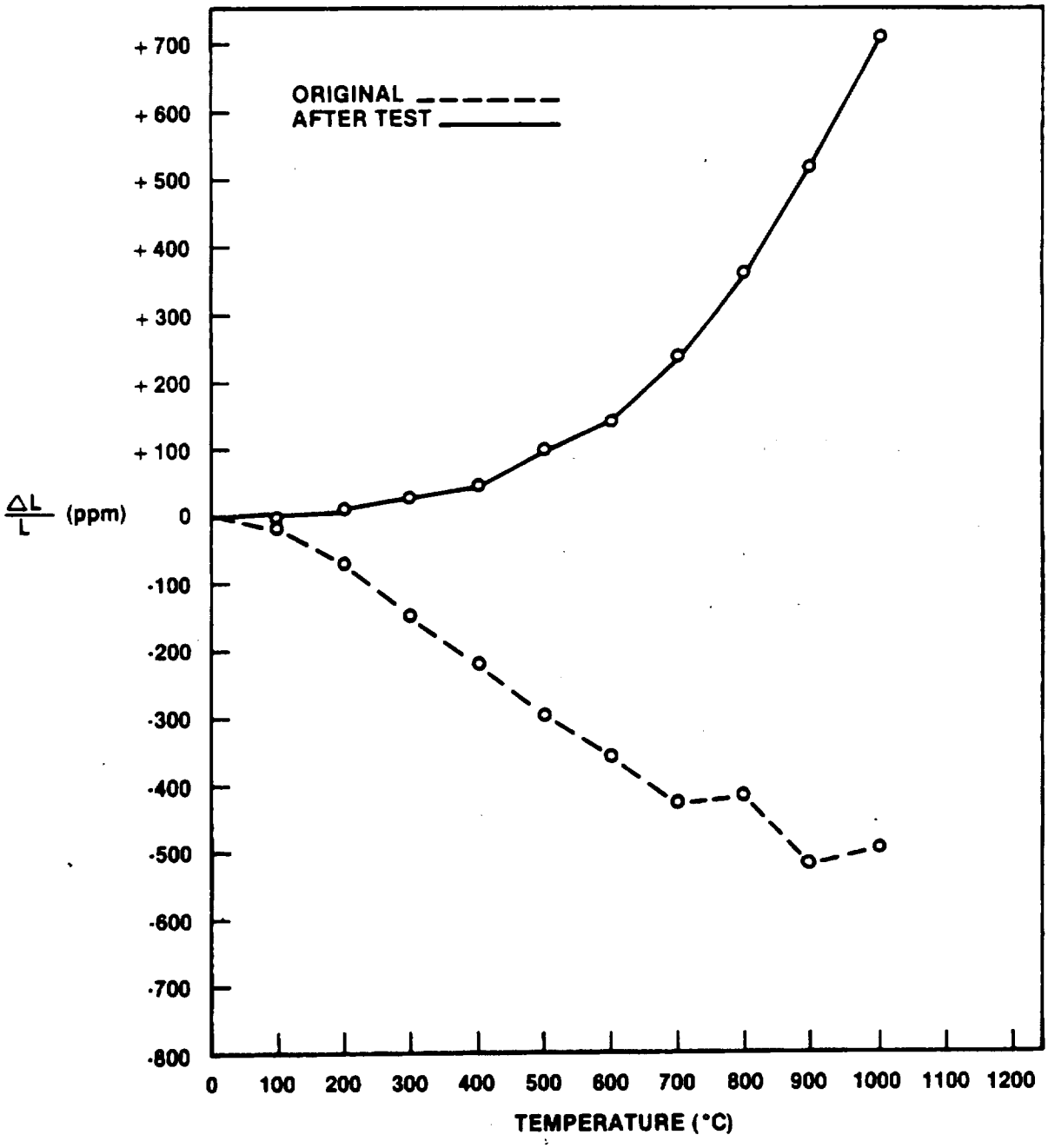

Figure VI.B.1.4 Supplier B, LAS; Thermal Expansion Behavior Before and After 1000°C (1832°F) Thermal Stability Testing with Sodium Present.

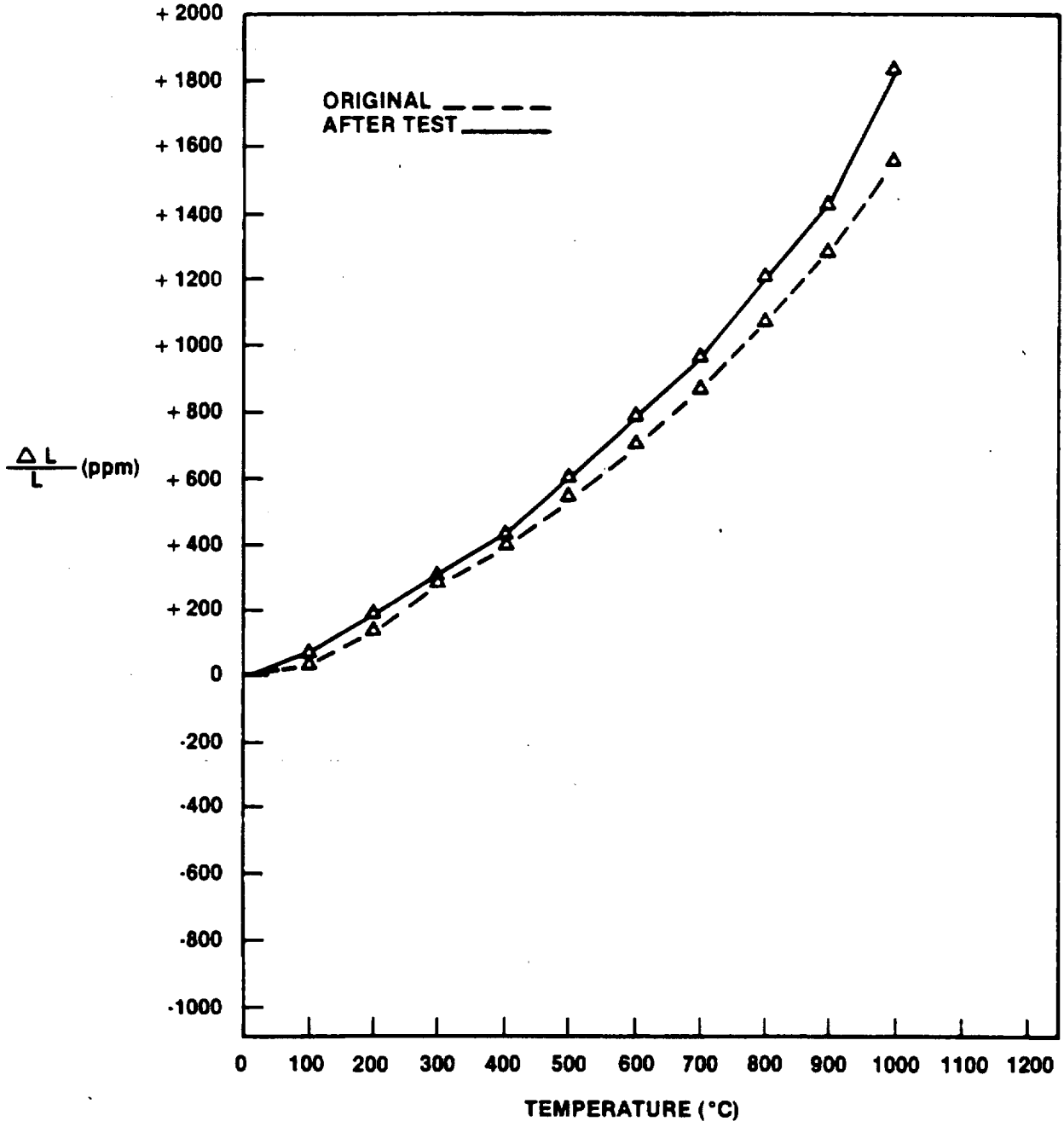

Figure VI.B.1.5 Supplier K, LAS/MAS; Thermal Expansion Behavior Before and After 1000°C (1832°F) Thermal Stability Testing with Sodium Present.

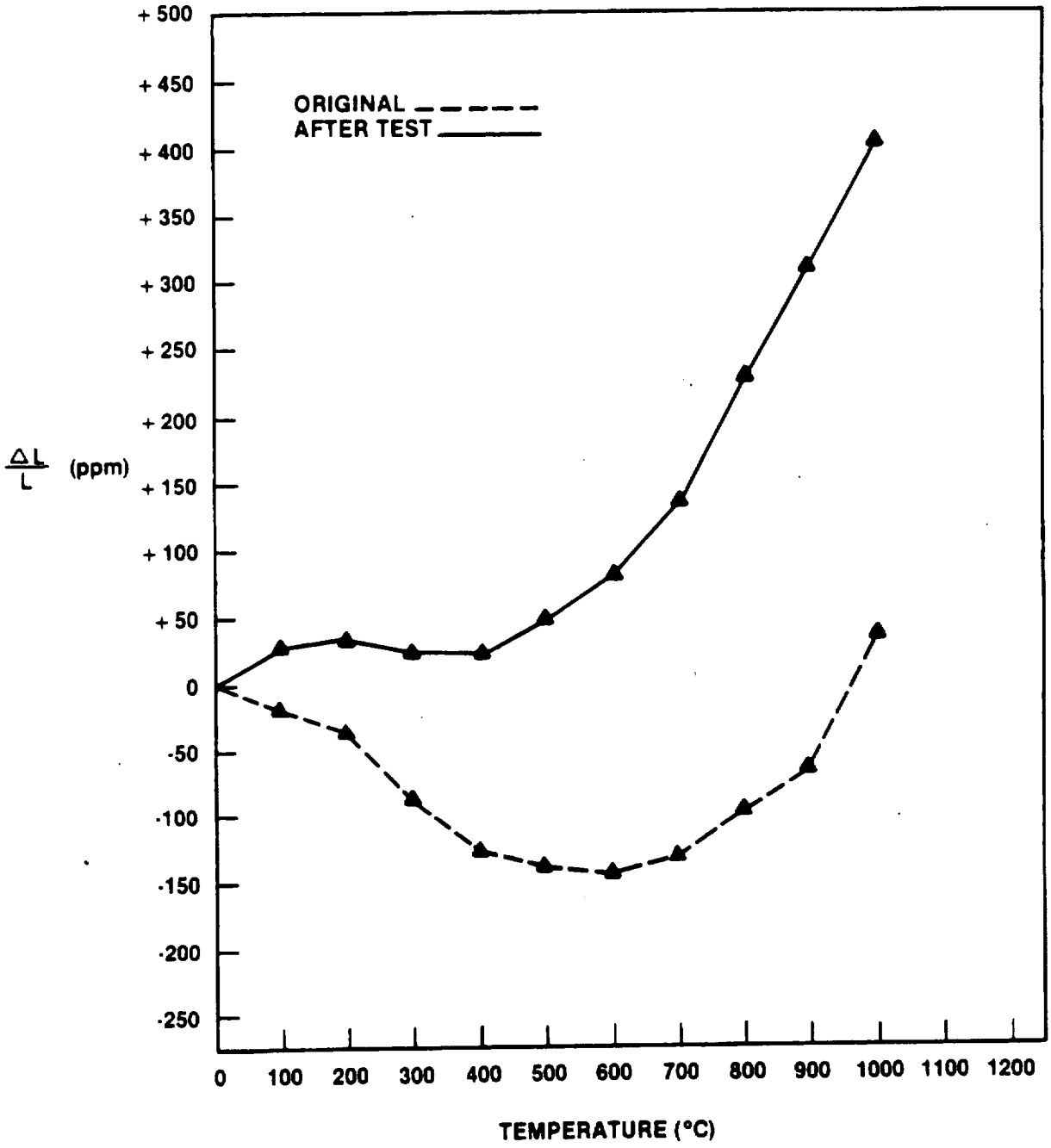

Figure VI.B.1.6 Supplier A, AS; Thermal Expansion Behavior Before and After 1000°C (1832°F) Thermal Stability Testing with Sodium Present.

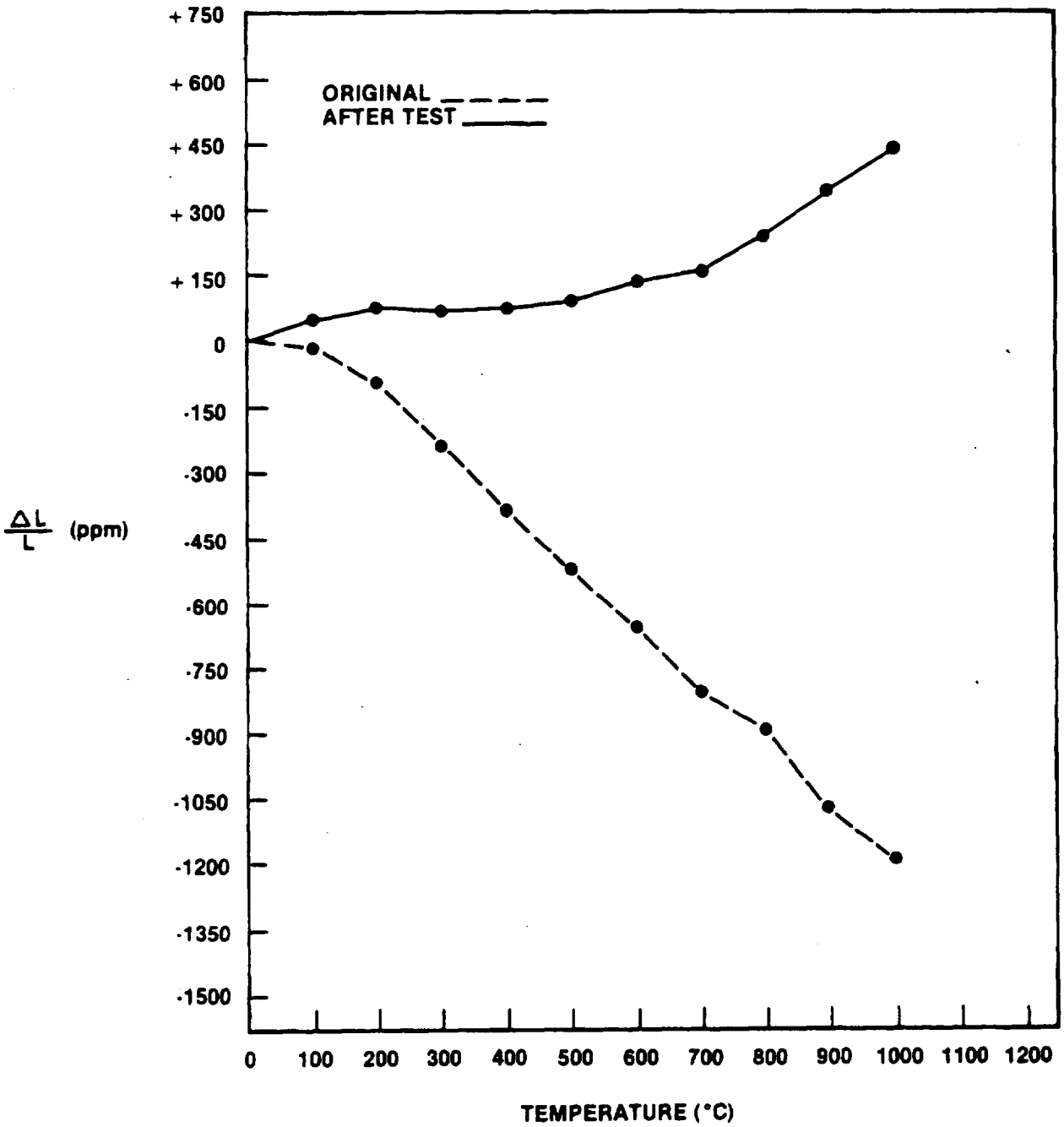

Figure VI.B.1.7 Supplier B, AS; Thermal Expansion Behavior Before and After 1000°C (1832°F) Thermal Stability Testing with Sodium Present.

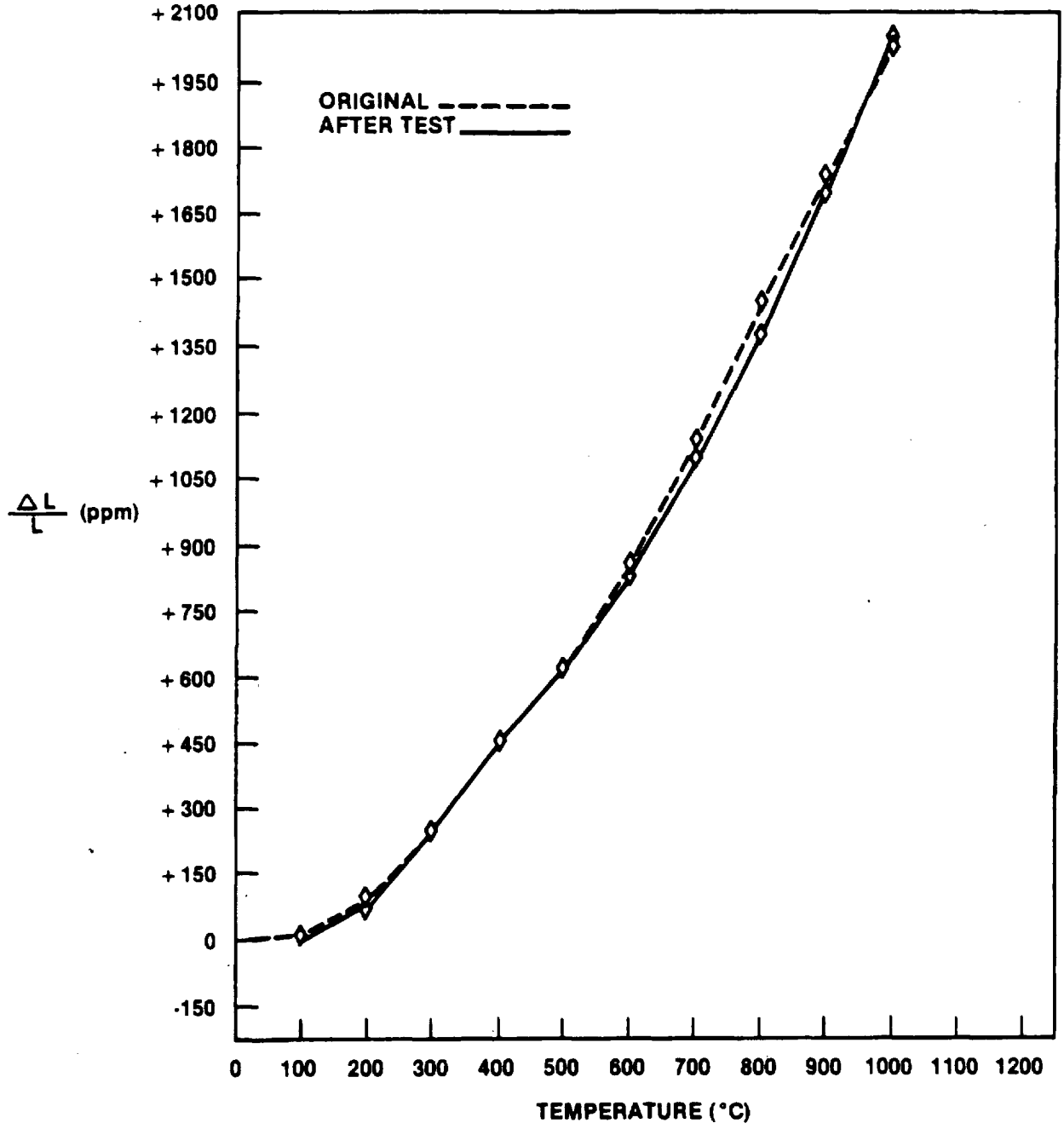

Figure VI.B.1.8 Supplier C, MAS; Thermal Expansion Behavior Before and After 1000°C (1832°F) Thermal Stability Testing with Sodium Present.

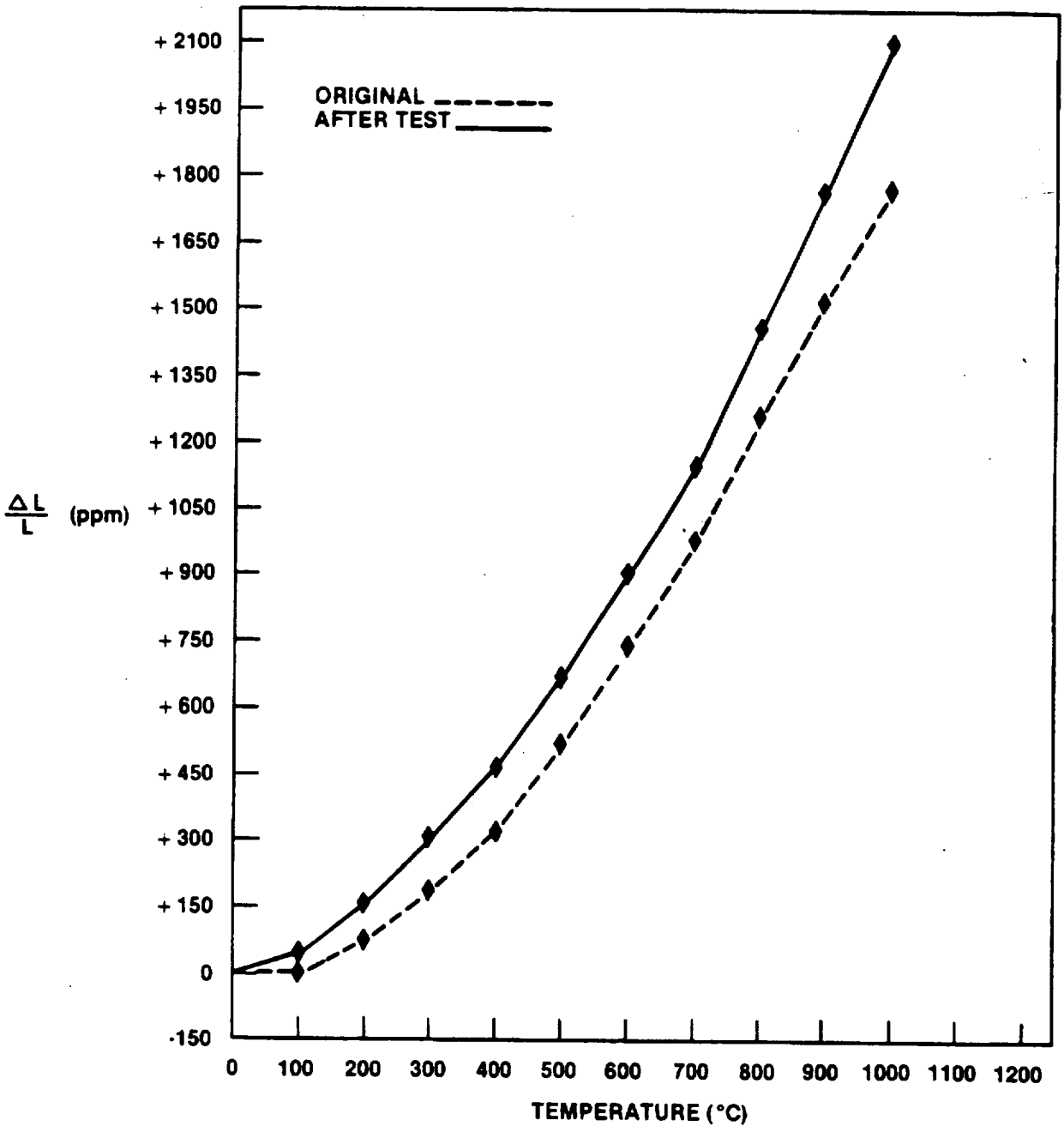

Figure VI.B.1.9 Supplier D, MAS; Thermal Expansion Behavior Before and After 1000°C (1832°F) Thermal Stability Testing with Sodium Present.

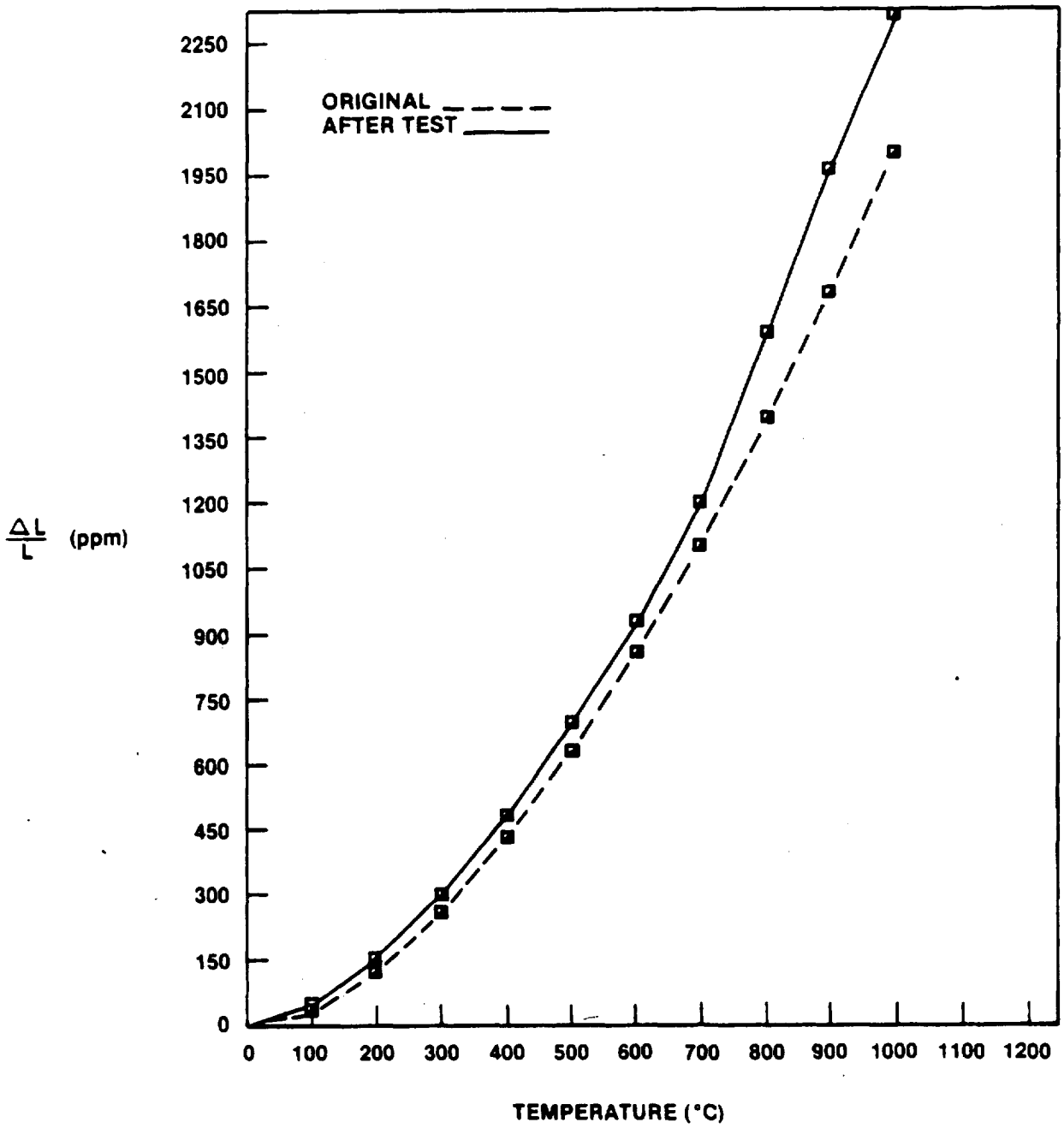

Figure VI.B.1.10 Supplier E, MAS #1; Thermal Expansion Behavior Before and After 1000°C (1832°F) Thermal Stability Testing with Sodium Present.

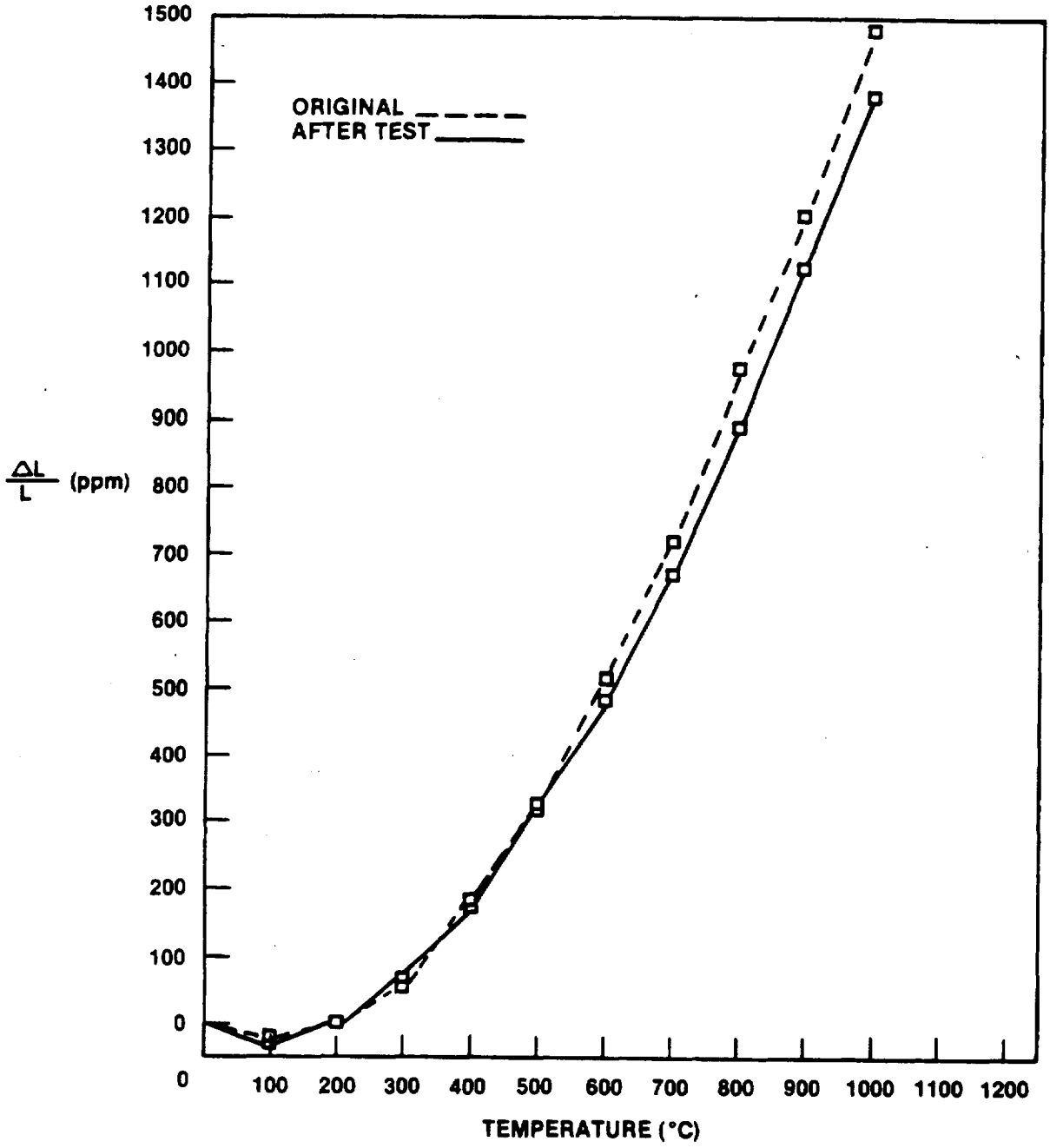

Figure VI.B.1.11 Supplier I, MAS; Thermal Expansion Behavior Before and After 1000°C (1832°F) Thermal Stability Testing with Sodium Present.

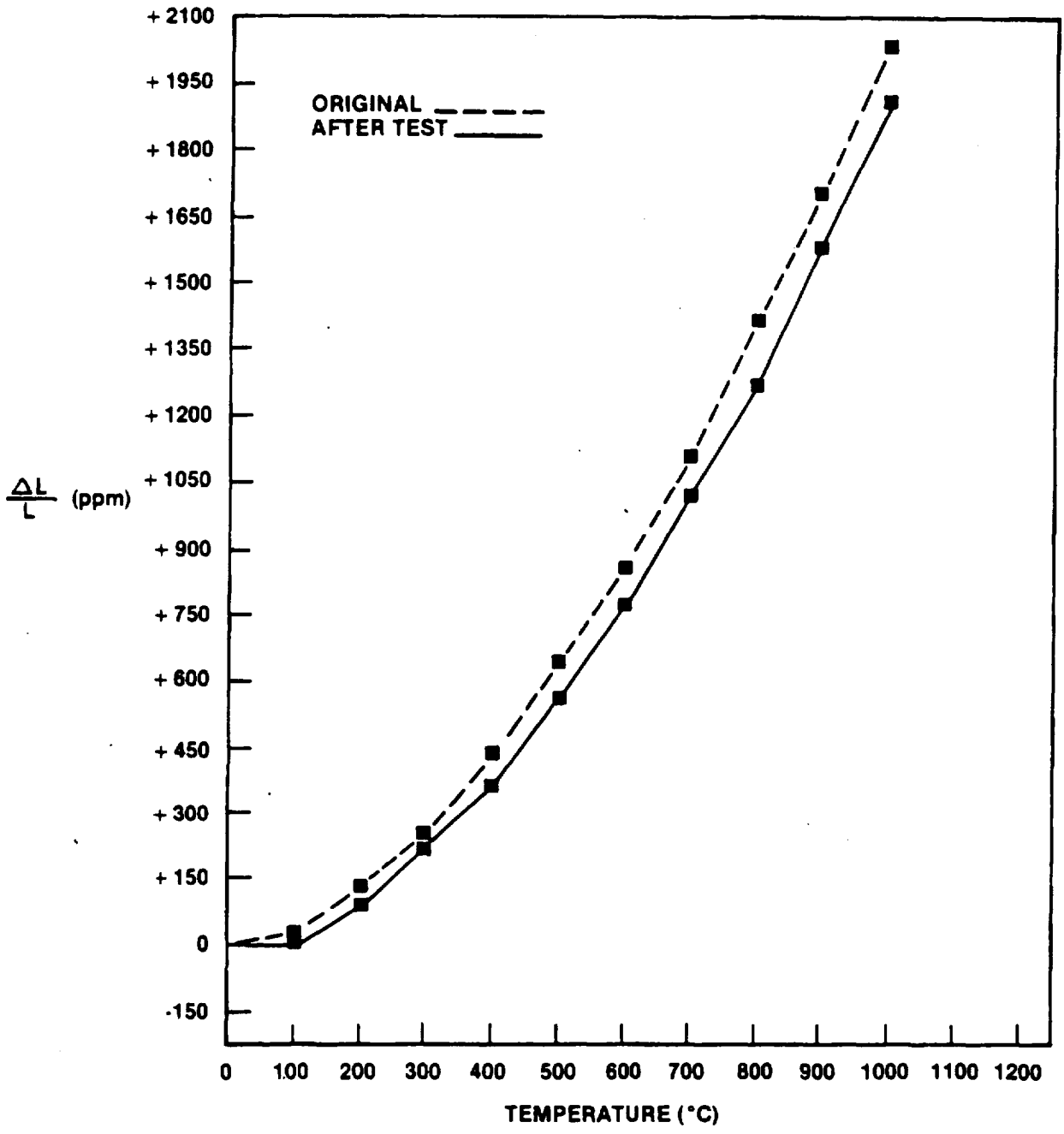

Figure VI.B.1.12 Supplier J, MAS; Thermal Expansion Behavior Before and After 1000°C (1832°F) Thermal Stability Testing with Sodium Present.

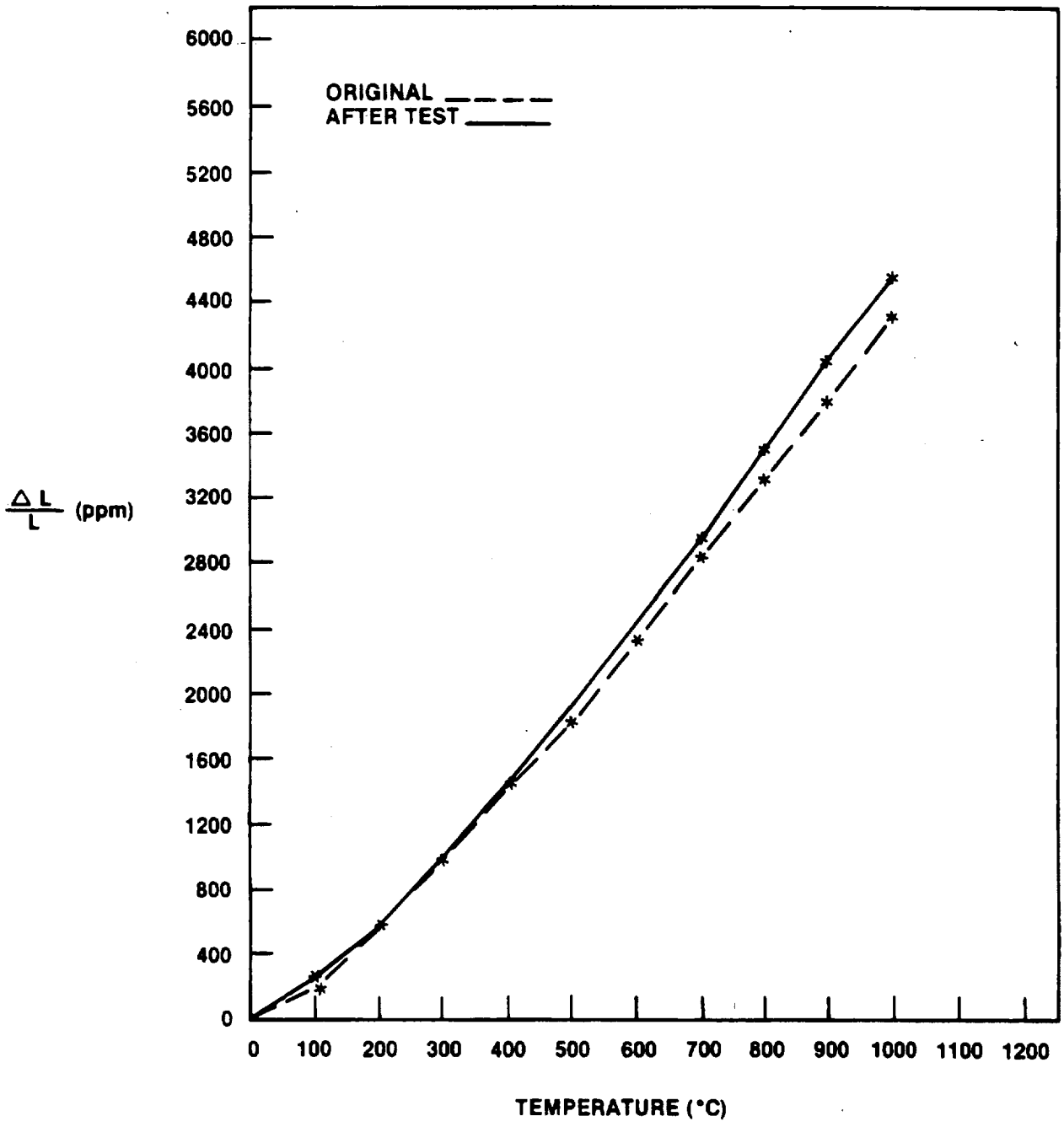

Figure VI.B.1.13 Supplier L, SiC; Thermal Expansion Behavior Before and After 1000°C (1832°F) Thermal Stability Testing with Sodium Present.

As expected the 9455 LAS standard is not very resistant to sodium exchange, and the change in thermal expansion behavior (Figure VI.B.1.3) indicates a significant material change. The point made earlier concerning the physical stability of the LAS material of Supplier B can be reinforced by comparing the thermal expansion plots for this material tested with sodium present (Figure VI.B.1.4) and without sodium present (Figure VI.B.1.3, Reference 6). Contrary to the impression created by the dimensional stability data alone, (Figures VI.B.1.1 and VI.B.1.2) this material has obviously suffered more damage as the result of the presence of sodium. In some manner, most likely sodium-for-lithium ion exchange, the sodium has mitigated the contractive nature of this material. This effect is the same as that observed in the accelerated corrosion testing of this material as a matrix insert and detailed in Task III.B.2 of this report.

The LAS/MAS mixture, while obviously unstable in this thermal environment, with or without sodium present, does not suffer a significant change in thermal expansion behavior (Figure VI.B.1.5). This effect remains somewhat of a mystery at this point.

The AS materials of Supplier A (Figure VI.B.1.6) and Supplier B (Figure VI.B.1.7) have both experienced a change in their thermal expansion behavior, rendering these originally contractive materials now expansive. Both of these materials underwent a dimensional contraction during testing (Figure VI.B.1.2). The reaction of the Supplier B material was a great deal larger in magnitude than the reaction of the material of Supplier A. This difference is also noted in the degree of change in thermal expansion behavior of the two materials. While the material of Supplier A has become more expansive (Figure VI.B.1.6), the nature of the thermal expansion response before and after testing bear a similarity to each other. The change noted for the AS material of Supplier B (Figure VI.B.1.7) is not only severe, but the nature of the material's response to changes in temperature has been altered. This observation, coupled with the greater dimensional instability observed, indicates that the AS of Supplier A is more resistant to sodium corrosion at 1000°C (1832°F) than the AS material of Supplier B.

The MAS materials all exhibited good dimensional stability under these test conditions. An examination of each material's thermal expansion behavior before and after testing (Figures VI.B.1.8 through VI.B.1.12 points out that these materials incur little, if any, change as a result of exposure to sodium at 1000°C (1832°F). It is concluded that any of these materials should prove to be of service in a regenerator application at 1000°C (1832°F).

Figure VI.B.1.13 indicates the thermal expansion behavior of SiC before and after testing at 1000°C (1832°F) with sodium present. The stability of this material in a corrosive environment at this temperature is excellent; however, the high thermal expansion, the high thermal conductivity, and the difficulty of processing will limit the use of this material in regenerator applications.

During this reporting period, a group of four additional materials (3-MAS, 1-LAS/-MAS) have been acquired, prepared, and placed on test. The tests are now in their initial stages, and graphical data will be included in subsequent reports.

VI.B.2 1050°C (1922°F) Test Temperature

While the initial testing plan defined a program of evaluation at 1000°C (1832°F), 1100°C (2012°F), and 1200°C (2192°F), it is the intent of this contract task to place an upper operating limit on the ceramic regenerator materials. Therefore, tests of three materials (2-AS, 1-LAS) which evidenced a loss of physical integrity at 1100°C (2012°F) and 1200°C (2192°F) were placed on test at this mid-point temperature (1050°C). These tests have just begun, and data will be reported at a later date.

VI.B.3 1100°C (2012°F) Test Temperature

The thermal stability tests, both with and without sodium present, for this test temperature were completed during this reporting period. Seven experimental materials (4-MAS, 2-AS, 1-LAS) and the 9455 LAS standard were included in the sample set.

Figure VI.B.3.1 is a graphical comparison of the material stability (as evidenced by dimensional measurement) of the sample set as a function of thermal stability test time at 1100°C (2012°F) without sodium present. The MAS materials and the 9455 LAS standard exhibit good thermal stability. The Supplier B LAS material has experienced some degree of growth as a result of this high temperature exposure, while the two AS materials have contracted to the point where physical deterioration was obvious, necessitating termination after 672 test hours. The numbers immediately adjacent to the graphing symbols for these materials indicate a degree of dimensional change too great to include in the graphing scale.

Figures VI.B.3.2 through VI.B.3.9 are comparisons of each individual material's change in thermal expansion behavior as a result of the 1100°C (2012°F) thermal stability testing. These data, combined with the dimensional stability measurements, afford one an insight into the effect of the test environment on each specific material.

Figures VI.B.3.2 and VI.B.3.3 represent the thermal expansion characteristics of the 9455 LAS standard and the LAS composition of Supplier B, respectively. The standard material (Figure VI.B.3.2) remains relatively unchanged as a result of the 1100°C (2012°F) thermal stability testing, although this material does exhibit a tendency to slump at a lower temperature after going through the test. In contrast, the LAS of Supplier B (Figure VI.B.3.3) has undergone a rather large change in thermal expansion behavior as a result of the 1008 cumulative hour exposure to a temperature of 1100°C (2012°F). This material, while originally contractive between room temperature and 1100°C (2012°F), has become expansive over this same temperature interval subsequent to the test. This observation corroborates the dimensional instability observed in this material during the course of the thermal stability testing.

Figures VI.B.3.4 and VI.B.3.5 dramatically illustrate the pronounced changes in thermal expansion behavior of the AS materials of Suppliers A and B respectively, as a result of the 1100°C (2012°F) thermal stability testing. Both of these materials were very unstable under the conditions of this test; and they were dropped from testing after a cumulative exposure of 672 hours. Both had suffered visible physical degradation. As can be seen in their thermal expansion plots, both materials have become quite expansive, with the material of Supplier A (Figure VI.B.3.4) undergoing the

greater change. This observation correlates well with the comparative dimensional instabilities (Figure VI.B.3.1). In this case, the difference in severity of attack is not important, as neither material appears to be thermally stable such that they might serve for extended periods of time at 1100°C (2012°F).

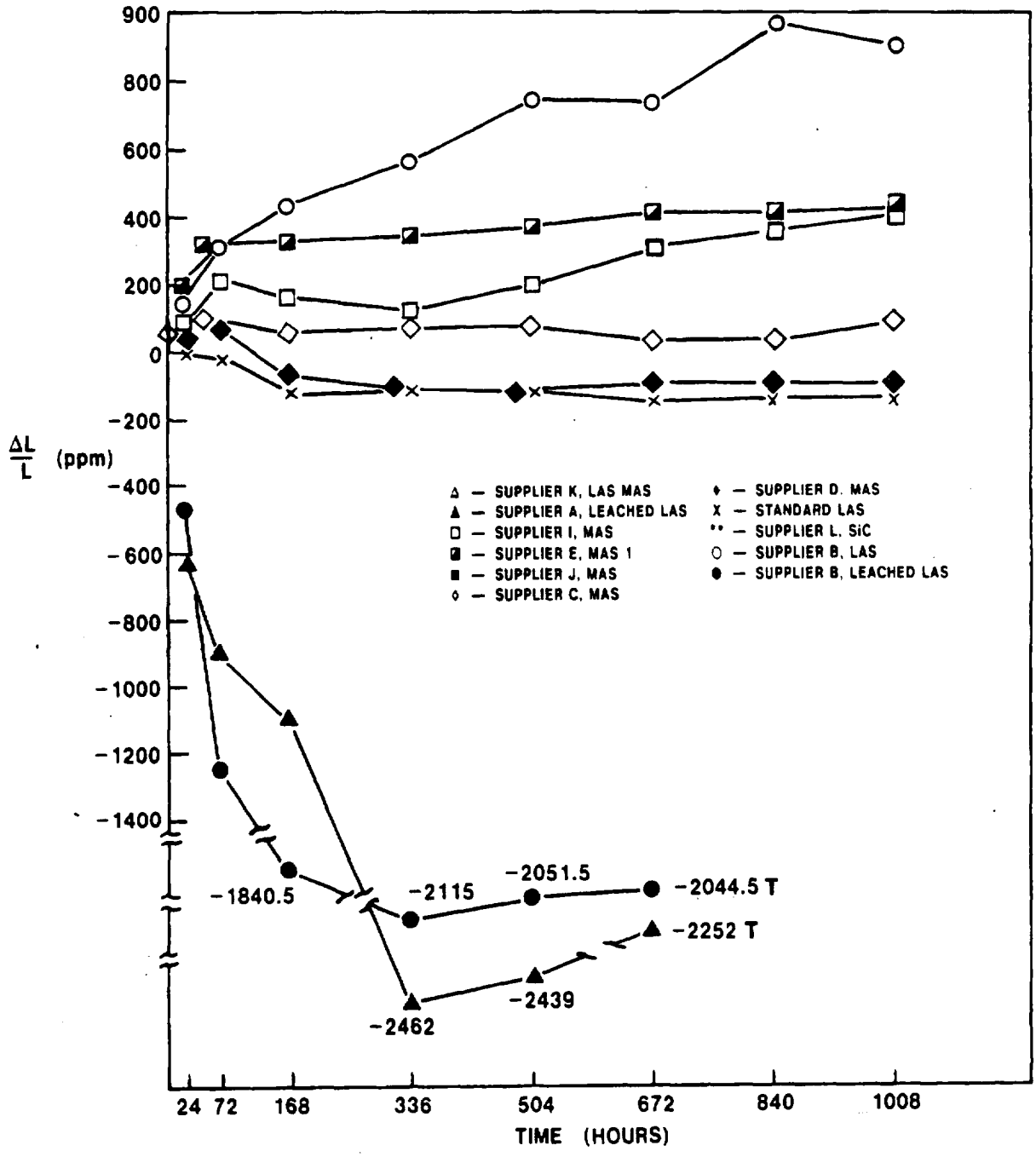

Figure VI.B.3.1 Physical Stability of Various Materials at 1100°C (2012°F).

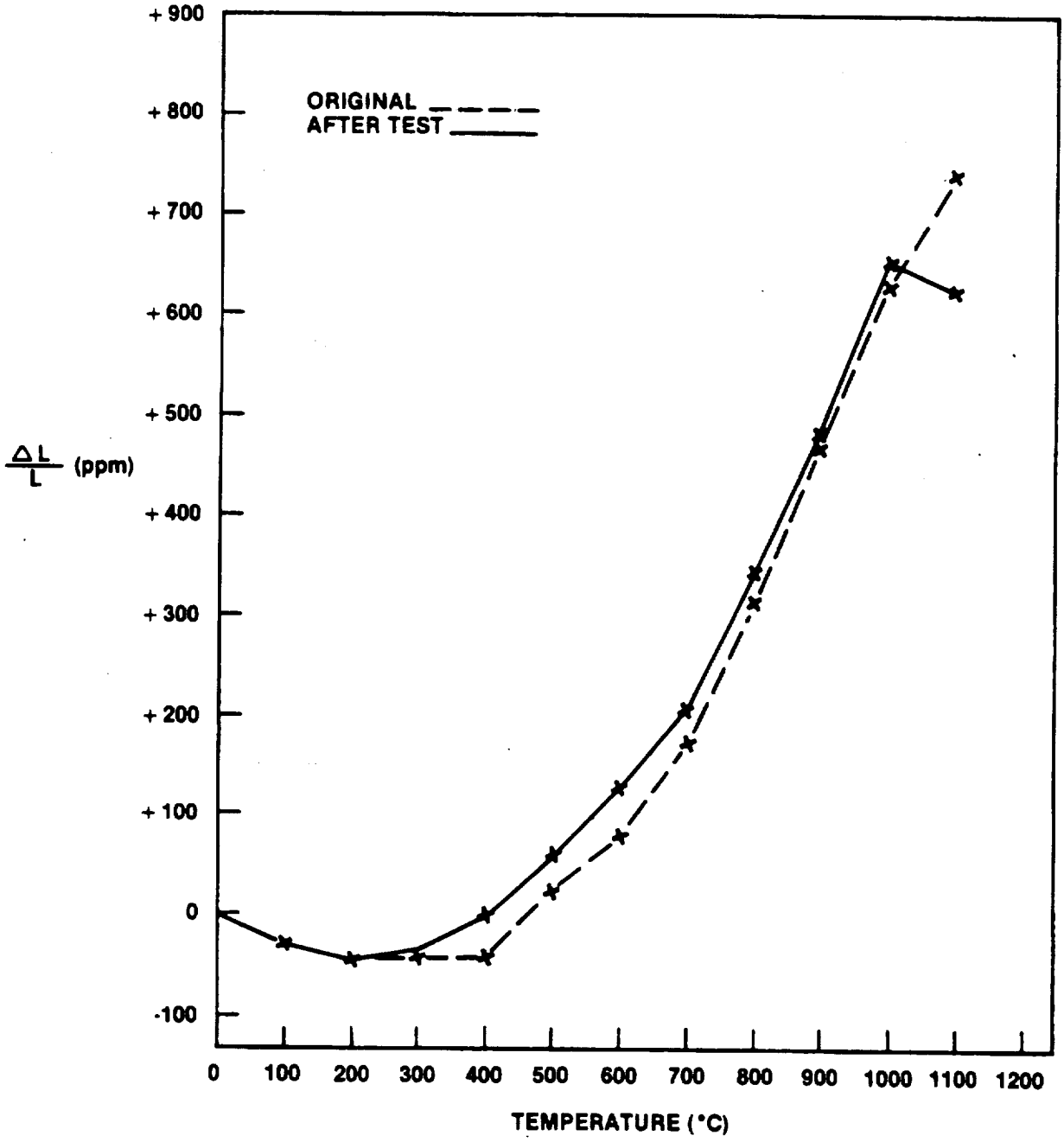

Figure VI.B.3.2 9455 LAS Standard; Thermal Expansion Behavior Before and After 1100°C (2012°F) Thermal Stability Testing.

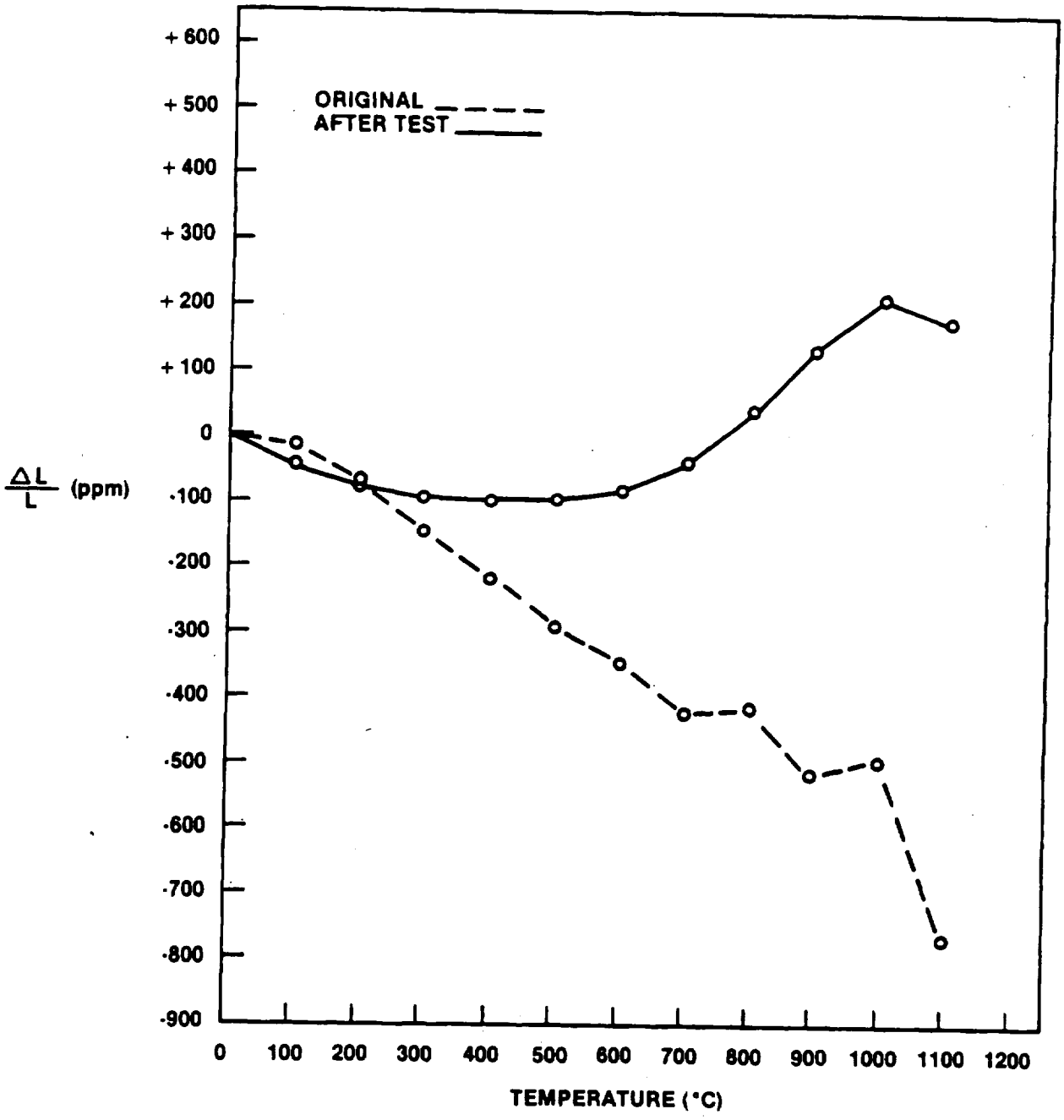

Figure VI.B.3.3 Supplier B, LAS; Thermal Expansion Behavior Before and After 1100°C (2012°F) Thermal Stability Testing.

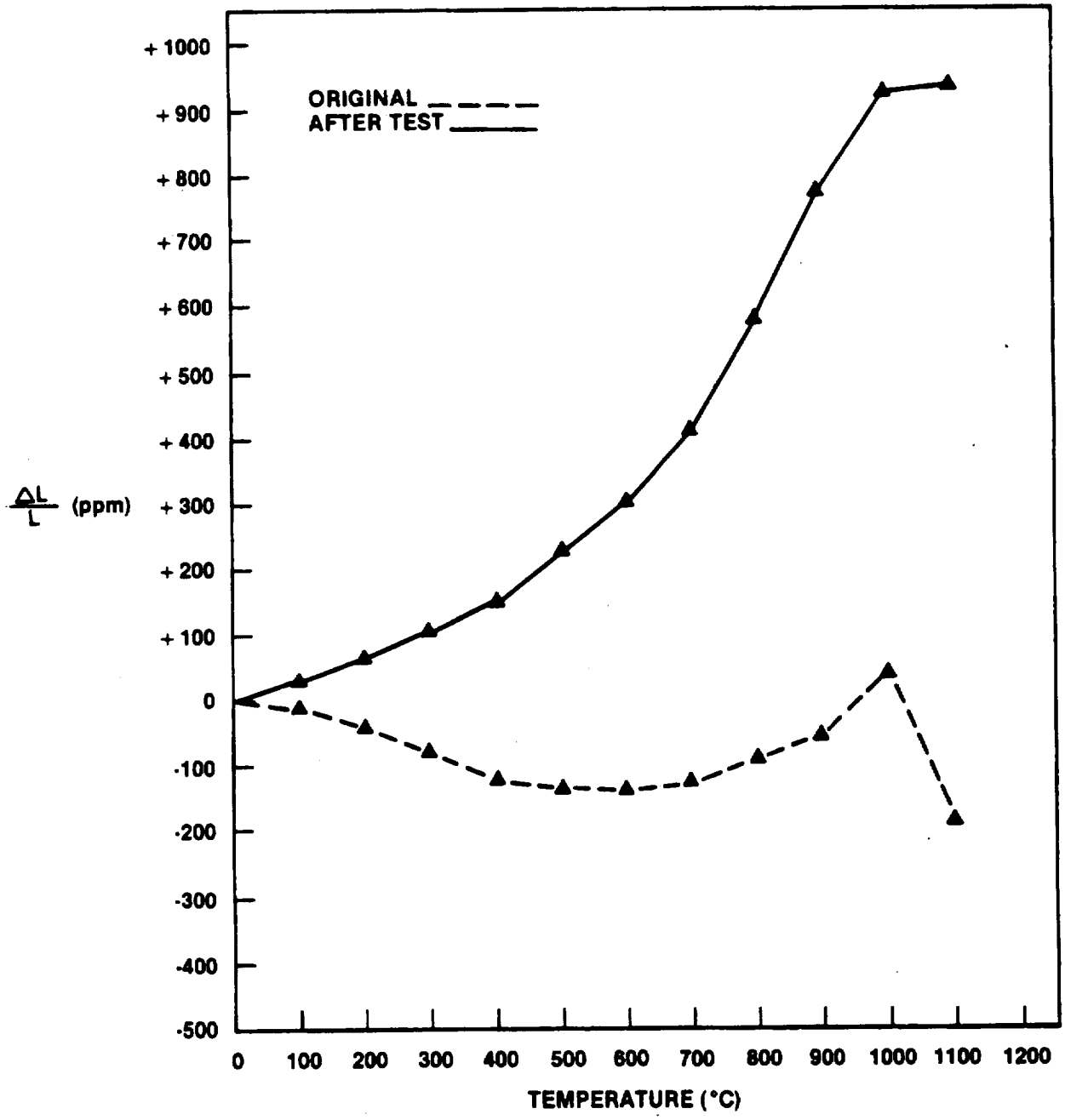

Figure VI.B.3.4 Supplier A, AS; Thermal Expansion Behavior Before and After 1100°C (2012°F) Thermal Stability Testing. (This material was terminated after 672 test hours).

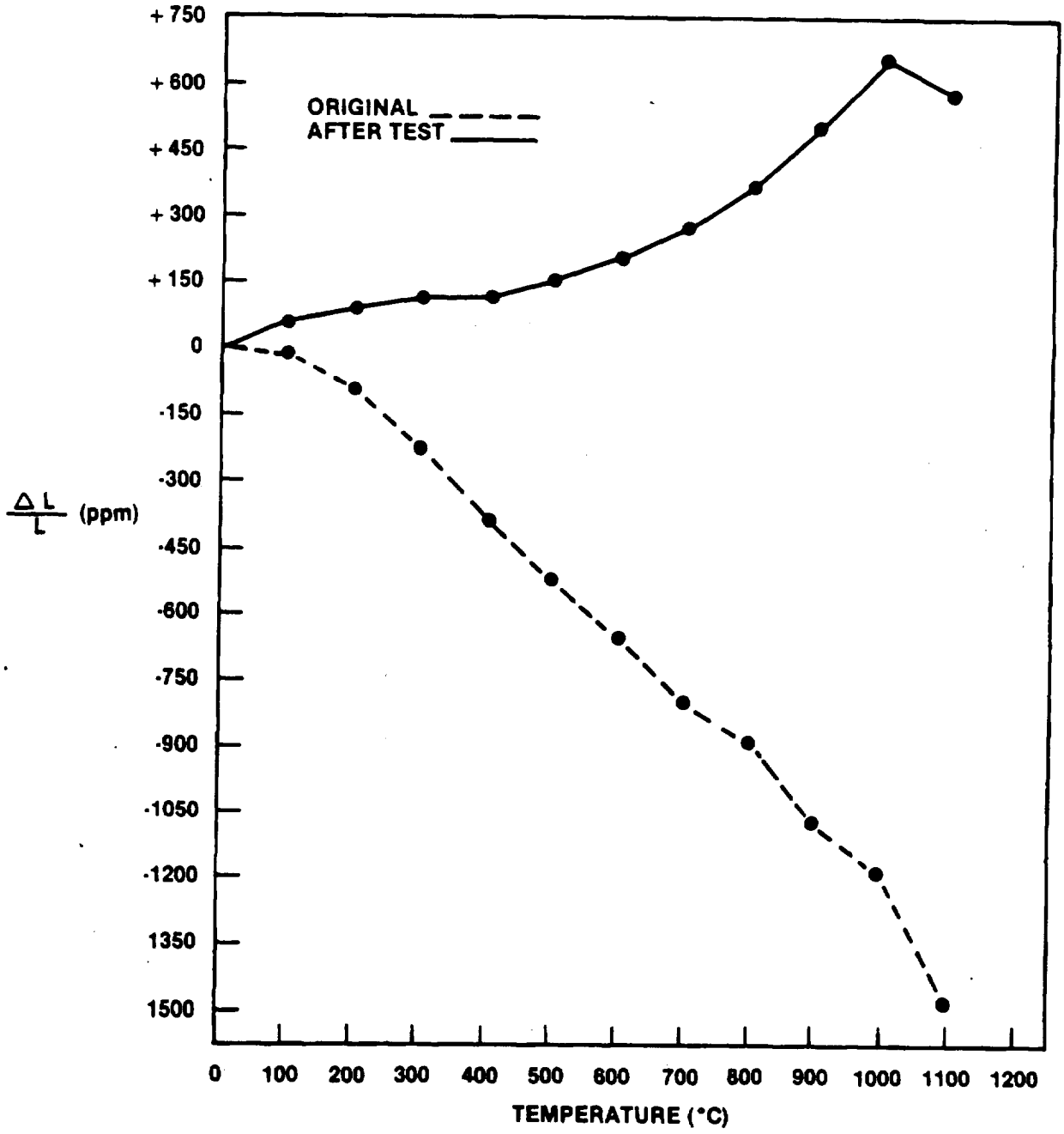

Figure VI.B.3.5 Supplier B, AS; Thermal Expansion Behavior Before and After 1100°C (2012°F) Thermal Stability Testing. (This material was terminated after 672 test hours).

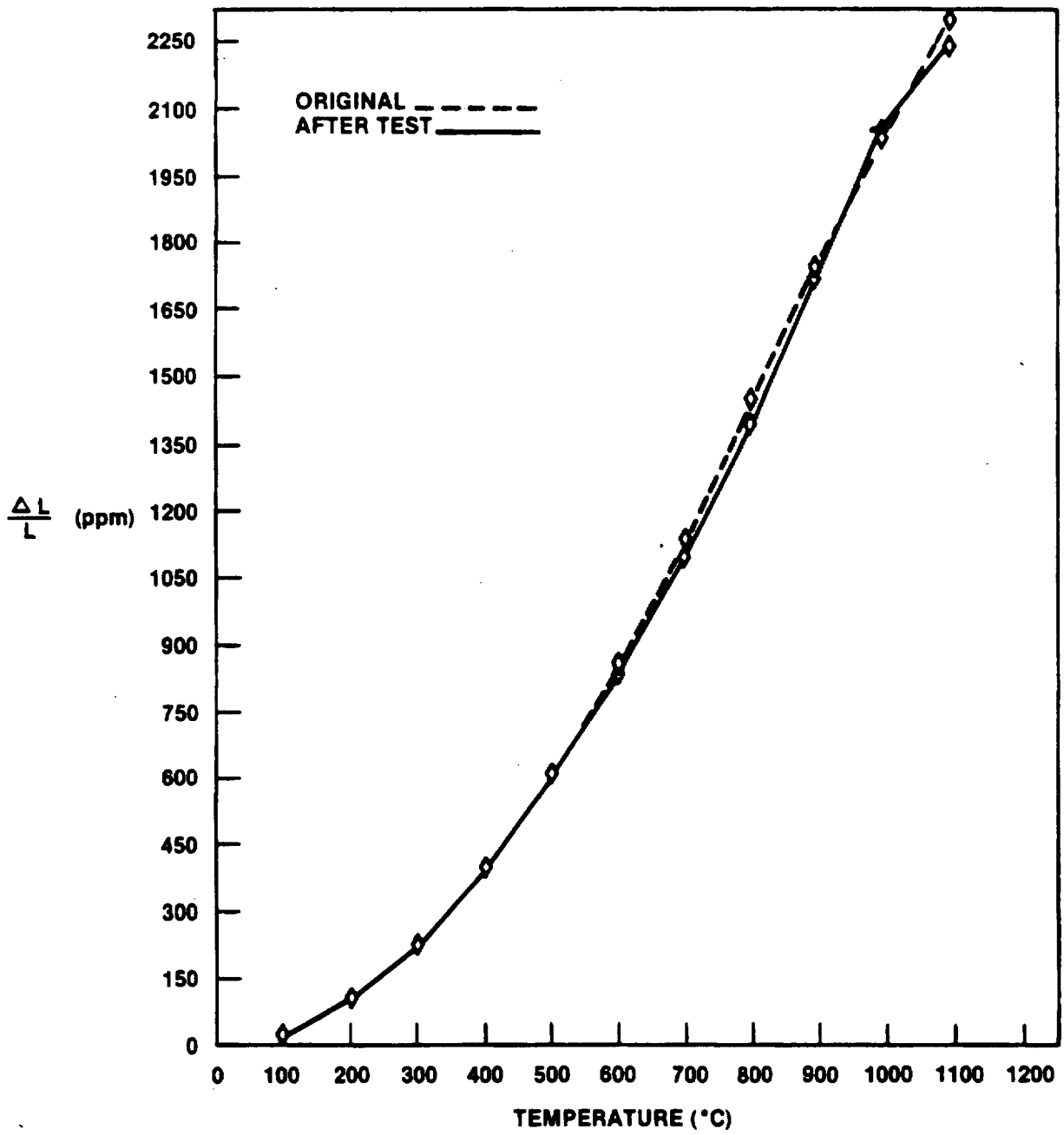

Figure VI.B.3.6 Supplier C, MAS; Thermal Expansion Behavior Before and After 1100°C (2012°F) Thermal Stability Testing.

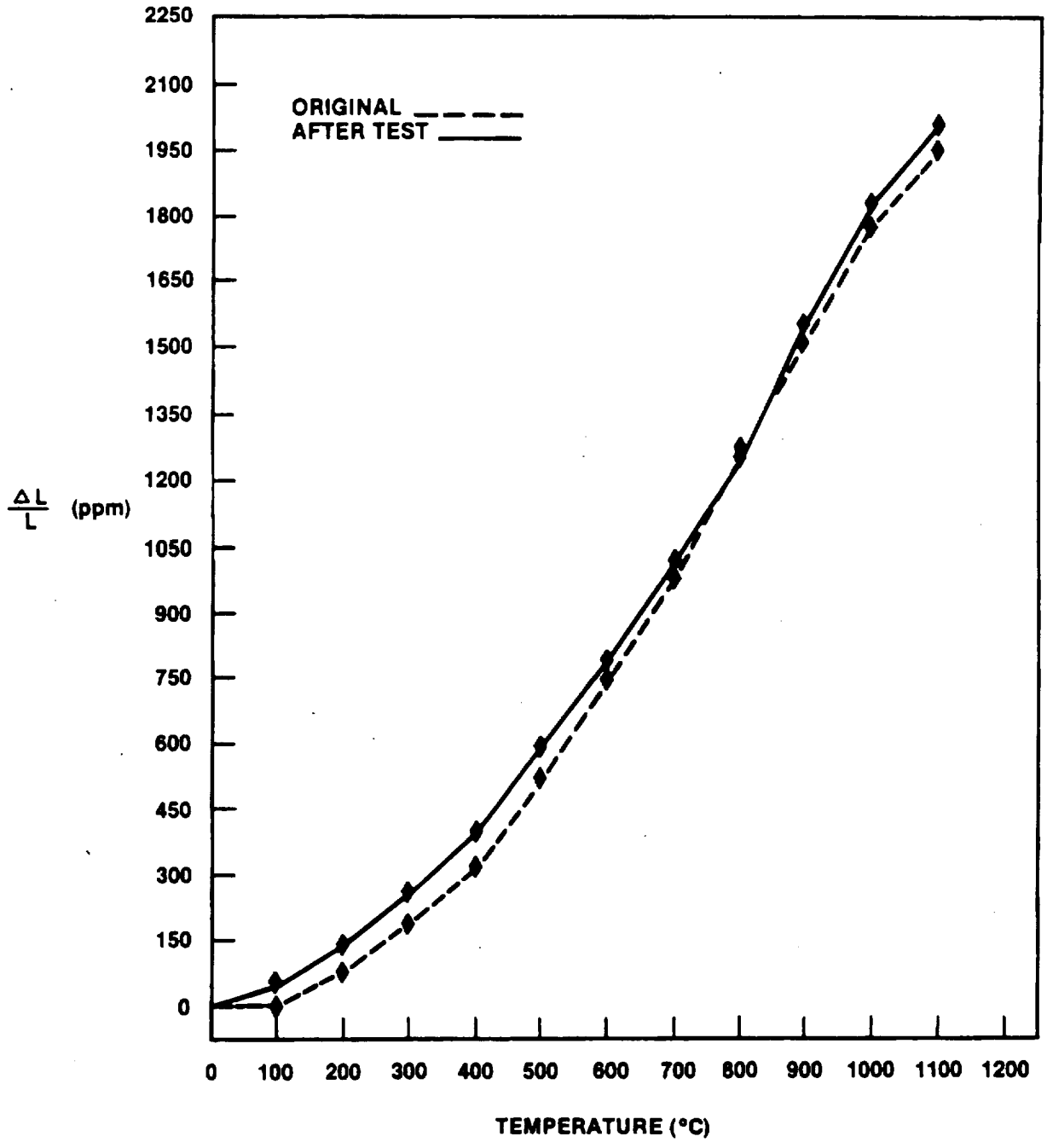

Figure VI.B.3.7 Supplier D, MAS; Thermal Expansion Behavior Before and After 1100°C (2012°F) Thermal Stability Testing.

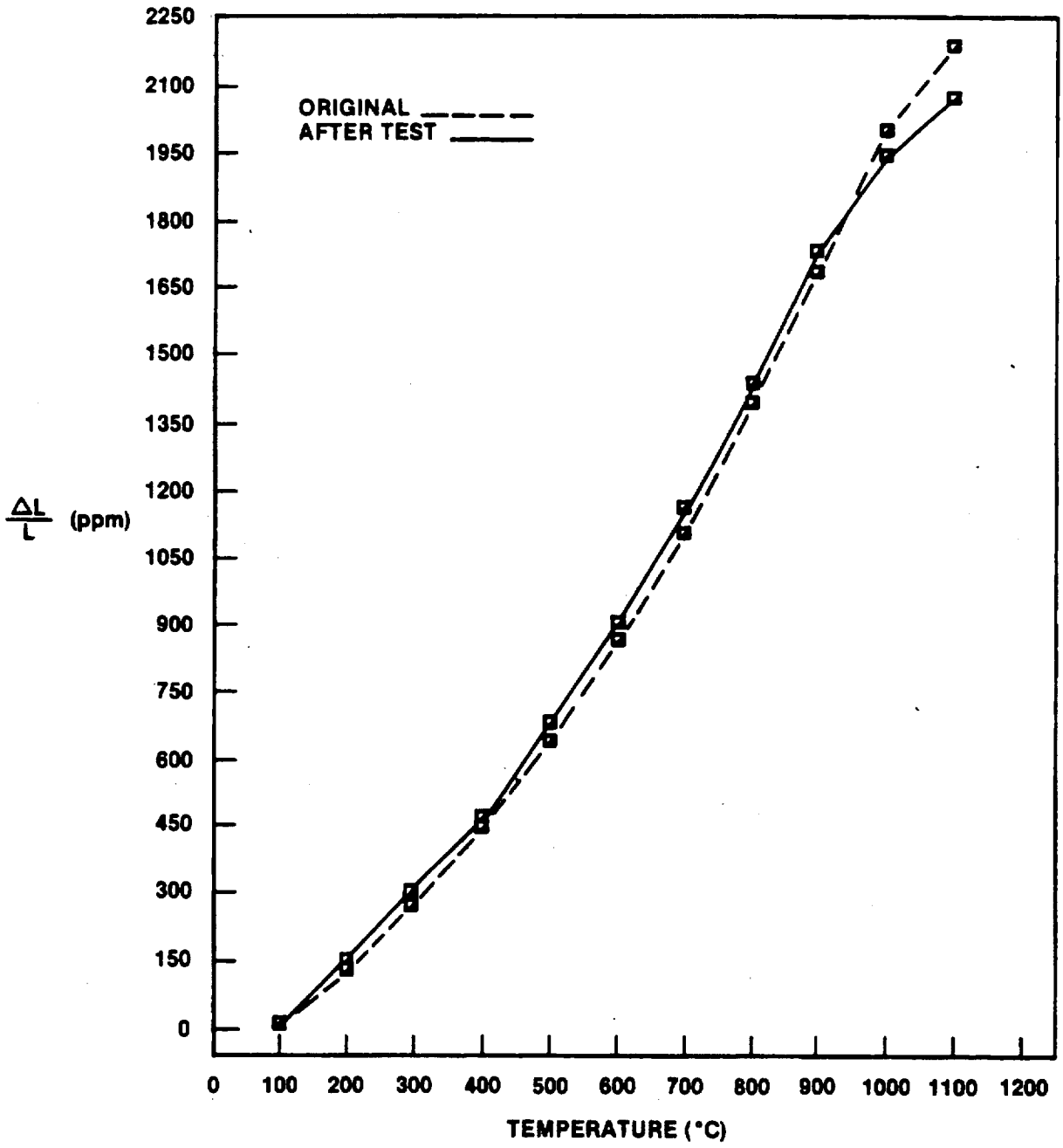

Figure VI.B.3.8 Supplier E, MAS #1; Thermal Expansion Behavior Before and After 1100°C (2012°F) Thermal Stability Testing.

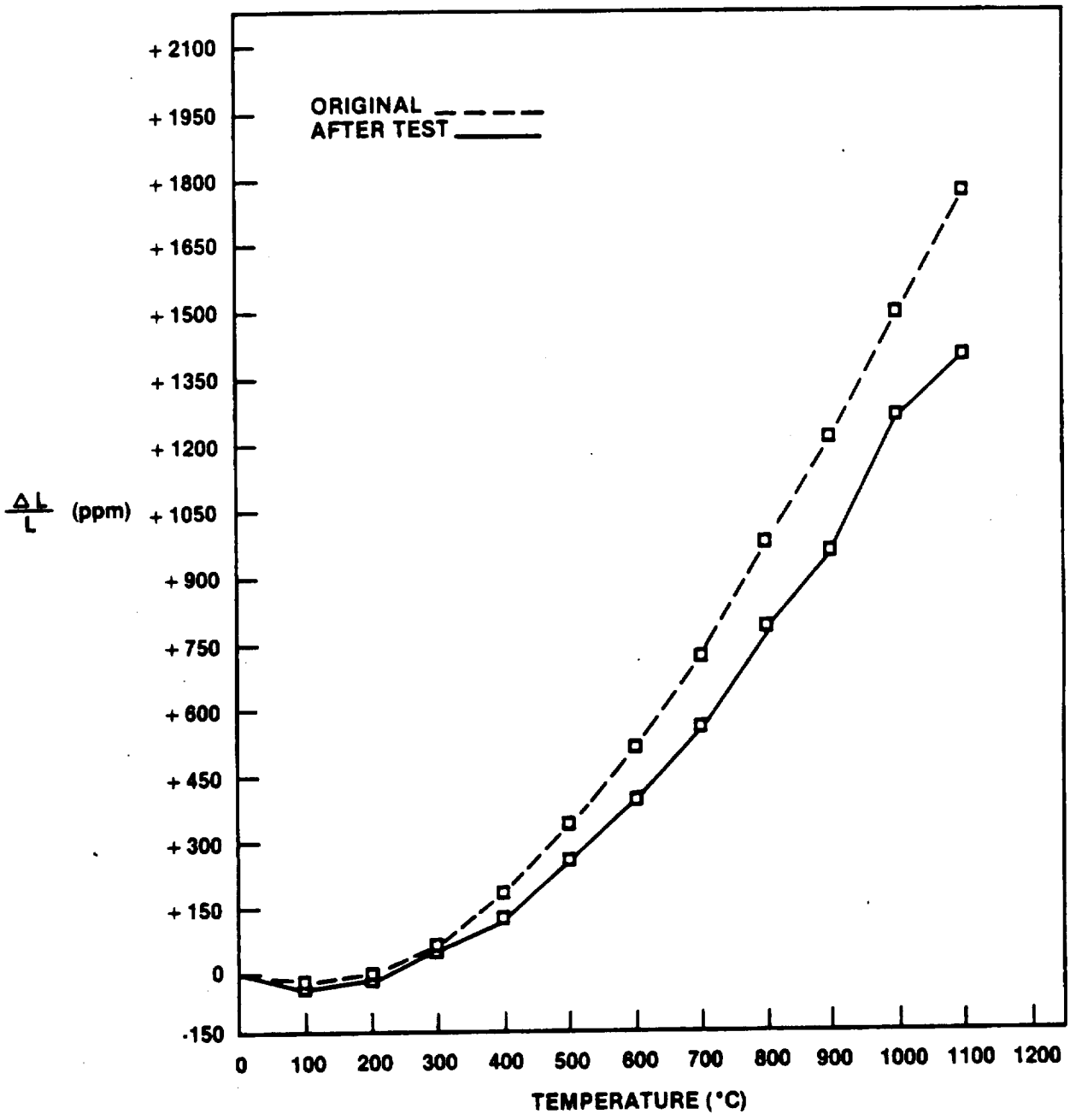

Figure VI.B.3.9 Supplier I, MAS; Thermal Expansion Behavior Before and After 1100°C (2012°F) Thermal Stability Testing.

At this test temperature, the MAS materials seem to be diverging into two groups, representing different levels of stability (Figure VI.B.3.1). Figures VI.B.3.6 and VI.B.3.7 indicate the essentially identical thermal expansion response of the very stable MAS materials of Suppliers C and D, respectively. Figures VI.B.3.8 and VI.B.3.9 illustrate the more marked change in thermal expansion experienced by the somewhat less stable MAS materials of Suppliers E (material #1) and I, respectively. While these measured differences do exist, the data would suggest that all of these MAS materials appear to be viable candidates for regenerator service at 1100°C (2012°F).

The results of the 1100°C (2012°F) thermal stability testing with sodium present, illustrated graphically in Figure VI.B.3.10, indicate that the introduction of sodium into the test environment at this temperature tends to accentuate the material responses noted in the thermal stability testing at this temperature without sodium present (Figure VI.B.3.1). The MAS materials, while all relatively stable under these test conditions, tend to divide more dramatically into the same two groups of differing stability. The Supplier B LAS and the two AS materials exhibited a marked physical deterioration early in the test sequence, and these materials were terminated after 168 cumulative hours of test time. Of curious interest is the lack of continuous growth, beyond the 24 hour test interval, of the 9455 LAS standard.

The effects of the 1100°C (2012°F) thermal stability testing with sodium on each material's thermal expansion behavior are presented in Figures VI.B.3.11 through VI.B.3.18. Figures VI.B.3.11 and VI.B.3.12 represent the original and final thermal expansions of the 9455 LAS standard and the LAS of Supplier B, respectively. As previously noted, the curious lack of long-term response by the standard material to the test environment is underscored by the significant change in thermal expansion behavior reported in Figure VI.B.3.11, especially when compared to the lack of change (Figure VI.B.3.2) resulting from the 1100°C (2012°F) thermal stability testing without sodium present. The LAS of Supplier B is clearly changed by the high-temperature, sodium-rich environment of the test, and has become so strongly expansive (Figure VI.B.3.12) as to become self-destructive.

Figures VI.B.3.13 and VI.B.3.14 illustrate the change in thermal expansion response for the AS materials of Suppliers A and B, respectively. The same relative effects are observed for both materials tested with sodium as were reported for the purely thermal tests: the AS of Supplier A (Figure VI.B.3.13) evidences more physical instability and a greater change in thermal expansion than does the AS of Supplier B (Figure VI.B.3.14). However, it should again be noted that this difference is not important, because both materials are obviously beyond the temperature limit at which they may serve in a regenerator application.

The MAS materials evidence the best resistance to corrosion at 1100°C (2012°F) of the three basic materials groups tested. Figures VI.B.3.15 through VI.B.3.18 indicate quite similar thermal expansion behaviors for these materials before and after the testing sequence. As was observed in the testing without sodium present (Figure VI. B.3.1) the MAS materials divide into two stability groups during testing with sodium present (Figure VI.B.3.10). The MAS materials of Suppliers C and D appear to be slightly more stable than those of Supplier E (Material #1) and Supplier I. This

division is not so dramatically supported by the thermal expansion data, as was the case in the 1100°C (2012°F) thermal stability testing without sodium present; but the conclusion to which one is drawn remains the same: all of these MAS materials would seem to be candidates for regenerator service at 1100°C (2012°F).

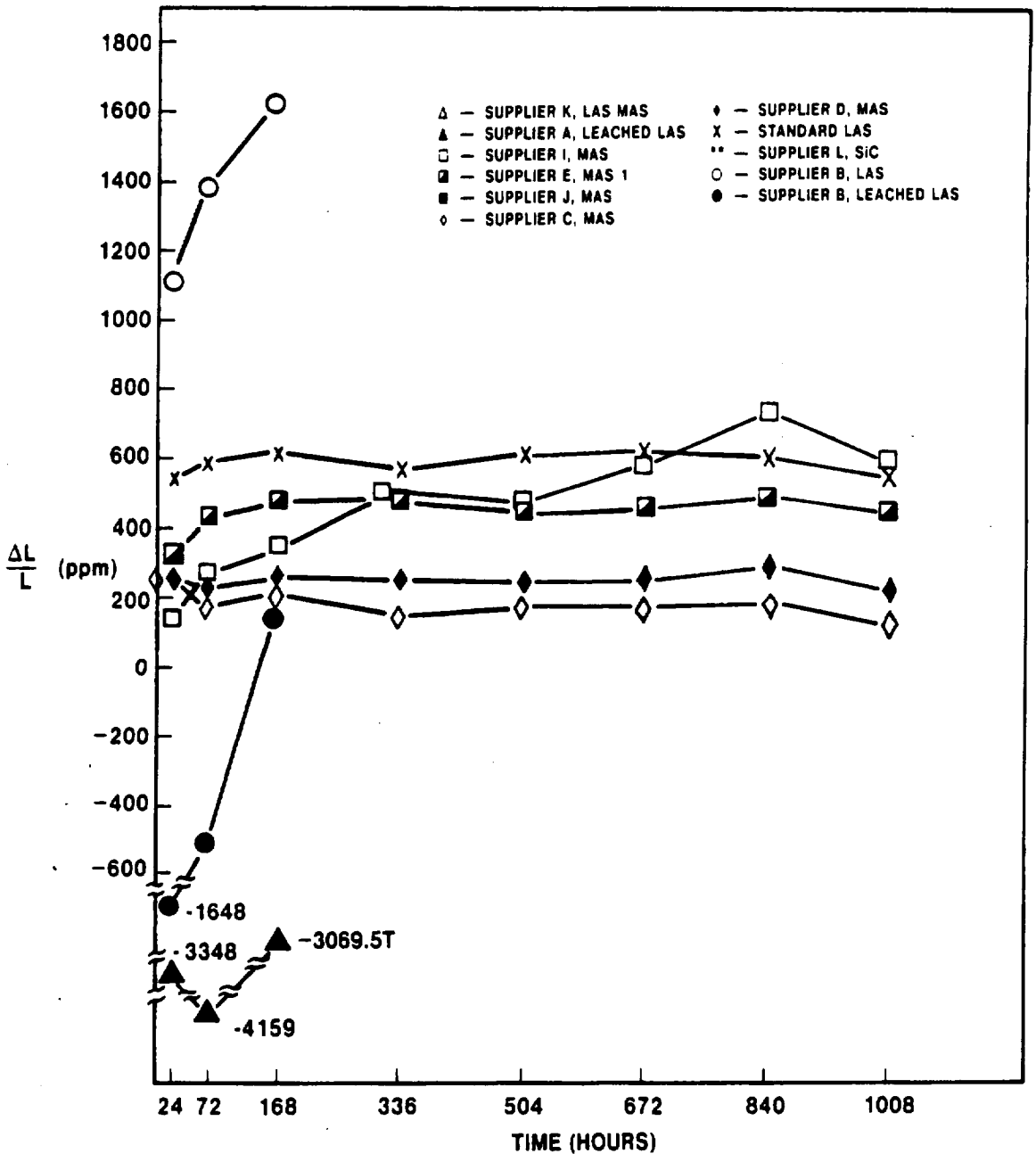

Figure VI.B.3.10 Physical Stability of Various Materials at 1100°C (2012°F) with Sodium Present.

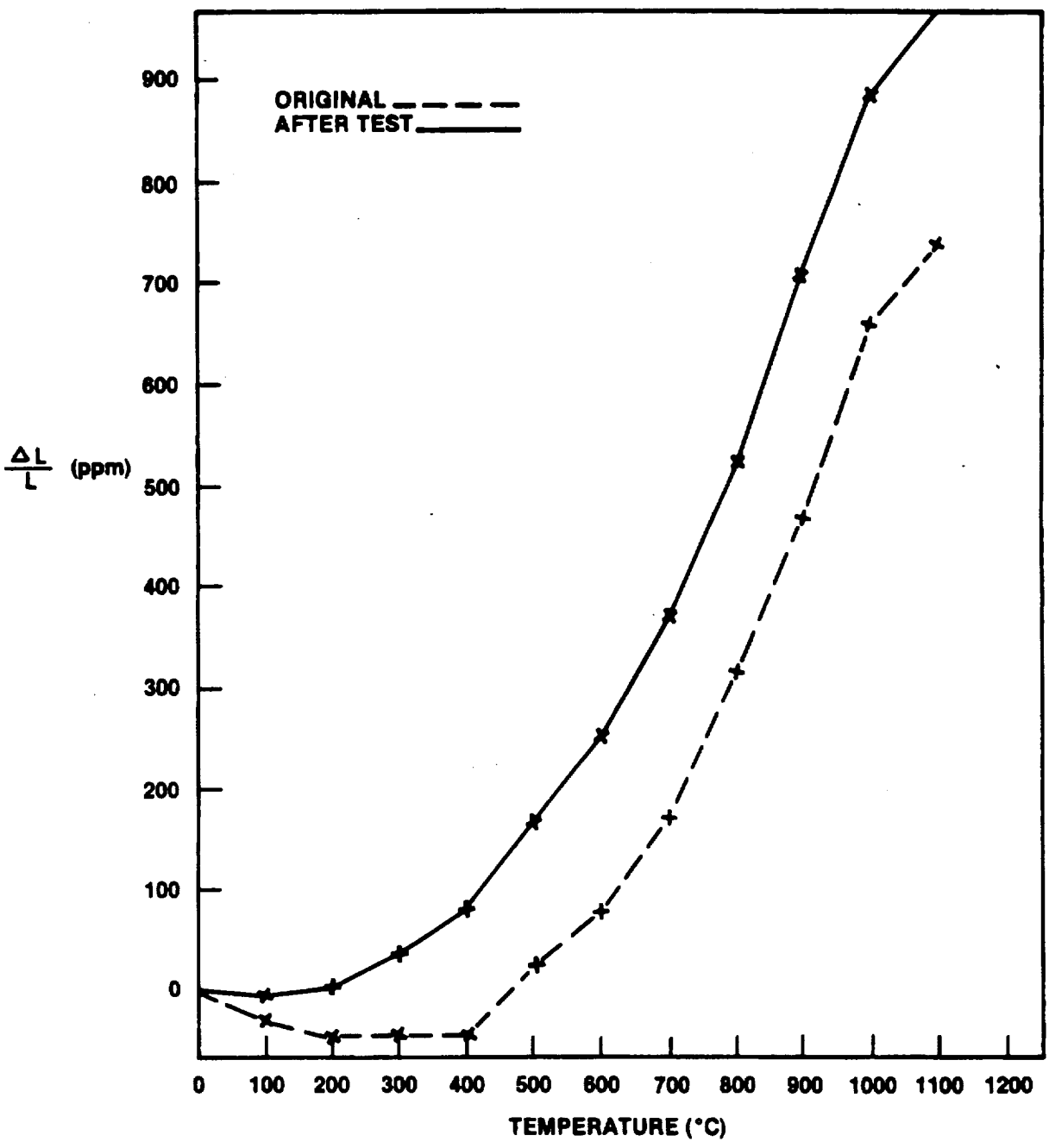

Figure VI.B.3.11 9455 LAS Standard; Thermal Expansion Behavior Before and After 1100°C (2012°F) Thermal Stability Testing with Sodium Present.

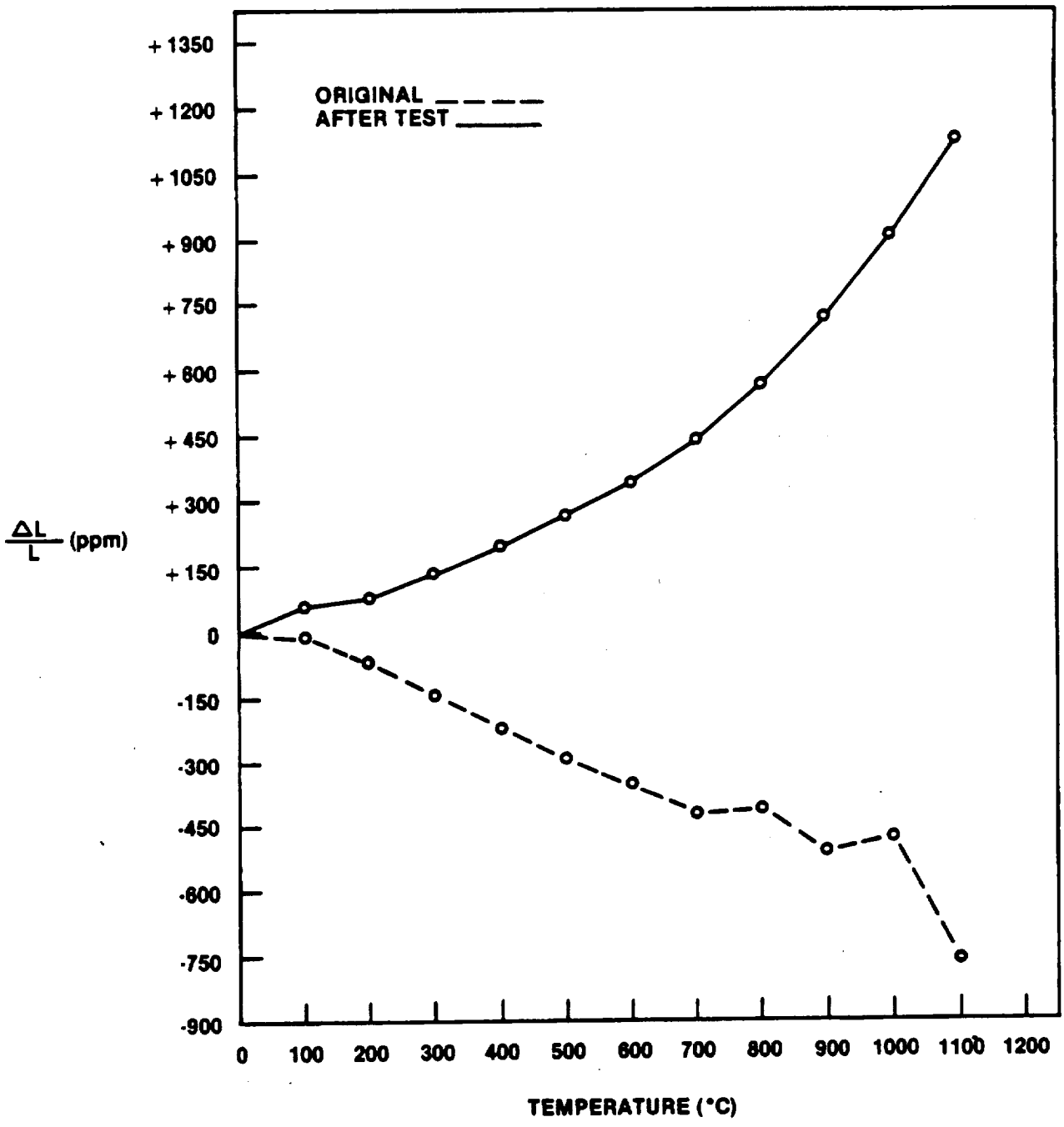

Figure VI.B.3.12 Supplier B, LAS; Thermal Expansion Behavior Before and After 1100°C (2012°F) Thermal Stability Testing with Sodium Present. (This material was terminated after 168 test hours).

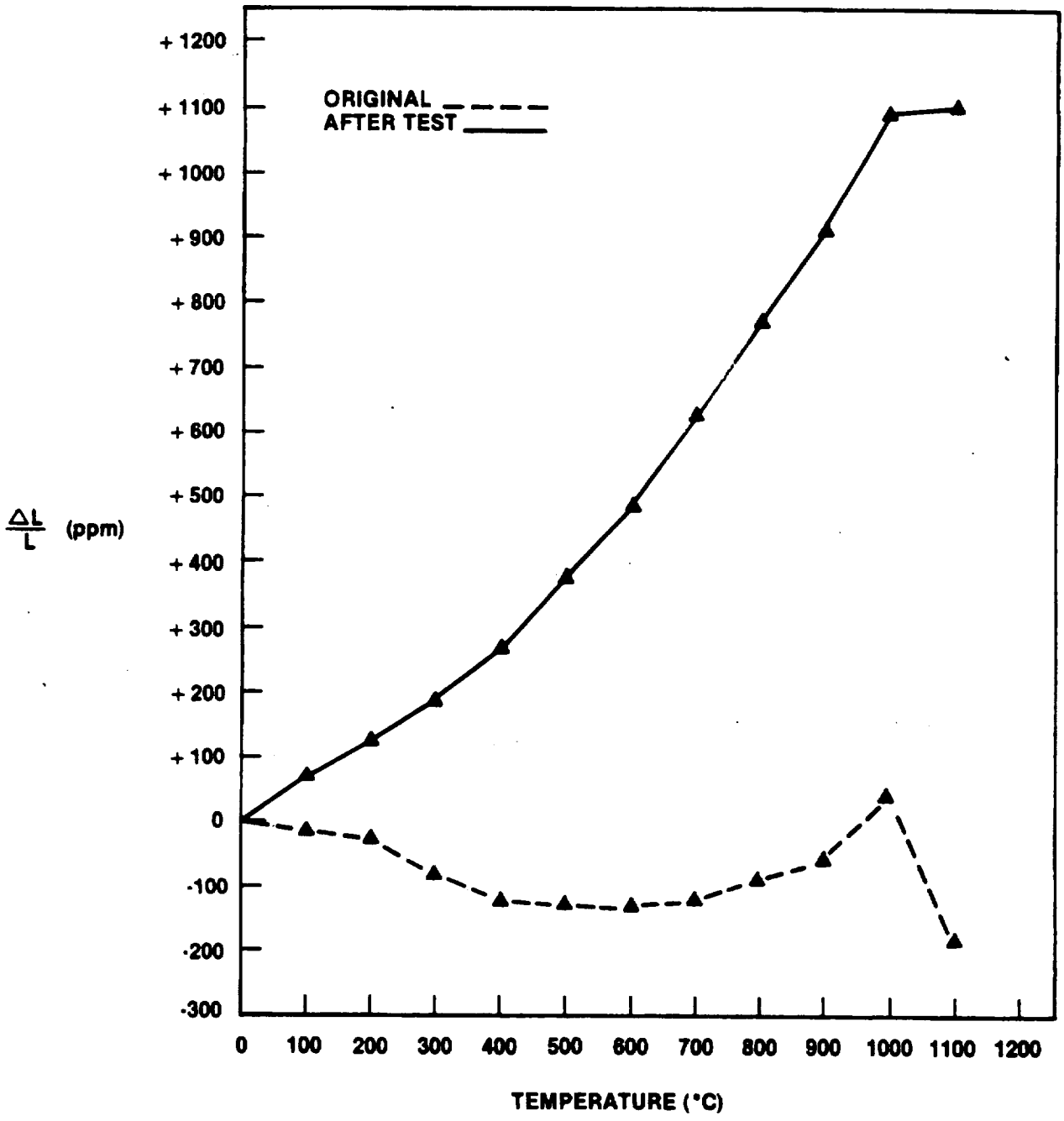

Figure VI.B.3.13 Supplier A, AS; Thermal Expansion Behavior Before and After 1100°C (2012°F) Thermal Stability Testing with Sodium Present. (This material was terminated after 168 test hours).

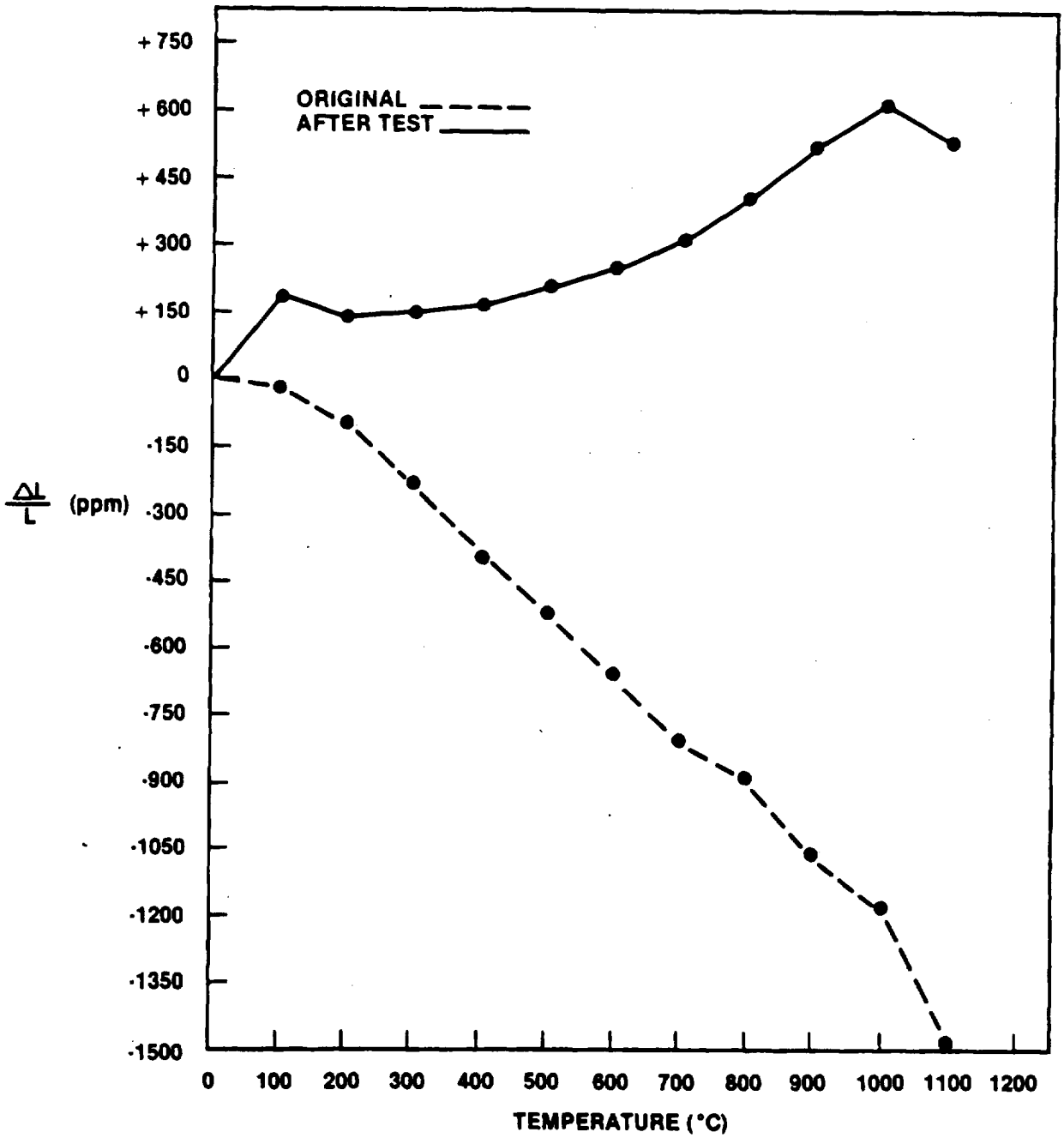

Figure VI.B.3.14 Supplier B, AS; Thermal Expansion Behavior Before and After 1100°C (2012°F) Thermal Stability Testing with Sodium Present. (This material was terminated after 168 test hours).

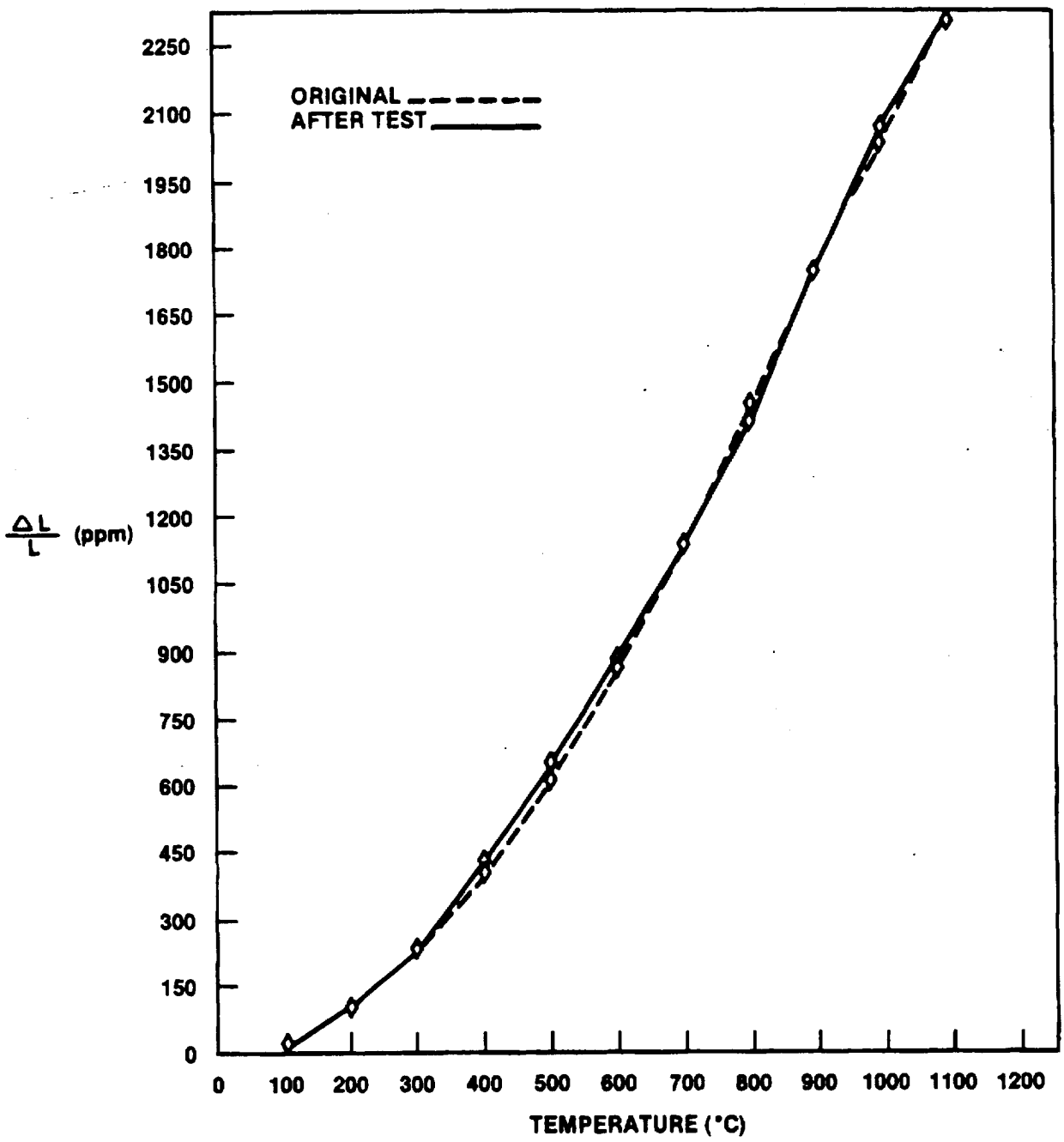

Figure VI.B.3.15 Supplier C, MAS; Thermal Expansion Behavior Before and After 1100°C (2012°F) Thermal Stability Testing with Sodium Present.

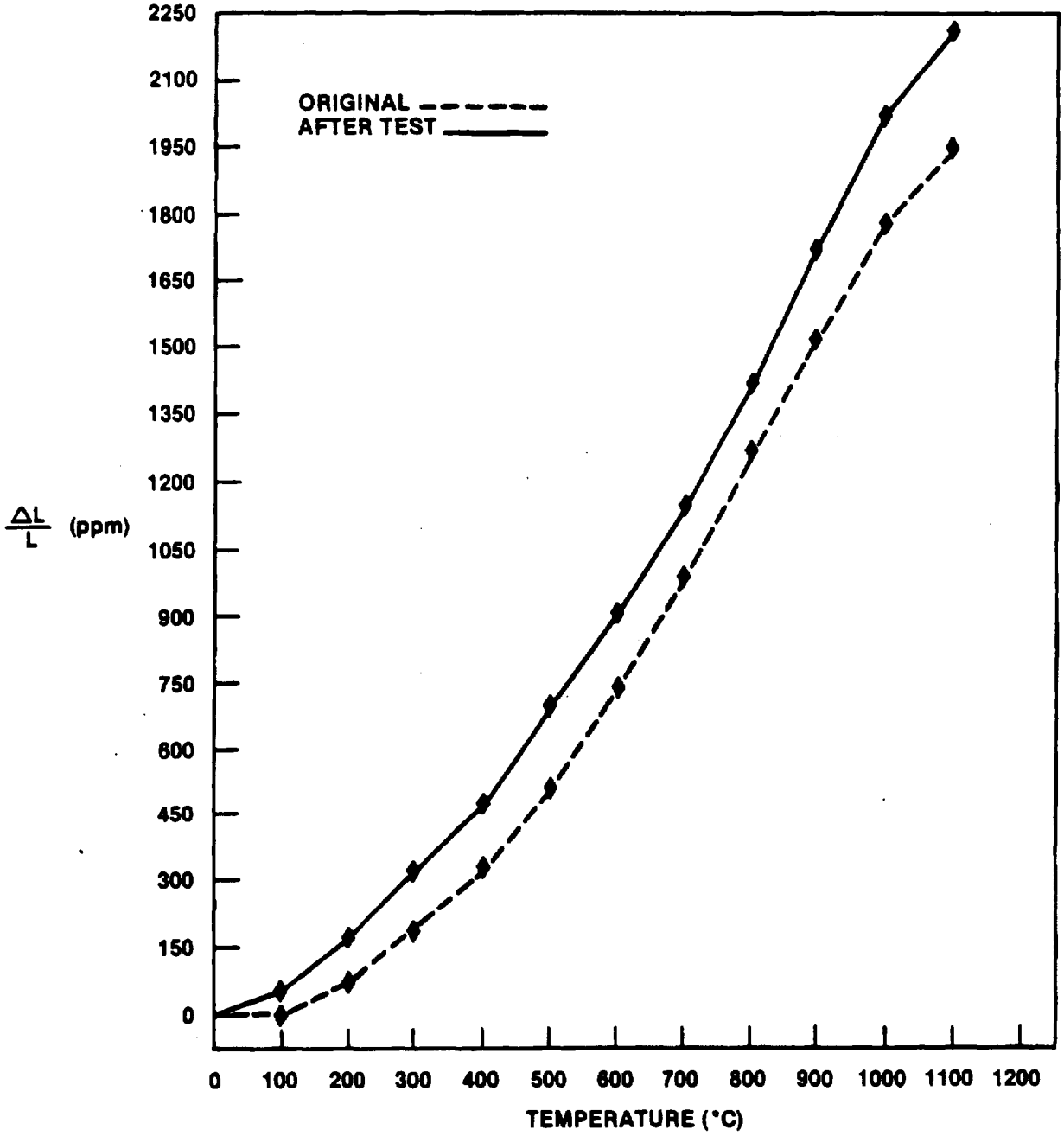

Figure VI.B.3.16 Supplier D, MAS; Thermal Expansion Behavior Before and After 1100°C (2012°F) Thermal Stability Testing with Sodium Present.

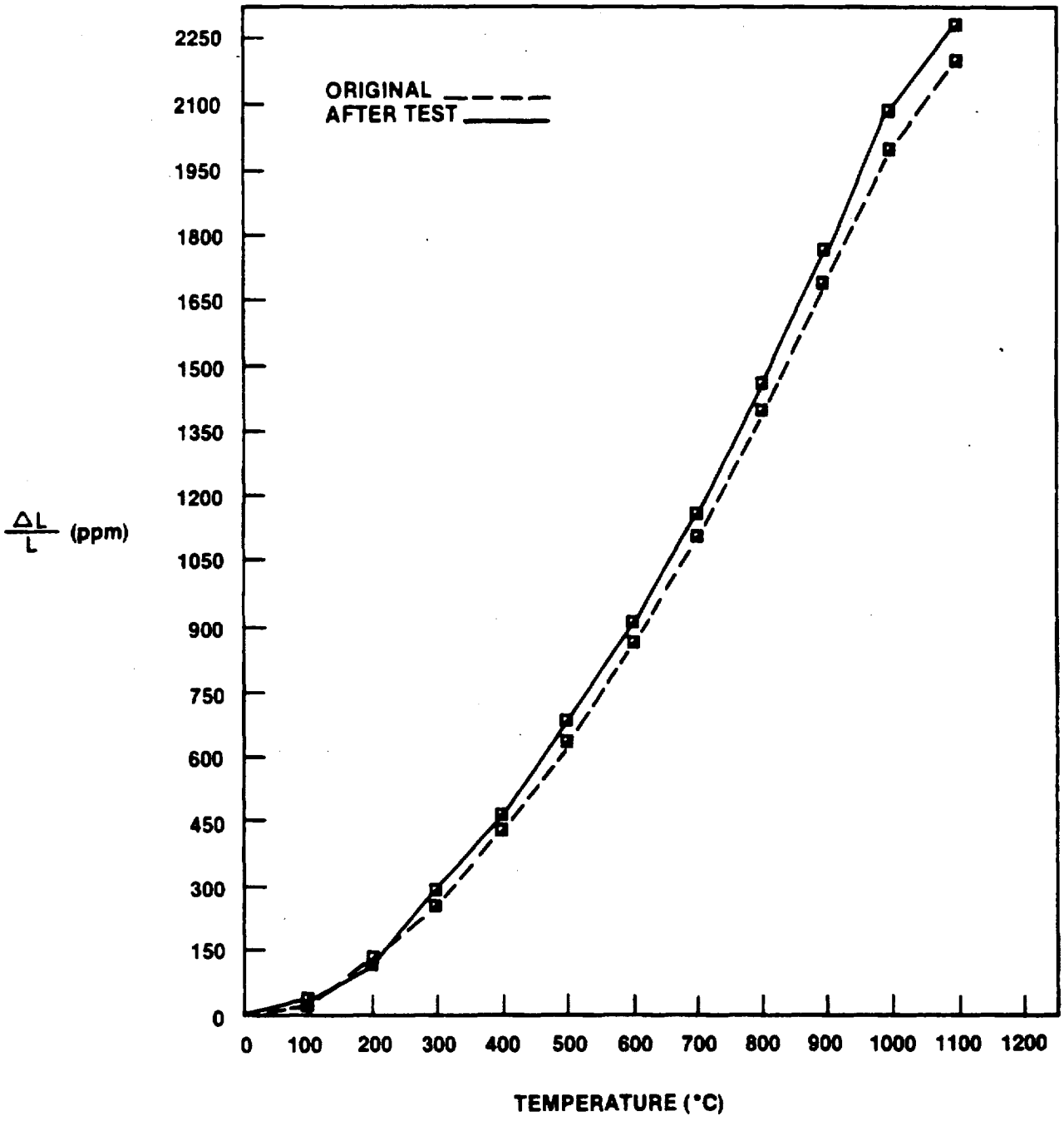

Figure VI.B.3.17 Supplier E, MAS #1; Thermal Expansion Behavior Before and After 1100°C (2012°F) Thermal Stability Testing with Sodium Present.

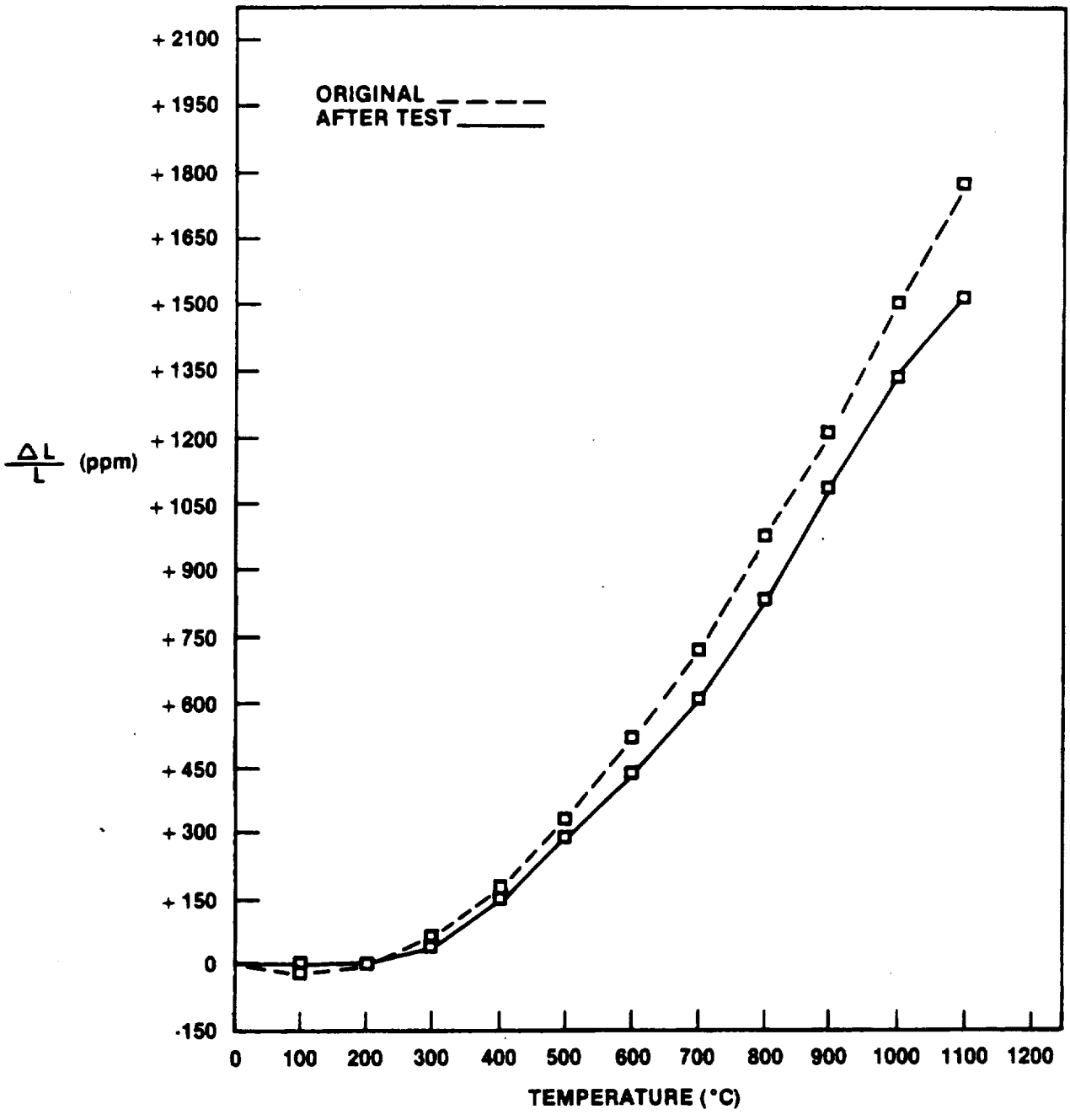

Figure VI.B.3.18 Supplier I, MAS; Thermal Expansion Behavior Before and After 1100°C (2012°F) Thermal Stability Testing with Sodium Present.

During this reporting period, four additional materials (3-MAS, 1-LAS/MAS) were procured, prepared, and introduced into the 1100°C (2012°F) thermal stability testing program. The test programs have been started, and the data will be included in future reports.

VI.B.4 1200°C (2192°F) Test Temperature

The original sample set submitted for testing at this temperature consisted of five experimental materials (4-MAS, 1-AS) plus the 9455 LAS standard. As the thermal stability testing program (without sodium present) progressed, it was necessary to terminate the AS material of Supplier A, as it exhibited physical deterioration after 168 cumulative test hours. During the time excursion to 672 test hours, a furnace overrun invalidated this specimen set. During this reporting period, materials have been gathered and prepared to create a new specimen set for thermal stability testing, without sodium present, at 1200°C (2192°F). This specimen set, consisting of eight experimental materials (7-MAS, 1-LAS/MAS) plus the 9455 LAS standard, is currently on test and results will be included in subsequent reports.

The 1200°C (2192°F) thermal stability testing with sodium present was completed during this reporting period, and the comparative data generated during the course of this test are presented in Figure VI.B.4.1. The results indicate that none of the materials tested are indifferent to the extremely hostile combined environment of high temperature and sodium chloride. The AS material was terminated after 168 hours of cumulative test time, as the samples were physically deteriorating and becoming difficult to handle. The extreme variations of the remainder of the materials suggest a deterioration of their properties as well.

Figures VI.B.4.2 through VI.B.4.7 illustrate the effect of the test environment on the thermal expansion behavior of each material between room temperature and the test temperature. The 9455 LAS standard does not exhibit a very marked change in thermal expansion (Figure VI.B.4.2) although the dimensional changes observed during testing (Figure VI.B.4.1) are quite uncharacteristic. Clearly, the AS of Supplier A is not the same material after having gone through the test, as the thermal expansion (Figure VI.B.4.3) is completely uncharacteristic of that of the original material.

The MAS materials, while all displaying a good deal of dimensional change during the course of the test (Figure VI.B.4.1), do not reflect, with the exception of that material from Supplier I (Figure VI.B.4.7) much change in their thermal expansion behaviors (Figures VI.B.4.4 through VI.B.4.7). The data accumulated to date at 1200°C (2192°F) are not as consistent and therefore, not as open to interpretation as those data gathered at the lower test temperatures. Before one should attempt to attach too much significance to these findings, it would be advantageous to compare this test to the corresponding thermal stability test without sodium present. Only then can the contribution of the sodium environment be evaluated; and, perhaps within that perspective, more meaningful conclusions drawn.

During this reporting period, the four new materials (3-MAS, 1-LAS/MAS) were also introduced into the 1200°C (2192°F) thermal stability testing program with sodium present. This insures a duplicate test sampling for both test conditions at this temperature. Testing of these materials has begun, and data will be subsequently reported.

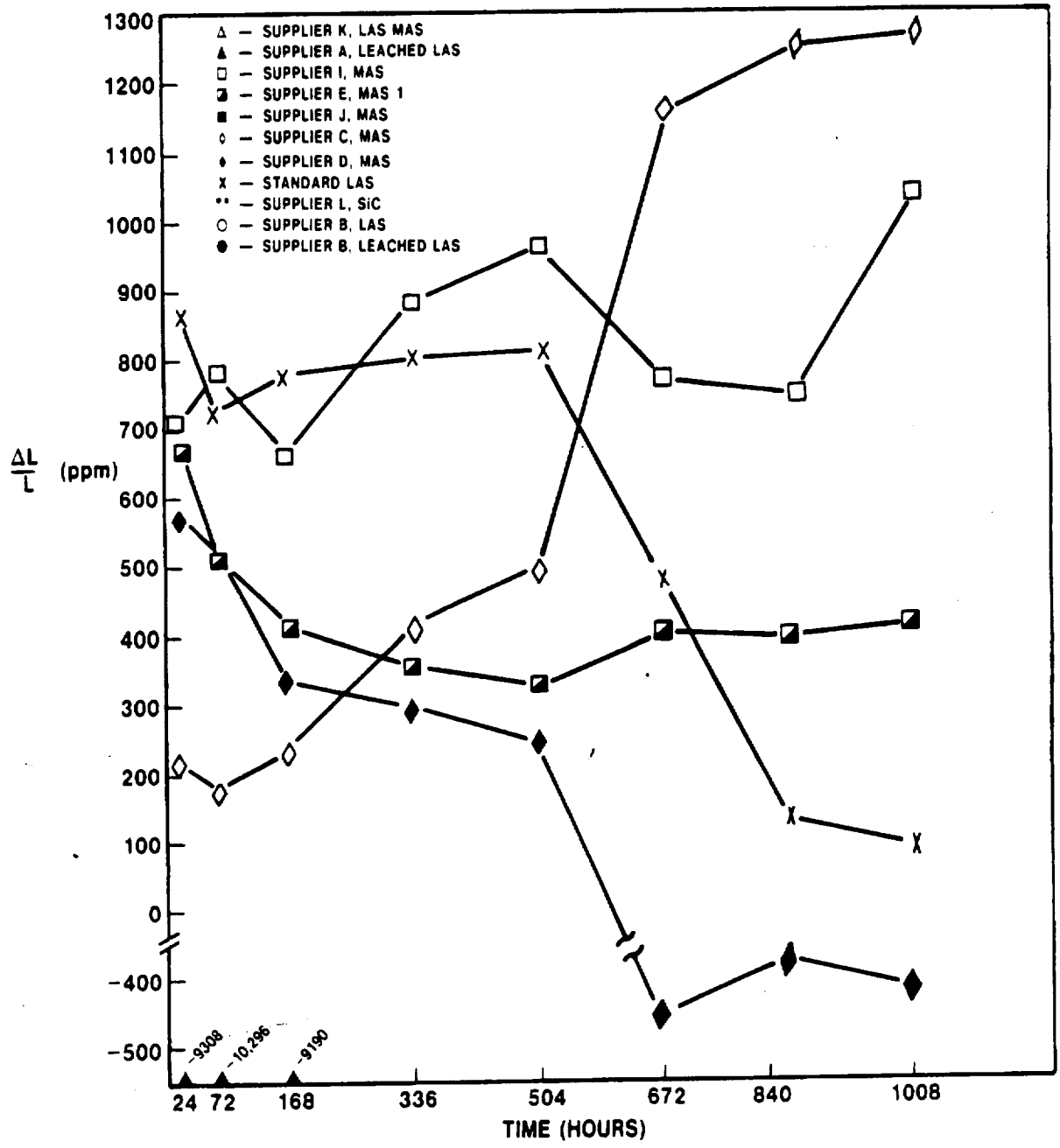

Figure VI.B.4.1 Physical Stability of Various Materials at 1200°C (2192°F) with Sodium Present.

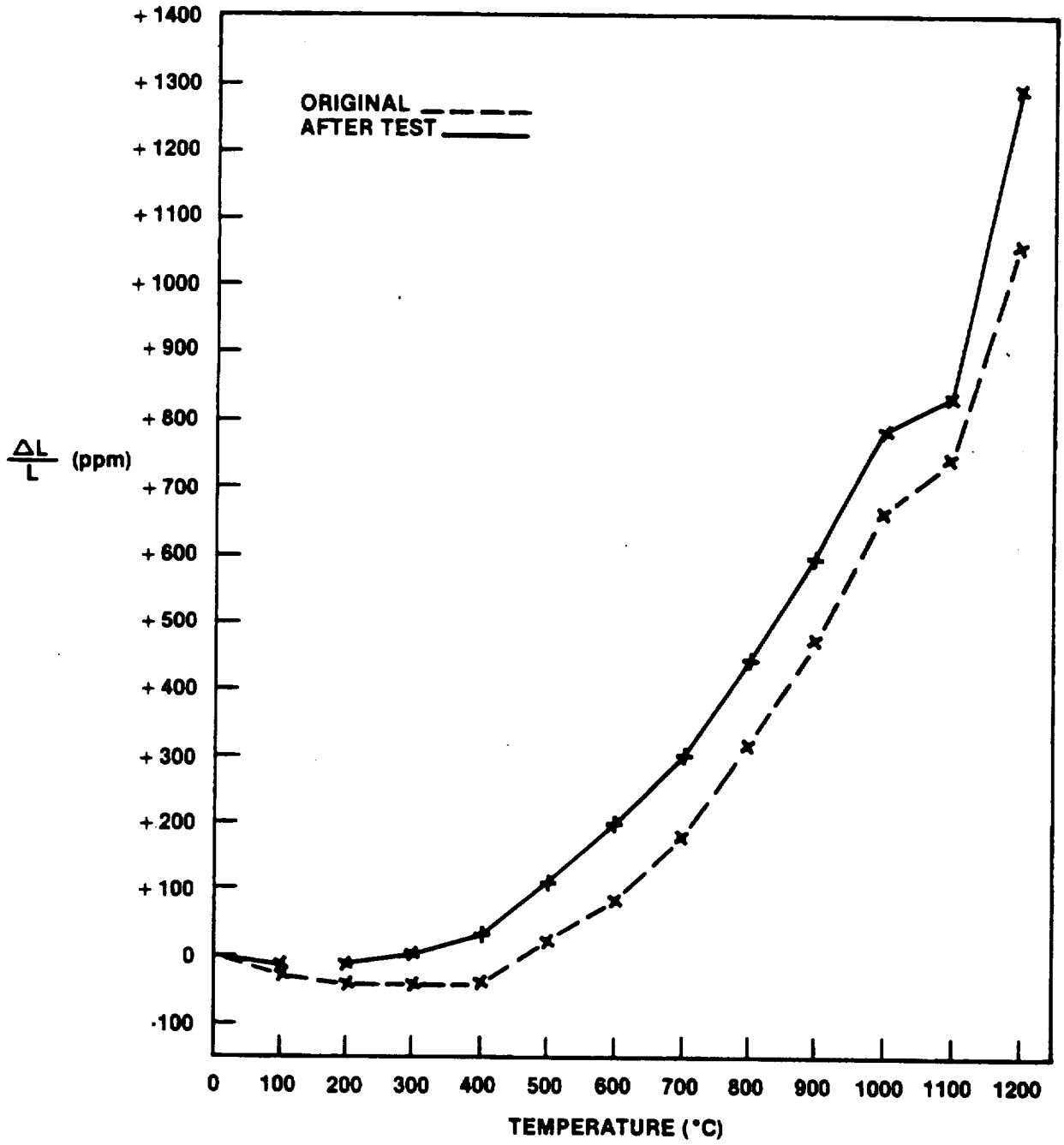

Figure VI.B.4.2 9455 LAS Standard; Thermal Expansion Behavior Before and After 1200°C (2192°F) Thermal Stability Testing with Sodium Present.

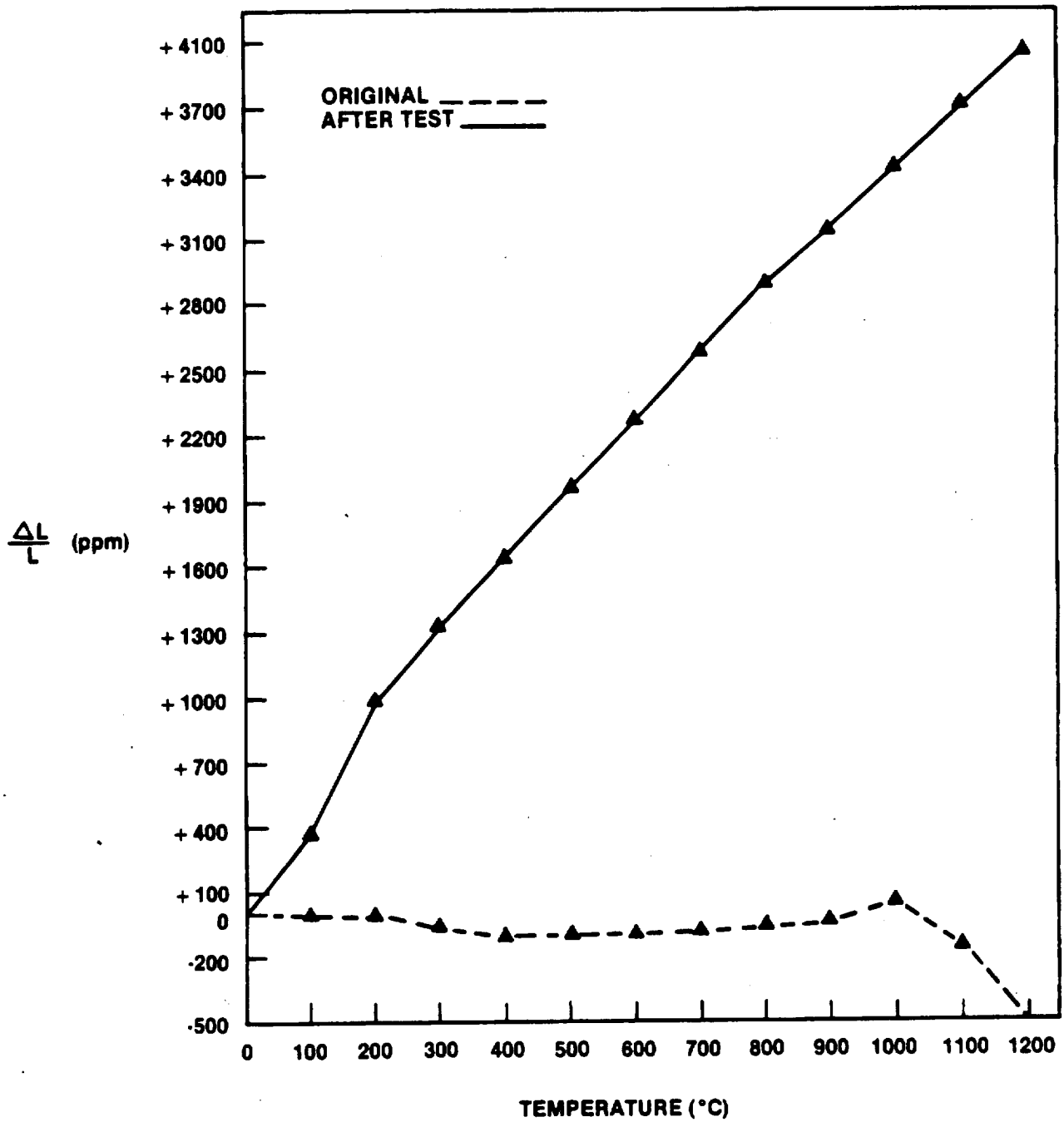

Figure VI.B.4.3 Supplier A, AS; Thermal Expansion Behavior Before and After 1200°C (2192°F) Thermal Stability Testing with Sodium Present. (This material was terminated after 168 test hours).

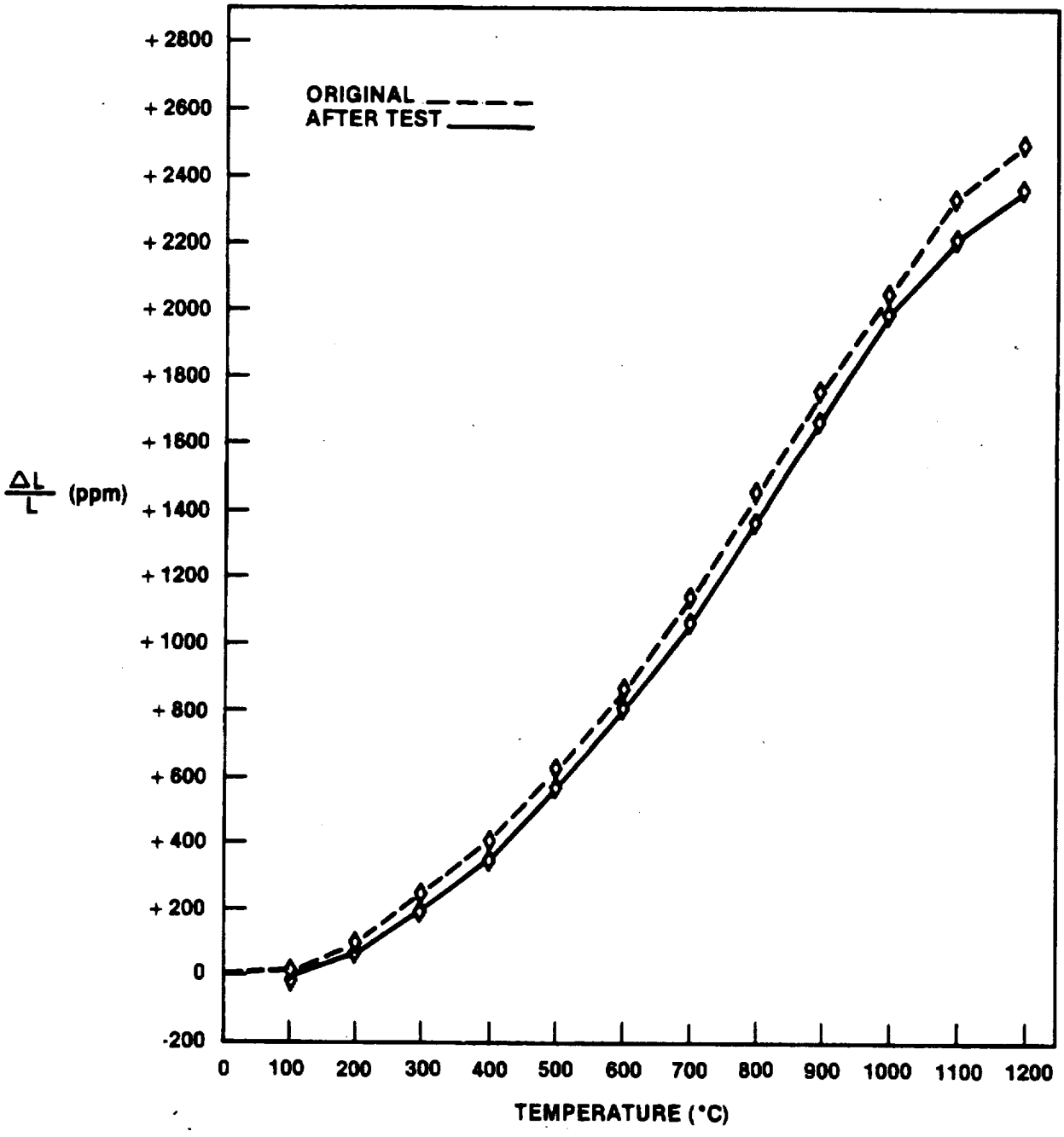

Figure VI.B.4.4 Supplier C, MAS; Thermal Expansion Behavior Before and After 1200°C (2192°F) Thermal Stability Testing with Sodium Present.

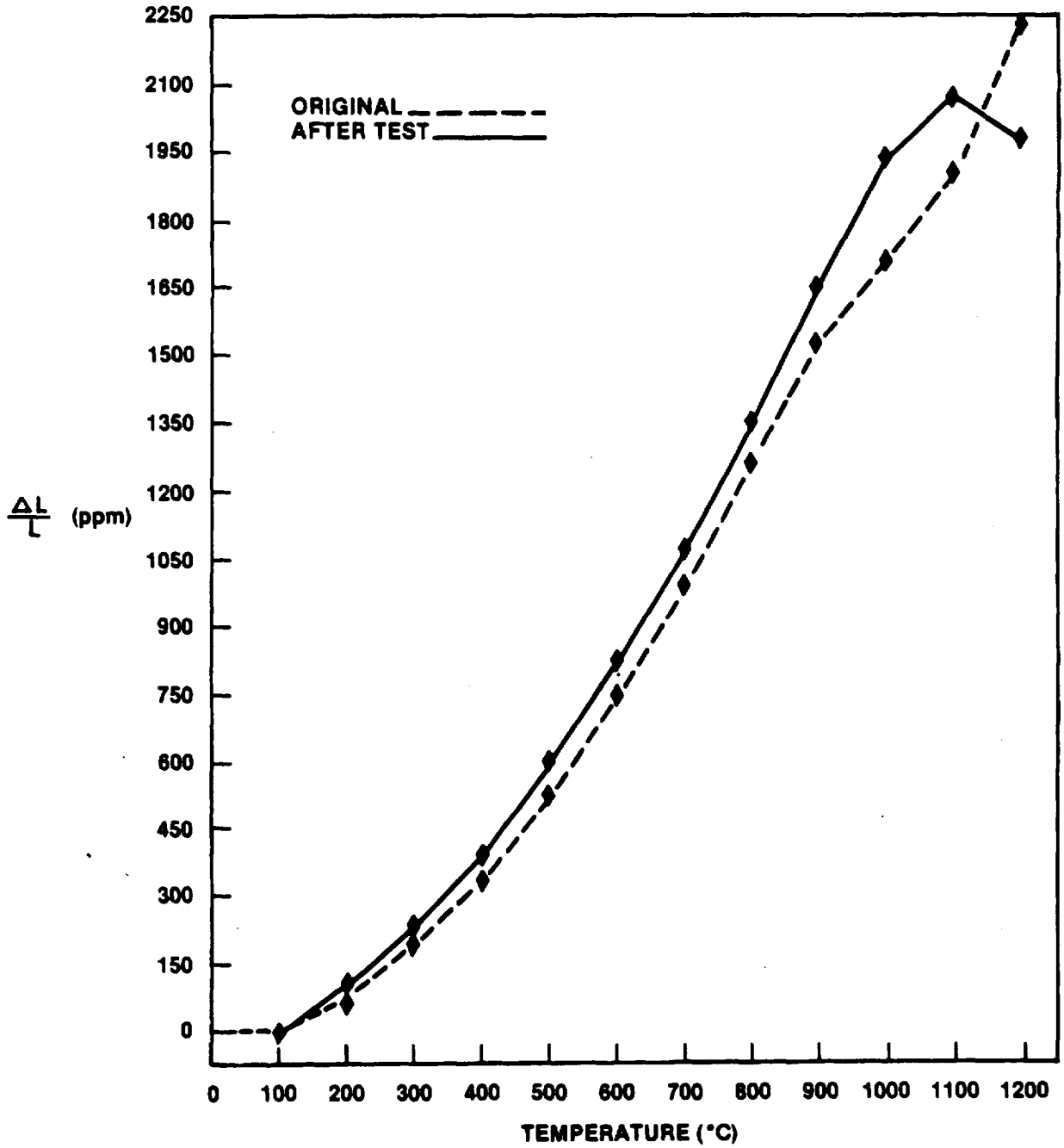

Figure VI.B.4.5 Supplier D, MAS; Thermal Expansion Behavior Before and After 1200°C (2192°F) Thermal Stability Testing with Sodium Present.

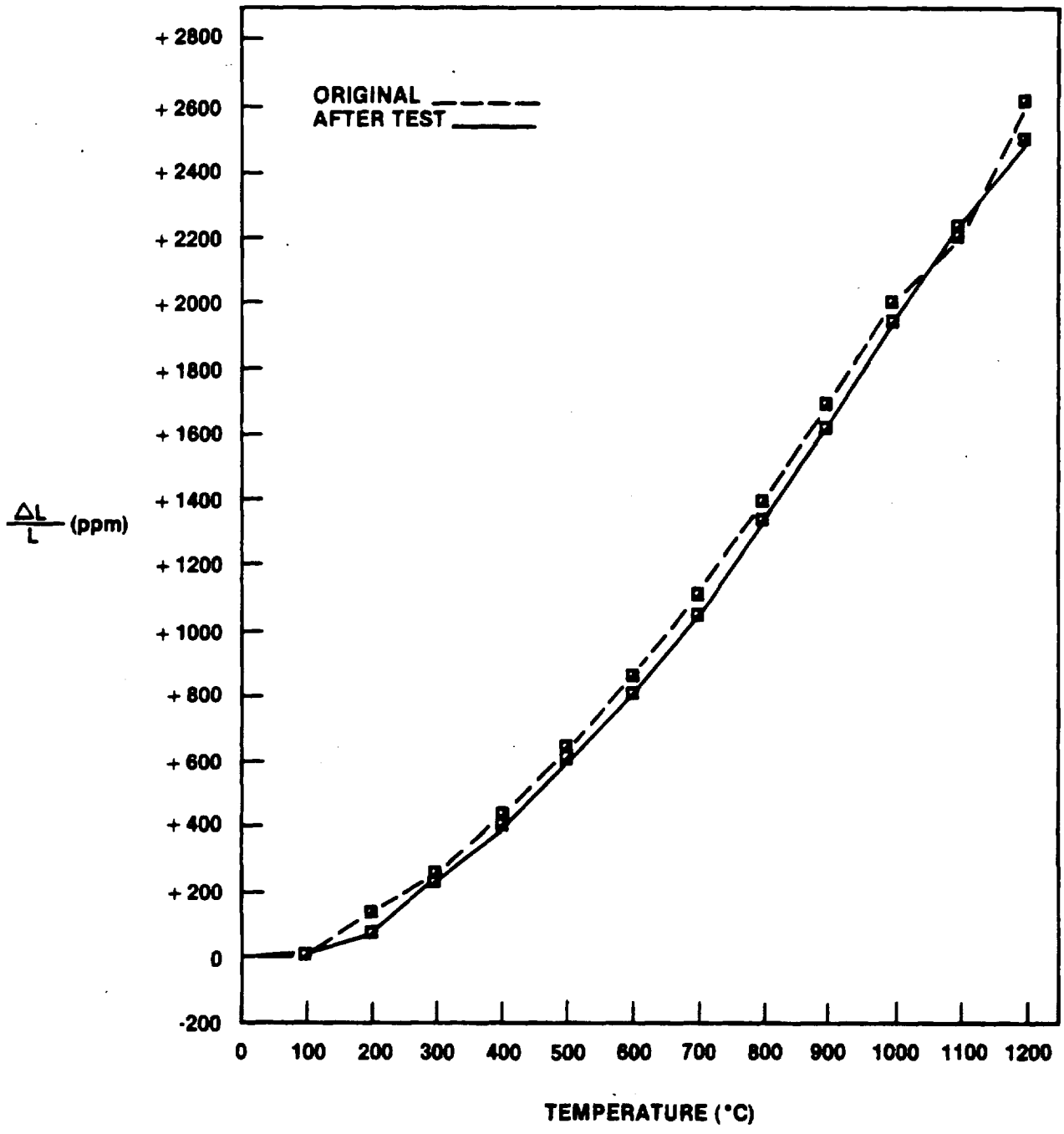

Figure VI.B.4.6 Supplier E, MAS #1; Thermal Expansion Behavior Before and After 1200°C (2192°F) Thermal Stability Testing with Sodium Present.

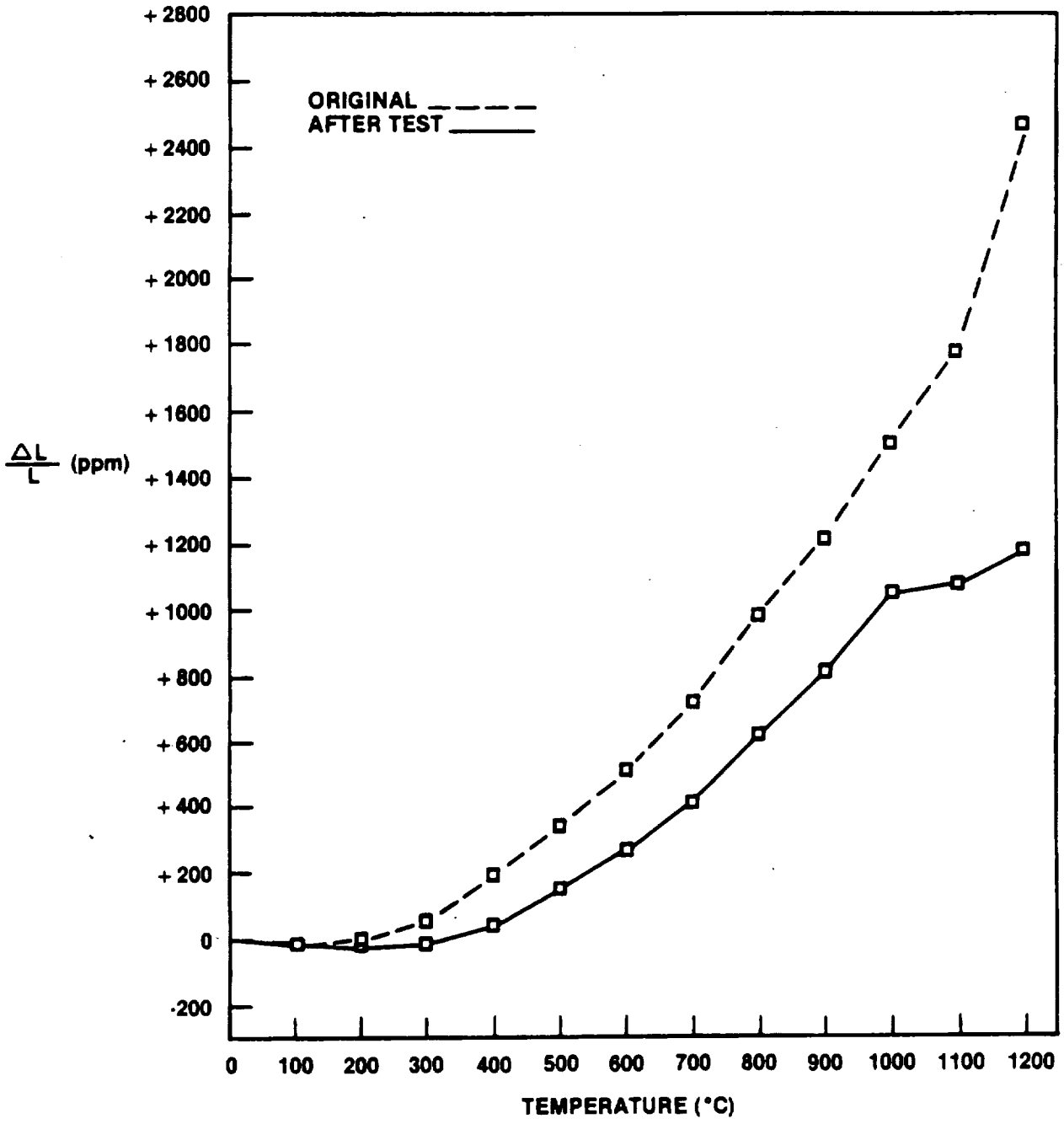

Figure VI.B.4.7 Supplier I, MAS; Thermal Expansion Behavior Before and After 1200°C (2192°F) Thermal Stability Testing with Sodium Present.

VI.C. PROBLEM AREAS

The crowning and tapering of the ends of the ceramic specimens has proven to be more severe and occurs at earlier test times at the elevated test temperatures. This effect reduces the precision of the length measurements. This problem is felt to be inherent in the manufacturing process of the matrix samples. Therefore, no effective method of eliminating this effect is available. It should be noted, however, that this is a real manifestation of the state of the fabricated material, and being such, most definitely speaks to the service potential of a particular supplier's material-fabrication combination.

VI.D. FUTURE PLANS

The thermal stability testing, with and without sodium present, of the new sample set (3-MAS, 1-LAS/MAS) will be pursued at 1000°C (1832°F), 1100°C (2012°F), and 1200°C (2192°F). A new sample set, including those materials invalidated by an earlier furnace overrun, will be tested at 1200°C (2192°F) without sodium present. The data resulting from these newly-initiated tests will be included in subsequent reports.

VI.E. TASK SUMMARY

During this reporting period, thermal stability testing was completed on the sample sets being evaluated at: 1000°C (1832°F), with sodium present; 1100°C (2012°F), without sodium present; 1100°C (2012°F), with sodium present; and 1200°C (2192°F), with sodium present.

Five MAS materials (those of Suppliers C, D, E, I, and J) are judged to have potential for regenerator service at 1000°C (1832°F). The AS material of Supplier A and the LAS material of Supplier B may also be useful at this temperature.

At 1100°C (2012°F) the four MAS materials tested (those of Suppliers C, D, E, and I) appear to have a physical and chemical stability necessary for regenerator service at this elevated temperature. The LAS, LAS/MAS, and AS materials tested are not recommended for service at 1100°C (2012°F).

The data at 1200°C (2192°F) are not complete, as only the testing with sodium present has been completed. Conclusions must await the completion of the 1200°C (2192°F) thermal stability testing without sodium present.

TASK VII. MANUFACTURING COST STUDIES

VII.A. INTRODUCTION

The purpose of this task is to update an existing cost study carried out in 1975, utilizing a 170 horsepower Stirling engine preheater model. The results of five independent vendor studies will be brought up to date by casting these results in the perspective of current and potential regenerator configurations and by accounting for inflation and the rising costs of production.

VIII.B. STATUS

In the previous report, projected costs for the volume production of regenerator cores of several configurations of interest were presented. During this reporting period, an evaluation of the extra cost of utilizing a zero-diameter (nominally 1″ or 25.4 mm) wind fabrication process was completed. Data for two core configurations are presented in Table VII.B.1. As can be readily deduced, a switch to the zero-wind fabrication process would increase unit costs approximately 15-18% for configuration (1) and 26% for configuration (2).

	Core Size (Finished)	Projected Cost/Unit
(1)	368.3 mm (14.5″) O.D. X 190.5 mm (7.5″) I.D. X 88.9 mm (3.5″) thick	$33 — 39
(1Z)	368.3 mm (14.5″) O.D. X 25.4. mm (1.0″) I.D. X 88.9 mm (3.5″) thick	$38 — 46
(2)	266.7 mm (10.5″) O.D. X 190.5 mm (7.5″) I.D. X 88.9 mm (3.5″) thick	$23 — 27
(2Z)	266.7 mm (10.5″) O.D. X 25.4 mm (1.0″) I.D. X 88.9 mm (3.5″) thick	$29 — 34

Table VII.B.1 — Comparison of difference in projected production costs between Regular and zero-wind fabrication of regenerator cores.

VII.C. PROBLEM AREAS

There are no current problems.

VII.D. FUTURE PLANS

A comparison of the costs of the rim mount and the hub mount drive systems will be concluded.

VII.E. TASK SUMMARY

A comparison of conventional and zero-wind fabrication costs was completed. Data for two regenerator core configurations indicate a production cost increase ranging from 15% to 26%, depending on core configurations.

TASK VIII. CORE MATERIAL AND DESIGN SPECIFICATION

VIII.A. INTRODUCTION

The volume procurement of regenerator cores necessitated a set list of criteria by which one could judge the quality of the finished product. Therefore, a regenerator material and design specification was assembled. This existing specification was recently updated, to include progressing technology, as a part of the charter of this contractural task.

The advancing temperature frontiers being addressed by turbine designers predict increased operating temperatures for the regenerator assembly. It is, then, quite important to learn as much as possible about the high temperature behavior of the material systems and design configurations being considered for future regenerator applications. This information, properly assembled, will serve as a high temperature material and design specification, useful to inform core manufacturers as to the demands to be placed upon their products.

VIII.B. STATUS

VIII.B.1 800°C (1472°F) Specification

This portion of the contract task has been completed. (Reference 4).

VIII.B.2 1000°C (1832°F) Specification

Laboratory tests of potential regenerator materials and engine tests of full size cores at elevated temperatures are proceeding. Studies of core mounting and drive systems compatible with increased operating temperatures are formulated. Design studies, including stress analysis modeled for elevated temperatures, will provide an input into this program.

VIII.C. PROBLEM AREAS

A temperature overrun in one of the Ford 707 gas turbine engines modified for elevated temperature operation prompted a premature engine shutdown and the resultant failure of a MAS test core.

VIII.D. FUTURE PLANS

Laboratory and engine testing will proceed during the next reporting period. Core mounting and drive studies will ensue, and computer modeling of operating stresses at elevated temperatures will be pursued.

VIII.E. TASK SUMMARY

The 800°C (1472°F) specification has been completed. Work is continuing to gather information for the 1000°C (1832°F) specification.

TASK IX. PROJECT MANAGEMENT

IX.A. INTRODUCTION

During the second quarter of 1978, Ford and NASA Project Management agreed to place more emphasis on 1000°C (1832°F) testing. Two engines were then converted from 800°C (1472°F) to 1000°C (1832°F) testing. This change in direction was done at no additional cost to NASA.

IX.B. STATUS

During this report period, Ford and NASA Project Management agreed to extend the program an additional six months at no additional cost to NASA. This will extend the completion date from June 30, 1979 to December 31, 1979. Consequently, an increase in core test hours of 13000 at 800°C (1472°F) and 2000 at 1000°C (1832°F) can be accommodated. The major advantage is that additional time will permit other suppliers to develop full size cores for test evaluation.

IX.C. PROBLEM AREAS

There are no problems associated with this task.

IX.D. FUTURE PLANS

Program emphasis and direction will be continually reviewed, and decisions affecting test content and priorities will be made as required.

IX.E. TASK SUMMARY

The program completion date has been extended from June 30, 1979 to December 31, 1979 at no additional cost to NASA. An increase in core test hours of 13000 at 800°C (1472°F) and 2000 at 1000°C (1832°F) can be accommodated. In addition this extension will permit other suppliers to develop full size cores for test evaluation.

TASK X. REPORTING REQUIREMENTS

X.A. INTRODUCTION

In addition to semi-annual Progress Reports, Ford will also publish three "Topical" reports as part of the NASA/Ford Ceramic Regenerator Program. The subjects of these three reports, which were determined by mutual agreement of Ford and NASA Project Management, are:

1. Evaluation of Advanced Regenerator Systems.

2. Feasibility Study of Silicon Nitride Heat Exchangers.

3. Regenerator Matrix Physical Data.

X.B. STATUS

During this report period the "Quarterly Progress Report for the Period from April 1, 1978 to June 30, 1978" was printed and distributed. In addition, the first "Topical" report, "Evaluation of Advanced Regenerator Systems", was printed and distributed.

X.C. PROBLEM AREAS

There are no problem areas associated with this task.

X.D. FUTURE PLANS

During the next report period a draft of the second "Topical" report, "Feasibility Study of Silicon Nitride Heat Exchangers", will be submitted to NASA Project Management for review, during May, 1979.

X.E. TASK SUMMARY

Publication of the "Semi-Annual Progress Reports" and "Topical Reports" are on schedule.

REFERENCES

1. Anderson, D. H., Fucinari, C. A., Rahnke, C. J., and Rossi, L. R., Annual Summary Report, No. 2630-1, Automotive Gas Turbine Ceramic Regenerator Design and Reliability Program, ERDA Contract No. E (11-1) 2630, Sept. 15, 1975.

2. Cook, J. A., Fucinari, C. A., Lingscheit, J. N., and Rahnke, C. J., Annual Summary Report, No. 2630-18, Automotive Gas Turbine Ceramic Regenerator Design and Reliability Program, ERDA Contract No. E (11-1) 2630, Oct. 15, 1976.

3. Cook, J. A., Fucinari, C. A., Lingscheit, J. N., and Rahnke, C. J., Annual Summary Report, No. NASA CR-135330, Ceramic Regenerator Systems Development Program, NASA Contract No. DEN3-8, Dec. 1977.

4. Cook, J. A., Fucinari, C. A., Lingscheit, J. N., Rahnke, C. J., Rao, V. D., Quarterly Progress Report for Oct.-Dec. 1977, No. NASA CR-135380, Ceramic Regenerator Systems Development Program, NASA Contract No. DEN3-8, Feb. 1978.

5. Cook, J. A., Fucinari, C. A., Lingscheit, J. N., Rahnke, C. J., Rao, V. D., Quarterly Progress Report for Jan.-Mar. 1978, No. NASA CR-135430, Ceramic Regenerator Systems Development Program, NASA Contract No. DEN3-8, May, 1978.

6. Cook, J. A., Fucinari, C. A., Lingscheit, J. N., Rahnke, C. J., Vallance, J. K., Quarterly Progress Report for April-June 1978, No. NASA CR-159432, Ceramic Regenerator Systems Development Program, NASA Contract No. DEN3-8, September, 1978.

7. C. P. Howard, "Heat Transfer and Flow Friction Characteristics of Skewed Passage and Glass-Ceramic Heat Transfer Surfaces," T. R. No. 59, Department of Mechanical Engineering, Stanford University, Oct. 1963.